

Investigation of Organogel Based Nanodispersion as a Novel Drug Delivery System

ジャンナトゥル, ファルドウス

<https://hdl.handle.net/2324/4496034>

出版情報 : Kyushu University, 2021, 博士 (工学), 課程博士
バージョン :
権利関係 :

**Investigation of Organogel Based Nanodispersion
as a Novel Drug Delivery System**

Jannatul FARDOUS

July 2021

Contents

Contents	i
List of Abbreviations.....	v
List of Tables.....	vii
List of Figures	viii
Abstract	xii
Chapter 1: Overview of Thesis.....	1
1.1 Introduction	1
1.2 Aim of the study	3
1.3 Originality of the study.....	3
1.4 Thesis outline	5
1.5 Reference.....	9
Chapter 2: Literature Review	13
2.1 Drug delivery system.....	13
2.2 Classification of drug	14
2.3 Advances in drug delivery system.....	15
2.4 Advantages and limitations of DDS	16
2.5 Gels in DDS.....	18
2.6 Organogels in DDS	18
2.6.1 Organogels in transdermal drug delivery.....	19
2.6.2 Organogels for parenteral formulations	19
2.6.3 Organogels for oral administration	20
2.6.4 Organogels in ocular drug delivery	20
2.6.5 Limitations of organogels	20
2.7 Conclusion.....	21
2.8 Reference.....	24
Chapter 3: Innovation and development of an organogel based gel-in-water nanodispersion for hydrophobic drug delivery	35
3.1 Introduction	35
3.2 Objectives	37
3.3 Materials and methods.....	37
3.3.1 Materials and their justification	37

3.3.2 Methods	39
3.4 Results and discussion.....	43
3.4.1 Preformulation study.....	43
3.4.2 Qualitative analysis of gel-in-water nanoemulsion	46
3.4.3 Stability study	50
3.5 Conclusion.....	52
3.6 Reference.....	53
Chapter 4: In vitro and in vivo evaluation of gel-in-water nanodispersion as a novel drug delivery system	59
4.1 Introduction	59
4.2 Objectives	60
4.3 Materials and methods.....	61
4.3.1 Biocompatibility of G/W nanoemulsion.....	61
4.3.2 In vitro cytotoxicity against cancer cells	63
4.3.3 In vitro cellular uptake by cancer cells	63
4.3.4 In vivo antitumor efficacy.....	64
4.3.5 Statistical analysis.....	65
4.4 Results and discussion.....	66
4.4.1 Biocompatibility of G/W nanoemulsion.....	66
4.4.2 In vitro anticancer efficacy	68
4.4.3 In vitro cellular uptake by cancer cells	69
4.4.4 In vivo antitumor efficacy.....	70
4.5 Conclusion.....	72
4.6 Reference.....	73
Chapter 5: Gel-in-water nanodispersion for potential application in intravenous delivery of anticancer drugs	78
5.1 Introduction	78
5.2 Objectives	79
5.3 Materials and methods.....	80
5.3.1 Preparation of Paclitaxel-loaded G/W nanoemulsion.....	80
5.3.2 In-vitro biocompatibility study	81
5.3.3 In vitro drug release from G/W nanodispersion	83
5.3.4 In vitro cellular uptake of nanoparticles	85
5.3.5 In vitro anticancer effect of G/W nanoemulsion	85

5.3.6 In vivo antitumor efficacy of paclitaxel-loaded G/W nanoemulsion	86
5.3.7 Statistical analysis.....	88
5.4 Results and discussion.....	88
5.4.1 In vitro biocompatibility study	88
5.4.2 In vitro drug release from nanodispersion	91
5.4.3 In vitro cellular uptake by lung cancer cells	93
5.4.4 In vitro anticancer effect against lung cancer cells.....	94
5.4.5 In vivo antitumor efficacy of paclitaxel-loaded G/W nanoemulsion	96
5.5 Conclusion.....	97
5.6 Reference.....	99

Chapter 6: Delivery of hydrophobic drug to the posterior region of eye as gel-in-water nanodispersion.....104

6.1 Introduction	104
6.2 Objectives.....	106
6.3 Materials and methods.....	106
6.3.1 Preparation of G/W nanoemulsion	106
6.3.2 Development of G/W nanoemulsion as an eyedrop	107
6.3.3 Characterization of G/W eyedrop.....	108
6.3.4 Effect of sterilization on particle size and its distribution	109
6.3.5 In vitro biocompatibility study of G/W nanoemulsion.....	110
6.3.6 Ocular surface irritation test in vivo	112
6.3.7 In vivo permeability study	113
6.3.8 Statistical analysis.....	114
6.4 Results and discussion.....	114
6.4.1 Determination of optimum concentration of oil to aqueous phase volume ratio, surfactant, and gelling agent concentration	114
6.4.2 Characterization of G/W eyedrop	116
6.4.3 Effect of sterilization on the particle size distribution	120
6.4.4 In vitro biocompatibility study	121
6.4.5 Ocular surface irritation test in vivo	123
6.4.6 In vivo permeability study	124
6.5 Conclusion.....	125
6.6 Reference.....	127

Chapter 7: Conclusion134
 7.1 Concluding remarks134
 7.2 Future Prospects135
Acknowledgements.....137

List of Abbreviations

12-HSA	12-Hydroxystearic Acid
A549	Adenocarcinomic human alveolar basal epithelial cells
AMD	Age-related Macular Regeneration
B16F10	Murine melanoma cell line
BCS	Biopharmaceutics Classification System
CLSM	Confocal Laser Scanning Microscopy
CT	Computed Tomography
CYP1A1	Cytochrome P450 family 1 subfamily A member 1
DDS	Drug Delivery System
DLS	Dynamic Light Scattering
DMEM	Dulbecco's Modified Eagle Medium
DMSO	Dimethyl Sulfoxide
EE	Encapsulation Efficiency
EGM-2	Endothelial Growth Medium 2
ELISA	Enzyme Linked Immunosorbent Assay
EPR	Enhanced Permeability and Retention
EROD	Ethoxyresorufin-O-Deethylase
FBS	Fetal Bovine Serum
G/W	Gel-in-Water
G/W/O	Gel-in-Water-in Oil
G/W-PTX	Paclitaxel-loaded gel-in-water Nano emulsion
HCO-60	Hydrogenated Castor Oil-60
HLB	Hydrophilic Lipophilic Balance

HUVEC	Human Umbilical Vein Endothelial Cells
L929	Murine fibroblasts cell line
LMOG	Low Molecular Weight Organogelator
MPS	Mononuclear Phagocyte System
NE	Nanoemulsion
NME	New Molecular Entities
O/W	Oil-in-Water
PBS	Phosphate Buffered Saline
PDI	Polydispersity Index
PSED	Posterior Segment Eye Diseases
PTX	Paclitaxel-loaded Gel-in-Water Nano Emulsion
SCID	Severe Combined Immunodeficient
TEM	Transmission Electron Microscopy
UV	Ultraviolet
WHO	World Health Organization
WST-8	Water Soluble Tetrazolium Salt 8

List of Tables

2-1	Advantages and limitations of currently available nanoparticles.	17
3-1	List of ingredients for gel-in-water nanoemulsion.	38
3-2	Physicochemical properties of G/W nanoemulsion.	47
6-1	Featured characteristics of G/W nanoemulsion.	118
6-2	Particle size analysis of G/W nanoemulsion before and after sterilization.	121

List of Figures

1-1	Schematic outline of the thesis.	8
2-1	Classification of nanoparticles with most common subclasses. This image is extracted from Mitchell et al ³² with permission.	16
3-1	Changes in the particle size and PDI of G/W nanoemulsion with the increasing volume of water and concentration of surfactant and organogelator, (A) oil-to-water volume ratio; (B) HCO-60 concentration; (C) 12-HSA concentration; (D) TEM micrograph of G/W nanoparticle; (E) Fluorescent image of G/W nanoemulsion.	44
3-2	Characterization of G/W nanoemulsion by (A) particle size distribution, (B) zeta potential distribution and (C) pH of G/W nanoemulsion before and after dilution with water, PBS, 0.9% saline, 5% dextrose.	48
3-3	Thermal sensitivity of G/W nanoparticles.	49
3-4	Comparative stability study of G/W NE and O/W NE, (A) particle size; (B) polydispersity index; (C) pH; (D) zeta potential, blue lines = O/W and red lines = G/W.	51
4-1	Changes in hepatocytes morphology and expression of liver functions, (A) hepatocyte morphology without G/W; (B) hepatocyte morphology with G/W; (C) live cell activity of hepatocytes; (D) albumin secretion rate by hepatocytes; (E) metabolic activity of hepatocytes; (F) metabolic activity per live cell. Bars represent standard deviation, n=3, scale bars = 200 μ m. G/W (+) = Cells	67

- incubated with G/W nanoemulsion, G/W (-) = Cells incubated with D-HDM.
- 4-2 In vitro cytotoxicity of paclitaxel-loaded G/W on melanoma cells, 69
(A) live cell activity showing significant cell death; bars represent standard deviation, n=3; (B) melanoma cell morphology in the culture medium; (C) melanoma cell morphology after treatment with paclitaxel-loaded G/W NE. Scale bars = 200 μ m.
- 4-3 In vitro cellular uptake of G/W nanoemulsion observed under 70
CLSM. Hoch = Hoechst, Rd = Rhodamine, C-6 = Coumarin-6, CLSM = Confocal laser scanning microscopy. Scale bars = 20 μ m.
- 4-4 In vivo cytotoxicity study, (A) changes in tumor volume over time; 71
(B) changes in tumor weight over time; (C) changes in mice body weight. Bars represent standard deviation, n=3, * p < 0.05.
- 5-1 Changes in cell morphology at day 1, 3, 5, and 7 days of culture 89
under phase-contrast microscope, (A) hepatocytes morphology incubated with D-HDM; (B) hepatocytes morphology incubated with G/W; (C) fibroblasts (L929) morphology incubated with DMEM; (D) fibroblasts morphology incubated with G/W. Scale bars = 200 μ m.
- 5-2 In vitro biocompatibility study of G/W nanodispersion, (A) live cell 91
activity of hepatocytes; (B) cell proliferation assay of L929 cell line; (C) relative cell viability of L929 cell line incubated with G/W. Bars represent standard deviation, n= 3.

- 5-3 In vitro drug release of paclitaxel from G/W nanodispersion and kinetic evaluation of release profile, (A) cumulative release of paclitaxel from nanoparticles; (B) paclitaxel release data fitted to Korsmeyer-Peppas model; (C) paclitaxel release data fitted to Higuchi model. Bars represent standard deviation, n= 3. 92
- 5-4 3D reconstruction of confocal analysis of the A549 cells exposed to coumarin-6 loaded G/W nanoemulsion. The staining of the cells is as follows: Blue - Hoechst-stained nuclei, Red – Rhodamine-stained cytoplasm, Green – Coumatin-6 loaded G/W nanoemulsion. Scale bar = 20 μm . 94
- 5-5 In vitro cytotoxicity of paclitaxel-loaded G/W nanoemulsion to lung cancer cells (A549), (A) live cell activity of A549 cells; (B) A549 cell morphology with DMEM; (C) A549 cell morphology with G/W-PTX. Bars represent standard deviation, n= 3, $*p < 0.05$. Scale bars = 200 μm . 95
- 5-6 Anti-tumor efficacy of paclitaxel-loaded G/W nanodispersion after intravenous injection on the tail vein, (A) changes in tumor volume over time; (B) tumor weight in control and treatment groups. Bars represent standard deviation, n= 5, $*p < 0.05$. 96
- 6-1 Formulation optimization for a stable G/W nanoemulsion, (A) selection of oil PBS volume ratio; (B) selection of surfactant concentration; (C) selection of organogelator concentration. Bars represent standard deviation, n=3. 115

6-2	Characterization of G/W nanoemulsion, (A) particle size distribution analysis by DLS, (B) zeta potential of G/W nanoparticles, n=3.	117
6-3	Rheological analysis of G/W nanoparticles, (A) comparative dynamic viscoelasticity of G/W and O/W nanoemulsion; (B) thermal sensitivity of G/W nanoparticles. Bars represent standard deviation, n=3, * $p < 0.05$.	119
6-4	In vitro biocompatibility of G/W nanoemulsion at different concentrations, (A) live cell activity of primary hepatocytes, (B) live cell activity of HUVECs, (C) cell viability of HUVECs in the presence of G/W nanoemulsion. Bars represent standard deviation, n = 3.	122
6-5	Effect of G/W nanoemulsion on cell morphology at different concentrations, (A) hepatocytes morphology; (B) HUVECs morphology. Scale bars = 200 μm .	123
6-6	Ocular surface irritation test for G/W nanoemulsion. Scale bar = 50 μm .	124
6-7	In vivo corneal permeability of G/W nanoemulsion, (A) relative fluorescence intensity of coumarin-6 in the retinal layer; (B) permeability for control group; (C) permeability of coumarin-6 in castor oil; (D) permeability of coumarin-6 loaded G/W nanoemulsion. Bars represent standard deviation, n=3, * $p < 0.05$. Scale bars = 50 μm .	125

Abstract

Formulation of poorly water-soluble drugs without compromising safety and therapeutic efficacy is challenging for researchers for years. With the advances in technology, currently available drug delivery strategies for hydrophobic drugs are based on nanoparticle systems and offer several advantages including increased drug absorption, enhanced bioavailability, and fewer side effects. Despite several advantages, nanoparticle-based drug delivery systems have certain limitations especially instability, immediate drug release owing to their large surface area, limited drug encapsulation efficiency, inadequate biocompatibility, non-specific localization, and so on. Organogels have gained attention in recent years as potential drug delivery systems due to their high bioavailability, no first-pass metabolism, and rapid action. Considering this, in the current study an organogel based nanoemulsion was developed aiming to effectively deliver hydrophobic drugs *via* encapsulation within *in situ* gellable organogel droplets, termed as gel-in-water (G/W) nanoemulsion.

G/W nanoemulsion was prepared using a combination of lipiodol and organogelator 12-hydroxystearic acid (12-HSA) as inner gel phase; dispersed in water by ultrasonication and stabilized with polyoxyethylene hydrogenated castor oil (HCO-60) as a surfactant. The fabricated nanoemulsion has monodispersed particles of ~ 206 nm in diameter and higher encapsulation efficiency (~97%). The narrow size distribution (PDI > 0.3) and higher surface charge of nanogel droplets ensure the stability of G/W nanoemulsion over six months at different storage temperatures. Additionally, ~67% of drugs released after 48h suggesting a diffusion-controlled drug release from the inner gel phase of nanodroplets. The nanoemulsion was found biocompatible to

different cell lines including primary rat hepatocytes, fibroblasts, and HUVECs with no significant change in live-cell activity as well as in other cellular functions. A significant decrease ($p < 0.05$) in cancer cell growth was found for paclitaxel-loaded G/W nanoemulsion to melanoma and lung cancer cells both in vitro and in vivo.

Similarly, the antitumor efficacy of paclitaxel-loaded G/W nanoemulsion after subcutaneous and intravenous administration confirms the feasibility of organogel nanodispersion application via various routes of administration. Moreover, this organogel nanoemulsion also emerges the possibility to administer as an eye drop with enhanced corneal permeability for the treatment of posterior segment eye diseases. All the results support the hypothesis that organogel based nanoemulsion can be a promising carrier for hydrophobic drugs with better stability, minimal side effects, and ease of administration through different routes.

Chapter 1: Overview of Thesis

1.1 Introduction

The poor water solubility of drug molecules is one of the major obstacles in the development of an effective drug delivery system (DDS) for various routes¹. Approximately, more than 40% of the marketed drugs are poorly water-soluble and the percentage is about 60% among the upcoming new molecular entities (NMEs) synthesized annually by pharmaceutical companies²⁻⁴. Poorly soluble drugs result in suboptimal dosing and subject to poor bioavailability and decreased therapeutic responses which make their formulation difficult or even impossible⁵. Hence, it is a challenge for researchers in both industry and academia to develop a DDS for the effective delivery of poorly water-soluble drugs without compromising safety and therapeutic efficacy.

Various strategies have been applied to deal with the poor aqueous solubility including chemical modification, particle size reduction, inclusion complexation using cyclodextrin, use of lipid carriers, solid dispersion etc⁶⁻⁸. With the advances in technology, researchers are progressively turning to nanotechnology-based DDS to improve the solubility and bioavailability of hydrophobic drugs⁹.

Currently, available drug delivery strategies for hydrophobic drugs based on nanoparticle systems like liposomes, polymeric micelles, solid lipid dispersions, micro/nanoemulsion offers several advantages. The most featured benefits of these DDSs are low drug toxicity, enhanced bioavailability, ease of administration through various routes, and higher biocompatibility¹⁰. These nanoparticle DDSs are suitable for a wide variety of drug entities including proteins and genetic materials. Particle

size in the nanoscale range leads to a significant increase in surface area to volume ratio along with increased saturation solubility, dissolution velocity, and further improved bioavailability^{3,11,12}. Recent developments in hydrophobic drug delivery systems include the use of hydrogels and organogels to encapsulate the drug substance within the three-dimensional network. Although hydrogels are limited to hydrophilic drug delivery, incorporation of hydrophobic moieties or micelles into the hydrogel has been studied for poorly water-soluble drug delivery¹³. On the other hand, organogels exert higher encapsulation of hydrophobic drugs but require further study to ensure their biocompatibility and stability.

Despite a number of advantages, hydrophobic drug delivery through nanoparticle-based DDSs has certain limitations. Firstly, nanoparticles are subject to instability by frequent cluster formation as the surface area to volume ratio and surface energy increase with a subsequent decrease in particle diameter to the nanoscale. Particle aggregation and flocculation also result from thermodynamic instability of nanoparticles and result in increased diameter of the particle with a wide size distribution. Nanoemulsions face such problems that need to be stored at a lower temperature to achieve better stability for a finite time^{14,15}. Secondly, the existing drug delivery causes immediate release of encapsulated drugs owing to their large surface area and has limited drug encapsulation efficiency. The use of polymers has been found effective in controlled drug release but their untimely elimination from the circulating blood is a major drawback^{15,16}. Thirdly, biocompatibility and targeted drug delivery are inevitable for a drug carrier. Concerns over cytotoxicity and in vivo toxicity have impeded the use of some nanoparticles and may result in both acute toxicity and long-term toxicity^{17,18}. Lastly, nanoparticle fabrication methods are both

times and cost-consuming and only suitable for the lab-scale synthesis of nanoparticles¹⁹.

1.2 Aim of the study

In light of these developments and limitations, the current research aims to develop an organogel based dispersion as a safe and effective carrier for hydrophobic drugs. The main target of this research is to design a nanotechnology-based DDS that will deliver poorly water-soluble drugs with high bioavailability, stability and will be applicable for the treatment of different diseases and various routes of administration. The primary objectives of this research are listed below-

- ✓ Design and fabrication of an organogel based emulsified system as a novel drug delivery system for poorly water-soluble drugs.
- ✓ Characterization of gel-in-water nanoemulsion as a drug delivery system.
- ✓ Encapsulation of a hydrophobic anticancer drug (Paclitaxel) in the core phase of nanodispersion and evaluate their application for chemotherapeutic agents.
- ✓ Administration of nanogel dispersion as a drug carrier via parenteral, transdermal, and ocular routes to evaluate possible therapeutic efficacy.

1.3 Originality of the study

Beyond several advantages of currently available nanoparticles, only a few nanoparticles are commercially available to deliver hydrophobic drugs. Nanoparticle-based DDSs especially nanoemulsions offer several advantages like increased absorption, higher bioavailability of poorly soluble drugs. But they are prone to

instability as the particles tend to agglomerate readily owing to their nanometric size. Similarly, burst release of drug and non-specific localization owing to the smaller size of <100 nm is of major concern in the development of a drug delivery system¹⁷. However, nanogels were found effective to overcome such problems of emulsion system in some instances as they comprise sustained drug release with active drug targeting properties. Nanogels are mainly hydrogel-based polymeric nanoparticles and have a higher drug loading capacity. But adverse effects from surfactants or monomers used in nanogel, possible interaction between drug and polymer leading to collapsed nanogel structure and limited use of nanogels in hydrophobic drug delivery^{20,21}.

Previous research showed the use of organogels to improve the bioavailability of hydrophobic drugs along with a controlled drug release. Organogels are biocompatible and biodegradable and have great potential in the pharmaceutical field particularly for lipophilic drugs^{22,23}. At the same time, iodinated oil lipiodol was widely used in the embolization of hepatocellular carcinoma (HCC) for its drug delivery and tumor-seeking performance along with its ability to induce transient embolization in tumors microcirculation²⁴⁻²⁶.

Considering the findings from previous studies, the current study relies on the development of a nanogel dispersion for lipophilic drug delivery. It is expected that the designed nanogel dispersion will sustain the drug release, ensure enhanced permeability and retention (EPR) of nanoparticles on the tumor site and improve the stability of nanoemulsion.

The use of lipiodol as an organic solvent will facilitate site-specific drug action, particularly for anticancer drugs. A cross-linked network of organogel will ensure

high drug loading efficiency and sustained drug release by diffusion and/or erosion. Additionally, scale-up of nanogel dispersion will be possible owing to the use of ultrasonication for homogenization. We believe that our organogel nanodispersion will be a novel approach in the field of pharmaceutical research with its unique features and will defeat current limitations.

1.4 Thesis outline

This thesis consists of 7 chapters. The chapters are arranged to achieve the basic objectives of this study. A glimpse of the work content of each chapter is given below-

Chapter 1: The first chapter of the thesis discusses the background and objective of this research. This chapter also highlights the novelty of this study and how this study was useful over currently available drug delivery systems.

Chapter 2: This chapter provides a comprehensive review of drug delivery systems. It also focuses on the use of organogel in drug delivery systems, application of organogel for transdermal, oral, parenteral, and ocular preparations, challenges with the use of organogel.

Chapter 3: In this chapter, a gel-in-water nanoemulsion was developed by optimization of oil-water volume ratio, surfactant, and gelling agent concentration. Characterization of nanoparticles was performed in this chapter in terms of particle size analysis, surface charge determination, pH to evaluate the feasibility of nanogel dispersion as a drug delivery system. Rheological analysis of nanoparticles was performed to confirm the gel formation in the inner core phase. Also, a stability study

was performed for six months at different storage conditions to assess the stability of nanoparticles and compared with the conventional oil-in-water nanoemulsion.

Chapter 4: Chapter 4 describes the applicability of gel-in-water nanoemulsion determined by in vitro and in vivo experiments. In vitro biocompatibility study of nanogel emulsion to primary rat hepatocytes was explained by different experiments including mitochondrial activity, albumin synthesis rate, and liver-specific function (CYP1A1) evaluation. In vitro cytotoxicity of Paclitaxel-loaded gel-in-water nanoemulsion was examined using skin cancer cell line (B16F10) along with an in vivo antitumor efficacy study after subcutaneous injection to tumor-bearing ICR mouse. Besides, in vitro cellular uptake of nanoparticles by B16F10 cells suggests the possible drug transfer capacity of nanogel particles inside the cytoplasm.

Chapter 5: This chapter mainly focuses on the potential application of gel-in-water nanoemulsion for the intravenous delivery of lipophilic anticancer drugs. Immunodeficient mice models (SCID mice) were used to develop ectopic tumors using humanized lung cancer cells (A549) followed by intravenous administration of paclitaxel-loaded gel-in-water nanoemulsion via the tail vein to assess the antitumor efficacy. Cytotoxicity of paclitaxel-loaded gel-in-water nanoemulsion to A549 cells was also evaluated in vitro. Besides, in vitro biocompatibility of nanoparticles to mice fibroblast (L929) and primary hepatocytes were also evaluated along with kinetic evaluation of paclitaxel release mechanism from nanoparticles using the Korsmeyer-Peppas model and Higuchi model.

Chapter 6: In chapter six, an attempt was made to develop an organogel based nanodispersion using beeswax as an organogelator for topical delivery of hydrophobic drugs in the posterior segment of the eye. Experiment results on formulation

Chapter 1: Overview of thesis

development and characterization of nanoparticles, in vitro biocompatibility study along with in vivo biocompatibility evaluation by ocular irritation test, were described in this chapter. In vivo corneal permeability of gel-in-water nanoemulsion as an eye drop was assessed in the ICR mouse model to determine the feasibility of organogel nanodispersion for ocular drug delivery.

Chapter 7: Finally, chapter 7 concludes with a summary of key findings in this thesis and future studies that can be embraced for further expansion of the current study.

An illustration of this thesis was given in figure 1-1 to explain the thesis structure at a glance.

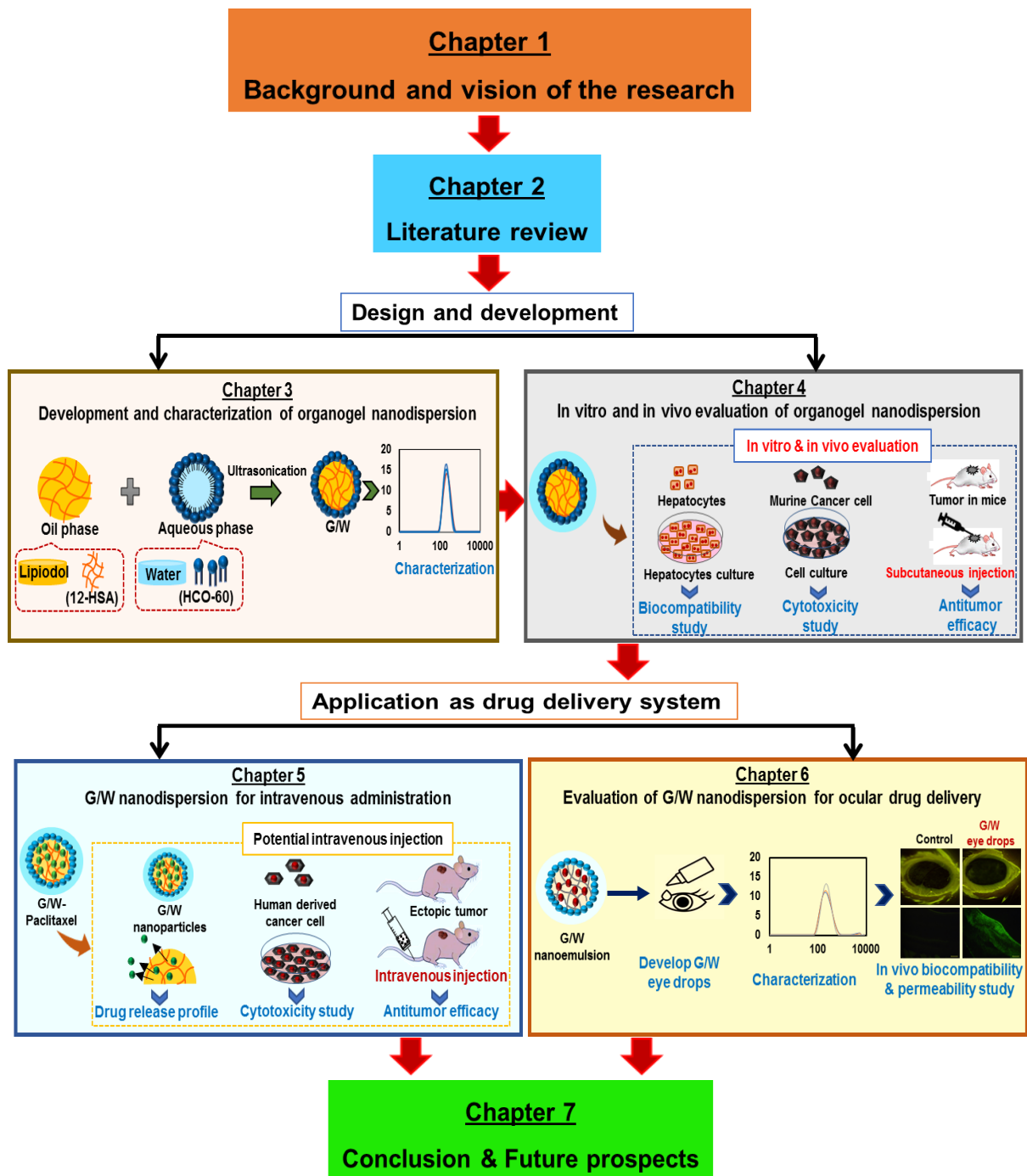


Figure 1-1: Schematic outline of the thesis.

1.5 Reference

1. Warnken Z, Smyth HDC, Williams RO. Route-specific challenges in the delivery of poorly water-soluble drugs. In: *AAPS Advances in the Pharmaceutical Sciences Series*. Vol 22. ; 2016:1-39. doi:10.1007/978-3-319-42609-9_1
2. Fahr A, Liu X. Drug delivery strategies for poorly water-soluble drugs. *Expert Opinion on Drug Delivery*. 2007;4(4):403-416. doi:10.1517/17425247.4.4.403
3. Kalepu S, Nekkanti V. Improved delivery of poorly soluble compounds using nanoparticle technology: a review. *Drug Delivery and Translational Research*. 2016;6(3):319-332. doi:10.1007/s13346-016-0283-1
4. Christopher Vimalson D, Parimalakrishnan S, Jeganathan NS, Anbazhagan S. Techniques to enhance solubility of hydrophobic drugs: An overview. *Asian Journal of Pharmaceutics*. 2016;10(2):S67-S75.
5. Kalepu S, Nekkanti V. Insoluble drug delivery strategies: review of recent advances and business prospects. *Acta Pharmaceutica Sinica B*. 2015;5(5):442-453. doi:10.1016/j.apsb.2015.07.003
6. Merisko-Liversidge EM, Liversidge GG. Drug Nanoparticles: Formulating Poorly Water-Soluble Compounds. *Toxicologic Pathology*. 2008;36(1):43-48. doi:10.1177/0192623307310946
7. Junghanns JUAH, Müller RH. Nanocrystal technology, drug delivery and clinical applications. *International Journal of Nanomedicine*. 2008;3(3):295-309.
8. Mohammed AR, Weston N, Coombes AGA, Fitzgerald M, Perrie Y. Liposome

- formulation of poorly water soluble drugs: Optimisation of drug loading and ESEM analysis of stability. *International Journal of Pharmaceutics*. 2004;285(1-2):23-34. doi:10.1016/j.ijpharm.2004.07.010
9. Bheemidi VS. An Imperative Note on Novel Drug Delivery Systems. *Journal of Nanomedicine & Nanotechnology*. 2011;02(07). doi:10.4172/2157-7439.1000125
 10. Mitchell MJ, Billingsley MM, Haley RM, Wechsler ME, Peppas NA, Langer R. Engineering precision nanoparticles for drug delivery. *Nature Reviews Drug Discovery*. 2021;20(2):101-124. doi:10.1038/s41573-020-0090-8
 11. Jia L. Nanoparticle Formulation Increases Oral Bioavailability of Poorly Soluble Drugs: Approaches, Experimental Evidences and Theory. *Current Nanoscience*. 2005;1(3):237-243. doi:10.2174/157341305774642939
 12. Rizvi SAA, Saleh AM. Applications of nanoparticle systems in drug delivery technology. *Saudi Pharmaceutical Journal*. 2018;26(1):64-70. doi:10.1016/j.jsps.2017.10.012
 13. Larrañeta E, Stewart S, Ervine M, Al-Kasasbeh R, Donnelly R. Hydrogels for Hydrophobic Drug Delivery. Classification, Synthesis and Applications. *Journal of Functional Biomaterials*. 2018;9(1):13. doi:10.3390/jfb9010013
 14. Phan HT, Haes AJ. What Does Nanoparticle Stability Mean? *Journal of Physical Chemistry C*. 2019;123(27):16495-16507. doi:10.1021/acs.jpcc.9b00913
 15. Vasir JK, Labhasetwar V. Biodegradable nanoparticles for cytosolic delivery of therapeutics. *Advanced drug delivery reviews*. 2007;59(8):718-728. doi:10.1016/j.addr.2007.06.003

16. Alexis F, Pridgen E, Molnar LK, Farokhzad OC. Factors Affecting the Clearance and Biodistribution of Polymeric Nanoparticles. *Molecular Pharmaceutics*. 2008;5(4):505-515. doi:10.1021/mp800051m
17. Blanco E, Shen H, Ferrari M. Principles of nanoparticle design for overcoming biological barriers to drug delivery. *Nature Biotechnology*. 2015;33(9):941-951. doi:10.1038/nbt.3330
18. De Jong WH, Borm PJA. Drug delivery and nanoparticles: Applications and hazards. *International Journal of Nanomedicine*. 2008;3(2):133-149. doi:10.2147/ijn.s596
19. Dang Y, Guan J. Nanoparticle-based drug delivery systems for cancer therapy. *Smart Materials in Medicine*. 2020;1:10-19. doi:10.1016/j.smaim.2020.04.001
20. Sharma A, Garg T, Aman A, et al. Nanogel - An advanced drug delivery tool: Current and future. *Artificial Cells, Nanomedicine and Biotechnology*. 2016;44(1):165-177. doi:10.3109/21691401.2014.930745
21. Mishra N, Wani TU, Rashid M, Kumar M, Chaudhary S, Kumar P. Targeting Aspects of Nanogels: An Overview. *International Journal of Pharmaceutical Sciences and Nanotechnology*. 2014;7(4):2612-2630. doi:10.37285/ijpsn.2014.7.4.3
22. Martin B, Brouillet F, Franceschi S, Perez E. Evaluation of Organogel Nanoparticles as Drug Delivery System for Lipophilic Compounds. *AAPS PharmSciTech*. 2017;18(4):1261-1269. doi:10.1208/s12249-016-0587-y
23. Esposito CL, Kirilov P, Roullin VG. Organogels, promising drug delivery

systems: an update of state-of-the-art and recent applications. *Journal of controlled release: official journal of the Controlled Release Society*. 2018;271:1-20. doi:10.1016/j.jconrel.2017.12.019

24. Song JE, Kim DY. Conventional vs drug-eluting beads transarterial chemoembolization for hepatocellular carcinoma. *World Journal of Hepatology*. 2017;9(18):808. doi:10.4254/wjh.v9.i18.808
25. You Y, Wang Z, Ran H, et al. Nanoparticle-enhanced synergistic HIFU ablation and transarterial chemoembolization for efficient cancer therapy. *Nanoscale*. 2016;8(7):4324-4339. doi:10.1039/C5NR08292G
26. Idée J-M, Guiu B. Use of Lipiodol as a drug-delivery system for transcatheter arterial chemoembolization of hepatocellular carcinoma: A review. *Critical Reviews in Oncology/Hematology*. 2013;88(3):530-549. doi:10.1016/j.critrevonc.2013.07.003

Chapter 2: Literature Review

2.1 Drug delivery system

A drug delivery system (DDS) is defined as a formulation or device that transports a pharmaceutical substance throughout the body¹. It acts as an interface between the patient and the drug and is intended to exert the therapeutic efficacy of that drug². DDS ensures the safe and effective delivery of a drug in the body by selective release of drug to the target site without affecting the healthy cells or tissues³. Moreover, DDS helps to achieve optimum bioavailability of drug after administration, improves drug stability, reduces drug-associated side effects, improves patient compliance^{2,4}. However, the key purpose of DDS is to deliver the active ingredient in a regulated way, to a particular site, and to maintain the drug level in the body within the therapeutic window⁴.

To confirm the effective delivery of drug substance, several drug delivery systems has been studied for years. The most common DDSs are tablets, capsules, injectables, creams, ointments, suppositories, powders and so on⁵. The efficacy and potency of a drug largely depend on both the physicochemical properties of the drug the physiologic conditions of the patient^{6,7}. Among the different physicochemical properties of drugs, drug solubility is of major concern during the formulation^{8,9}. With the advances in technology, DDS is moving now towards the application of nanotechnology to overcome the barriers associated with the therapeutic benefits of a drug substance^{10,11}.

2.2 Classification of drug

The physical and chemical properties of the drug and its release from a dosage form along with the drug action are studied in biopharmaceutics¹². This branch of pharmaceutical science relates the in vitro characteristics of a DDS to the in vivo performance¹³. To predict the in vivo performance of drugs Amidon et al. and Lipinski et al. have been developed a qualitative model named Biopharmaceutics Classification System (BCS) based on drug substances solubility and permeability^{14,15}. According to BCS, drugs are classified into four groups¹⁶⁻¹⁹.

- i) Class I- High solubility-high permeability drugs: Drugs included in this class show higher absorption and lower excretion. But their bioavailability is limited owing to their rapid clearance by the first-pass metabolism. Paracetamol, Aspirin, Propranolol, Metoprolol, etc. are examples of Class I drugs.
- ii) Class II- Low solubility-high permeability drugs: Class II drugs have poor absorption than Class I drugs because of their lack of solubility. The bioavailability of these drug products is regulated by the solvation rate. Ibuprofen, Ketoprofen, Carbamazepine, Aceclofenac etc. drugs are included in this class.
- iii) Class III- High solubility-low permeability: A non-uniform drug absorption is observed for drugs of class III. Although the drug dissolves very fast, the bioavailability is limited by the intestinal permeation rate. Ranitidine, Acyclovir, Chloramphenicol, etc. are examples of Class III drugs.

iv) Class IV- Low solubility-low permeability drugs: Drugs of this class are more challenging to deliver via oral route owing to their poor absorption and often require an alternate route of administration. Hydrochlorothiazide, Ritonavir, and most of the chemotherapeutic agents e.g. Paclitaxel, Docetaxel, are members of this class.

2.3 Advances in drug delivery system

Conventional drug delivery systems i.e. tablets, capsules, liquids, injectables often cause systemic adverse effects due to their non-specific drug release, poor absorption, non-uniform distribution, higher dosage, and frequent administration²⁰⁻²³. Similarly, poorly water-soluble drugs are more challenging to deliver through traditional DDS and suffer from poor bioavailability issues followed by subtherapeutic activity^{24,25}. Research is moving towards the use of advanced technologies in order to overcome the limitations of conventional DDSs for the past few decades. The design and development of novel drug delivery systems are one of the fastest expanding segments in the field of pharmaceutical research²². Sustained drug delivery to the target site, enhanced bioavailability, and reduced side effects are the prime rationales for the advancement of novel drug delivery systems²⁶⁻²⁸.

Among the different types of novel drug delivery systems, nanocarrier-based DDS are emerging in recent days particularly for hydrophobic drugs that belong to Class IV. Liposomes, niosomes, self-emulsifying nanoparticles, nanoemulsions, polymeric nanoparticles, micelles, dendrimers, etc. are studied broadly as DDSs and offer several advantages compared to traditional DDSs^{29,30}.

2.4 Advantages and limitations of DDS

Nanoparticle-based novel drug delivery systems are widely investigated owing to their nanometric size followed leading to higher absorption and bioavailability along with safe and effective delivery of therapeutic agents to target cells³¹. Nanoparticles are applicable for both hydrophilic and hydrophobic drugs through various routes with high loading capacity for their tunable size, shape, and morphology^{29,31}. Different classes of nanoparticles with subclasses are shown in figure 2-1 and their characteristics are summarized in Table 2-1

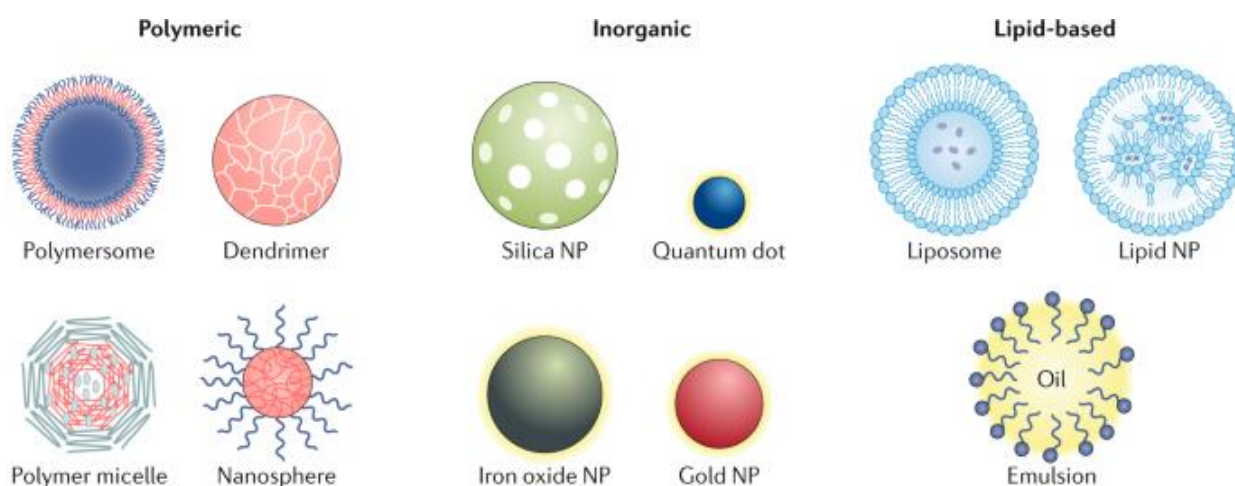


Figure 2-1: Classification of nanoparticles with most common subclasses. This image is extracted from Mitchell et al³² with permission.

Table 2-1: Advantages and limitations of currently available nanoparticles

Types of Nanoparticulate	Advantages	Limitations	Ref.
Polymeric nanoparticles or organic nanoparticles (Polymerosome, polymeric micelles, dendrimer, nanocapsules, nanospheres)	<ul style="list-style-type: none"> • Particle sizes range from 20-1000 nm. • Suitable for a wide variety of therapeutic agents including hydrophilic and hydrophobic drugs, proteins, genetic materials. • Drugs remain encapsulated in the inner core phase as dispersed or dissolved form. • Biodegradable, biocompatible, and stable during storage. 	<ul style="list-style-type: none"> • Increased risk of particle aggregation. • Requires surface modification to get targeted action. • Rapid elimination by lymphatic drainage and mononuclear phagocyte system (MPS) leads to subtherapeutic effects. • Inadequate toxicological data is available, only a few polymeric nanoparticles are approved by FDA. 	33-38
Inorganic nanoparticles (Silica nanoparticles, Gold nanoparticles, quantum dots, iron oxide nanoparticles)	<ul style="list-style-type: none"> • Particles are of 2-100 nm and successfully deliver both drugs and genes. • Inorganic materials e.g. gold, silica, iron are used to form the nanoparticle. • Can be engineered in a wide variety of size, shape, and structures. • Inorganic nanoparticles are uniquely qualified for applications such as diagnostics, imaging, and photothermal therapies due to their magnetic, radioactive, or plasmonic properties. • Have good biocompatibility and stability. • Localized and targeted delivery, magnetically or antibody-targeted nanoparticles to specific tissue/disease sites can be attained. 	<ul style="list-style-type: none"> • Limited in their clinical application by low solubility and toxicity concerns, especially in formulations using heavy metals. 	32,39-45
Lipid-based nanoparticles (Liposome, emulsion, niosomes, solid-lipid nanoparticles)	<ul style="list-style-type: none"> • Nanoparticle size ranges from 10-200 nm. • Non-toxic, higher bioavailability. • Have thermodynamic and thermokinetic stability. • Suitable for both hydrophilic and hydrophobic drugs. • Can be administered by various routes, e.g. oral, topical, parenteral, transdermal, and so on. 	<ul style="list-style-type: none"> • A higher amount of surfactant/ co-surfactant is required for stabilization. • Stability is affected by pH and temperature. • Burst release of the drug due to large surface area. • Nanoparticles are often susceptible to oxidation and Ostwald ripening. • Low drug loading capacity. 	46-49

2.5 Gels in DDS

Gels are semi-solid structures where a gelling agent immobilizes a solvent in an elastic or viscoelastic cross-linked network⁵⁰. Based on the immobilized solvent gels are mainly of two types, where hydrophilic solvents form hydrogel and organic solvents form the organogel⁵¹. Hydrogels are used extensively in DDS for their high biocompatibility, flexibility, higher swelling tendency, ease of fabrication in different shapes^{52,53}. However, hydrogels are not suitable for poorly water-soluble drugs for their limited drug loading capacity. Similarly, the high water content and large pore size of hydrogels lead to an immediate release of the drug. Clinical application of some hydrogels is restricted for their low tensile strength that causes rapid dissolution and clearance of the drug from the target site⁵⁴⁻⁵⁶.

In the last decade, research interest on organogels increased dramatically and the functionality of organogels has been studied widely for drug delivery^{50,51}. Previously the use of organogels in the pharmaceutical field was limited as most of the organic solvents used to form organogel were toxic. Research on the use of more biocompatible, biodegradable organic solvents and organogelators emerges the platform for their use in DDS that is proved both pharmaceutically acceptable and eco-friendly⁵⁷⁻⁵⁹.

2.6 Organogels in DDS

Organogels present fascinating advantages in DDS for their self-assembled micro/nanostructure and allows entrapping of a wide variety of drug substances, particularly hydrophobic drugs. Thermo-reversible properties of organogels along with their three-dimensional network have been explored to release the drug in a

controlled manner. At the same time, organogels could deliver drugs via various routes like transdermal, oral, ophthalmic, and parenteral administrations^{57,58}.

2.6.1 Organogels in transdermal drug delivery

Organogels represent a promising category of vehicles with excellent characteristics to deliver drugs into and beyond the skin layers by percutaneous or transdermal routes. Organogels are intrinsic in nature, lipophilic, non-irritating, and readily absorb via the lipophilic layers of skin. Hence, organogels have been largely developed and studied for the topical administration of pharmaceutical molecules in the treatment of various diseases e.g. neuropathy, hormone-dependent cancer, and diabetes⁶⁰⁻⁶².

2.6.2 Organogels for parenteral formulations

Organogels have gained attention in parenteral formulations mainly for their in situ gel formation characteristics⁶³. The sol-gel transition in the physiologic environment after injection prevents burst release of drug and presents a long-term sustained drug delivery with higher biocompatibility. Besides, organogels improve drug stability by preventing enzymatic degradation after parenteral administration. Studies showed that organogels successfully encapsulate various drugs like contraceptive drugs (levonorgestrel), drugs used in Alzheimer's disease (rivastigmine), chemotherapeutic agents (doxorubicin), and exert therapeutic efficacy along with sustained drug release⁶⁴⁻⁶⁶.

2.6.3 Organogels for oral administration

As the safest and convenient route of administration, organogels were designed to deliver both hydrophilic and hydrophobic drugs via the oral route. The main advantages of organogels are increased bioavailability of poorly water-soluble drugs and protection from degradation by gastric enzymes. Drug-loaded organogels result in sustained release of drugs with a significant increase in plasma concentration^{67,68}.

2.6.4 Organogels in ocular drug delivery

Ocular drug delivery is challenging owing to the complex anatomy of the eye and physiological ocular barriers. A wide range of hydrogel materials has been studied to date with various successes and efficiencies⁶⁹. However, hydrogels are limited for hydrophilic drug delivery and have low drug loading capacity and poor bioavailability to the posterior segment of the eyes⁷⁰. Organogels are promising materials to improve the long-term release of both hydrophilic and hydrophobic drugs, biocompatibility, and drug permeability through the ocular site. Owing to their sustained release profiles, organogels are emerging as new delivery systems which might broadly improve hydrophobic drug delivery to the anterior and posterior segment of the eye^{50,71}.

2.6.5 Limitations of organogels

Beyond several advantages of organogels in DDS, organogels represent some inconveniences that impair their pharmaceutical performances. The purity of the organogelator along with the choice of organic solvent is of major concern affecting

the gel network stability by physicochemical interactions. Organogels are subject to instability during storage due to syneresis and require special storage conditions^{72,73}.

2.7 Conclusion

Considering the above-mentioned advances and challenges in DDS, the current research aimed to develop an organogel based nanoemulsion as a safe and effective drug delivery system for poorly soluble drugs of class II and class IV.

To achieve such a target, both characteristics of a nanoemulsion and clinical efficacy of organogel based nanoemulsion as DDS were considered that is assumed as a prerequisite for an ideal DDS.

At first, a nanoemulsion of particle diameter in 200-300 nm will be developed using a biodegradable and biocompatible organogelator. Particles of 200-300 nm in diameter will provide enhanced permeability and retention (EPR) effect in the tumor, being small enough to pass through the tumor microcirculation and large enough to avoid rapid clearance by MPS or p-glycoprotein efflux and non-specific accumulation. The nanometric size range of nanoemulsion will be obtained by ultrasonication and considered to facilitate absorption of hydrophobic drugs along with higher encapsulation efficiency owing to their large surface area. 12-Hydroxystearic acid (12-HSA) was selected as an organogelator that can form gel even at a lower concentration and lipiodol as an organic solvent which is widely used for their tumor-seeking nature, transient embolization in tumor microcirculation, and high retention time. Emulsification by ultrasonication is a high-energy method that will help to overcome the large scale-up challenge with organogels.

Secondly, the stability of organogel nanoemulsion was considered prominently in this research as instability of nanoemulsion is a major concern. The size distribution will be maintained < 0.3 that will indicate a homogenous preparation with monodispersed nanogel droplets. Besides, a higher surface charge of nanoparticles will prevent coagulation and flocculation of nanogel droplets followed by enhanced stability of nanoemulsion. The stability of nanogel droplets at different storage conditions is considered to be attained for the higher melting point of 12-HSA.

Thirdly, apart from the higher bioavailability and stability of the nanogel emulsion, another important matter to focus on is the biocompatibility of nanogel dispersion as a drug delivery system since organogels use in the pharmaceutical field is limited for their toxic interactions. A small amount of surfactant was used for emulsification in order to avoid cytotoxicity related to higher concentrations of surfactant and co-surfactant mixture used in conventional nanoemulsions. Although both the gelling agent and organic solvent used in this study are considered safe and biocompatible, we will evaluate the biocompatibility of nanoemulsion both *in vitro* and *in vivo*.

Finally, the efficacy of nanogel dispersion as a DDS for hydrophobic drugs in animal models will be evaluated. The applicability of developed organogel based nanoemulsion for different routes of administration, especially parenteral and ocular administration was assessed. Sustained drug delivery with site-specificity is believed to be achieved from this organogel based nanodispersion with minimal side effects associated with chemotherapeutic agents.

To the best of my knowledge, this is the first report on the development of organogel nanodispersion as a DDS for hydrophobic drugs using 12-HSA and lipiodol to form

the inner core phase. It is presumed that such valuable findings can overcome the challenges associated with nanoparticle-based drug delivery systems for the effective delivery of hydrophobic drugs.

2.8 Reference

1. Vega-Vásquez P, Mosier NS, Irudayaraj J. Nanoscale Drug Delivery Systems: From Medicine to Agriculture. *Frontiers in Bioengineering and Biotechnology*. 2020;8. doi:10.3389/fbioe.2020.00079
2. Jain KK. An Overview of Drug Delivery Systems. In: *Methods in Molecular Biology*. Vol 2059. ; 2020:1-54. doi:10.1007/978-1-4939-9798-5_1
3. Rojo J, Sousa-Herves A, Mascaraque A. Perspectives of Carbohydrates in Drug Discovery. In: *Comprehensive Medicinal Chemistry III*. Vol 1-8. ; 2017:577-610. doi:10.1016/B978-0-12-409547-2.12311-X
4. Coelho JF, Ferreira PC, Alves P, et al. Drug delivery systems: Advanced technologies potentially applicable in personalized treatments. *EPMA Journal*. 2010;1(1):164-209. doi:10.1007/s13167-010-0001-x
5. Nayak AK, Ahmad SA, Beg S, Ara TJ, Hasnain MS. Drug delivery: Present, past, and future of medicine. In: *Applications of Nanocomposite Materials in Drug Delivery*. ; 2018:255-282. doi:10.1016/B978-0-12-813741-3.00012-1
6. Maheshwari R, Sharma P, Seth A, Taneja N, Tekade M, Tekade RK. Drug Disposition Considerations in Pharmaceutical Product. In: *Dosage Form Design Considerations: Volume I*. ; 2018:337-369. doi:10.1016/B978-0-12-814423-7.00010-1
7. Lajiness MS, Vieth M, Erickson J. Molecular properties that influence oral drug-like behavior. *Current Opinion in Drug Discovery and Development*.

2004;7(4):470-477.

8. Savjani KT, Gajjar AK, Savjani JK. Drug Solubility: Importance and Enhancement Techniques. *ISRN Pharmaceutics*. 2012;2012:1-10. doi:10.5402/2012/195727
9. Tambosi G, Coelho PF, Luciano S, et al. Challenges to improve the biopharmaceutical properties of poorly water-soluble drugs and the application of the solid dispersion technology. *Matéria (Rio de Janeiro)*. 2018;23(4). doi:10.1590/s1517-707620180004.0558
10. Simonazzi A, Cid AG, Villegas M, Romero AI, Palma SD, Bermúdez JM. Nanotechnology applications in drug controlled release. In: *Drug Targeting and Stimuli Sensitive Drug Delivery Systems*. ; 2018:81-116. doi:10.1016/B978-0-12-813689-8.00003-3
11. Sun J, Yang Z, Teng L. Nanotechnology and Microtechnology in Drug Delivery Systems. *Dose-Response*. 2020;18(2):155932582090781. doi:10.1177/1559325820907810
12. Panchagnula R, Thomas NS. Biopharmaceutics and pharmacokinetics in drug research. *International Journal of Pharmaceutics*. 2000;201(2):131-150. doi:10.1016/S0378-5173(00)00344-6
13. Yang Y, Zhao Y, Duan JZ, Zhao P, Zhao L, Zhang X. Predictive biopharmaceutics and pharmacokinetics: Modeling and simulation. In: *Developing Solid Oral Dosage Forms: Pharmaceutical Theory and Practice: Second Edition*. ; 2017:399-413. doi:10.1016/B978-0-12-802447-8.00015-7

14. Amidon GL, Lennernäs H, Shah VP, Crison JR. A Theoretical Basis for a Biopharmaceutic Drug Classification: The Correlation of in Vitro Drug Product Dissolution and in Vivo Bioavailability. *Pharmaceutical Research: An Official Journal of the American Association of Pharmaceutical Scientists*. 1995;12(3):413-420. doi:10.1023/A:1016212804288
15. Lipinski CA, Lombardo F, Dominy BW, Feeney PJ. Experimental and computational approaches to estimate solubility and permeability in drug discovery and development settings. *Advanced Drug Delivery Reviews*. 2012;64(SUPPL.):4-17. doi:10.1016/j.addr.2012.09.019
16. Kumar S, Kaur R, Rajput R, Singh M. Bio pharmaceutics classification system (BCS) class IV drug nanoparticles: Quantum leap to improve their therapeutic index. *Advanced Pharmaceutical Bulletin*. 2018;8(4):617-625. doi:10.15171/apb.2018.070
17. Farah K, Syed MFH, Madiha M, et al. Comparative analysis of biopharmaceutic classification system (BCS) based biowaiver protocols to validate equivalence of a multisource product. *African Journal of Pharmacy and Pharmacology*. 2020;14(7):212-220. doi:10.5897/ajpp2020.5130
18. Charalabidis A, Sfouni M, Bergström C, Macheras P. The Biopharmaceutics Classification System (BCS) and the Biopharmaceutics Drug Disposition Classification System (BDDCS): Beyond guidelines. *International Journal of Pharmaceutics*. 2019;566:264-281. doi:10.1016/j.ijpharm.2019.05.041
19. Papich MG, Martinez MN. Applying Biopharmaceutical Classification System

- (BCS) Criteria to Predict Oral Absorption of Drugs in Dogs: Challenges and Pitfalls. *AAPS Journal*. 2015;17(4):948-964. doi:10.1208/s12248-015-9743-7
20. Liu D, Yang F, Xiong F, Gu N. The smart drug delivery system and its clinical potential. *Theranostics*. 2016;6(9):1306-1323. doi:10.7150/thno.14858
21. Khan R, Irchhaiya R. Niosomes: a potential tool for novel drug delivery. *Journal of Pharmaceutical Investigation*. 2016;46(3):195-204. doi:10.1007/s40005-016-0249-9
22. Bheemidi VS. An Imperative Note on Novel Drug Delivery Systems. *Journal of Nanomedicine & Nanotechnology*. 2011;02(07). doi:10.4172/2157-7439.1000125
23. Makadia MH a, Bhatt MAY, Parmar RB, Paun MJS, Tank HM. Self-nano Emulsifying Drug Delivery System (SNEDDS): Future Aspects. *Asian Journal Pharmaceutical Research*. 2013;3(1):21-27.
24. Laffleur F, Keckeis V. WITHDRAWN: Advances in drug delivery systems: Work in progress still needed? *International Journal of Pharmaceutics: X*. 2020;2:100050. doi:10.1016/j.ijpx.2020.100050
25. Bhagwat RR, Vaidhya IS. Novel Drug Delivery Systems: An Overview. *International Journal Of Pharmaceutical Sciences and Research*. 2013;4(3):970-982.
26. Akhtar N. Vesicles: A Recently Developed Novel Carrier for Enhanced Topical Drug Delivery. *Current Drug Delivery*. 2014;11(1):87-97.

doi:10.2174/15672018113106660064

27. Jain S, Jain V, Mahajan SC. Lipid Based Vesicular Drug Delivery Systems. *Advances in Pharmaceutics*. 2014;2014:1-12. doi:10.1155/2014/574673
28. Jain S, Patel N, Shah MK, Khatri P, Vora N. Recent Advances in Lipid-Based Vesicles and Particulate Carriers for Topical and Transdermal Application. *Journal of Pharmaceutical Sciences*. 2017;106(2):423-445. doi:10.1016/j.xphs.2016.10.001
29. Rizvi SAA, Saleh AM. Applications of nanoparticle systems in drug delivery technology. *Saudi Pharmaceutical Journal*. 2018;26(1):64-70. doi:10.1016/j.jsps.2017.10.012
30. Martinelli C, Pucci C, Ciofani G. Nanostructured carriers as innovative tools for cancer diagnosis and therapy. *APL Bioengineering*. 2019;3(1):011502. doi:10.1063/1.5079943
31. Cong H, Wang K, Zhou Z, et al. Tuning the Brightness and Photostability of Organic Dots for Multivalent Targeted Cancer Imaging and Surgery. *ACS Nano*. 2020;14(5):5887-5900. doi:10.1021/acsnano.0c01034
32. Mitchell MJ, Billingsley MM, Haley RM, Wechsler ME, Peppas NA, Langer R. Engineering precision nanoparticles for drug delivery. *Nature Reviews Drug Discovery*. 2021;20(2):101-124. doi:10.1038/s41573-020-0090-8
33. Thakor AS, Gambhir SS. Nanooncology: The future of cancer diagnosis and therapy. *CA: A Cancer Journal for Clinicians*. 2013;63(6):395-418.

doi:10.3322/caac.21199

34. Anselmo AC, Mitragotri S. Nanoparticles in the clinic: An update. *Bioengineering & Translational Medicine*. 2019;4(3). doi:10.1002/btm2.10143
35. Fenton OS, Olafson KN, Pillai PS, Mitchell MJ, Langer R. Advances in Biomaterials for Drug Delivery. *Advanced Materials*. 2018;30(29):1705328. doi:10.1002/adma.201705328
36. Liu X, Li C, Lv J, et al. Glucose and H₂O₂ Dual-Responsive Polymeric Micelles for the Self-Regulated Release of Insulin. *ACS Applied Bio Materials*. 2020;3(3):1598-1606. doi:10.1021/acsabm.9b01185
37. Valcourt DM, Dang MN, Scully MA, Day ES. Nanoparticle-Mediated Co-Delivery of Notch-1 Antibodies and ABT-737 as a Potent Treatment Strategy for Triple-Negative Breast Cancer. *ACS Nano*. 2020;14(3):3378-3388. doi:10.1021/acsnano.9b09263
38. Kahraman E, Güngör S, Özsoy Y. Potential enhancement and targeting strategies of polymeric and lipid-based nanocarriers in dermal drug delivery. *Therapeutic Delivery*. 2017;8(11):967-985. doi:10.4155/tde-2017-0075
39. Manshian BB, Jiménez J, Himmelreich U, Soenen SJ. Personalized medicine and follow-up of therapeutic delivery through exploitation of quantum dot toxicity. *Biomaterials*. 2017;127. doi:10.1016/j.biomaterials.2017.02.039
40. Xu C, Nam J, Hong H, Xu Y, Moon JJ. Positron emission tomography-guided photodynamic therapy with biodegradable mesoporous silica nanoparticles for

- personalized cancer immunotherapy. *ACS Nano*. 2019;13(10):12148-12161. doi:10.1021/acsnano.9b06691
41. Huang K-W, Hsu F-F, Qiu JT, et al. Highly efficient and tumor-selective nanoparticles for dual-targeted immunogene therapy against cancer. *Science Advances*. 2020;6(3):eaax5032. doi:10.1126/sciadv.aax5032
42. Arias L, Pessan J, Vieira A, Lima T, Delbem A, Monteiro D. Iron Oxide Nanoparticles for Biomedical Applications: A Perspective on Synthesis, Drugs, Antimicrobial Activity, and Toxicity. *Antibiotics*. 2018;7(2):46. doi:10.3390/antibiotics7020046
43. Yang W, Liang H, Ma S, Wang D, Huang J. Gold nanoparticle based photothermal therapy: Development and application for effective cancer treatment. *Sustainable Materials and Technologies*. 2019;22:e00109. doi:10.1016/j.susmat.2019.e00109
44. Pandey P, Dahiya M. A Brief Review on Inorganic Nanoparticles. *Journal of Critical Reviews*. 2016;3(3):18-26.
45. Khan I, Saeed K, Khan I. Nanoparticles: Properties, applications and toxicities. *Arabian Journal of Chemistry*. 2019;12(7):908-931. doi:10.1016/j.arabjc.2017.05.011
46. Ghasemiyeh P, Mohammadi-Samani S. Solid lipid nanoparticles and nanostructured lipid carriers as novel drug delivery systems: Applications, advantages and disadvantages. *Research in Pharmaceutical Sciences*. 2018;13(4):288-303. doi:10.4103/1735-5362.235156

47. Kesrevani RK, Sharma AK. Nanoarchitected Biomaterials: Present Status and Future Prospects in Drug Delivery. In: *Nanoarchitectonics for Smart Delivery and Drug Targeting*. ; 2016. doi:10.1016/B978-0-323-47347-7.00002-1
48. Maher PG, Roos YH, Fenelon MA. Physicochemical properties of spray dried nanoemulsions with varying final water and sugar contents. *Journal of Food Engineering*. 2014;126:113-119. doi:10.1016/j.jfoodeng.2013.11.001
49. Vasir JK, Labhasetwar V. Biodegradable nanoparticles for cytosolic delivery of therapeutics. *Advanced drug delivery reviews*. 2007;59(8):718-728. doi:10.1016/j.addr.2007.06.003
50. Esposito CL, Kirilov P, Roullin VG. Organogels, promising drug delivery systems: an update of state-of-the-art and recent applications. *Journal of controlled release: official journal of the Controlled Release Society*. 2018;271:1-20. doi:10.1016/j.jconrel.2017.12.019
51. Murdan S. Organogels in drug delivery. *Expert Opinion on Drug Delivery*. 2005;2(3):489-505. doi:10.1517/17425247.2.3.489
52. Jacob S, Nair AB, Shah J, Sreeharsha N, Gupta S, Shinu P. Emerging Role of Hydrogels in Drug Delivery Systems, Tissue Engineering and Wound Management. *Pharmaceutics*. 2021;13(3):357. doi:10.3390/pharmaceutics13030357
53. Ma X, Sun X, Hargrove D, et al. A Biocompatible and Biodegradable Protein Hydrogel with Green and Red Autofluorescence: Preparation, Characterization and In Vivo Biodegradation Tracking and Modeling. *Scientific Reports*.

2016;6(1):19370. doi:10.1038/srep19370

54. Hoare TR, Kohane DS. Hydrogels in drug delivery: Progress and challenges. *Polymer*. 2008;49(8):1993-2007. doi:10.1016/j.polymer.2008.01.027
55. Ghasemiyeh P, Mohammadi-Samani S. *Hydrogels as Drug Delivery Systems; Pros and Cons*. Vol 5.; 2019. doi:10.30476/TIPS.2019.81604.1002
56. Yin ZC, Wang YL, Wang K. A pH-responsive composite hydrogel beads based on agar and alginate for oral drug delivery. *Journal of Drug Delivery Science and Technology*. 2018;43:12-18. doi:10.1016/j.jddst.2017.09.009
57. Sahoo S, Kumar N, Bhattacharya C, et al. Organogels: Properties and applications in drug delivery. *Designed Monomers and Polymers*. 2011;14(2):95-108. doi:10.1163/138577211X555721
58. Vintiloiu A, Leroux JC. Organogels and their use in drug delivery - A review. *Journal of Controlled Release*. 2008;125(3):179-192. doi:10.1016/j.jconrel.2007.09.014
59. Rehman K, Zulfakar MH. Recent advances in gel technologies for topical and transdermal drug delivery. *Drug Development and Industrial Pharmacy*. 2014;40(4):433-440. doi:10.3109/03639045.2013.828219
60. Barton DL, Wos EJ, Qin R, et al. A double-blind, placebo-controlled trial of a topical treatment for chemotherapy-induced peripheral neuropathy: NCCTG trial N06CA. *Supportive Care in Cancer*. 2011;19(6):833-841. doi:10.1007/s00520-010-0911-0

61. Pandey M, Belgamwar V, Gattani S, Surana S, Tekade A. Pluronic lecithin organogel as a topical drug delivery system. *Drug Delivery*. 2010;17(1):38-47. doi:10.3109/10717540903508961
62. Kumar R, Katare OP. Lecithin organogels as a potential phospholipid-structured system for topical drug delivery: A review. *AAPS PharmSciTech*. 2005;6(2):E298-E310. doi:10.1208/pt060240
63. Wang D, Zhao J, Liu X, et al. Parenteral thermo-sensitive organogel for schizophrenia therapy, in vitro and in vivo evaluation. *European Journal of Pharmaceutical Sciences*. 2014;60:40-48. doi:10.1016/j.ejps.2014.04.020
64. Hu Y, Xu L, Zhou C, Wu H, Gao W. Intratumoral injectable in situ-forming low-molecular-weight organogels against subcutaneous tumor. *Nanomedicine: Nanotechnology, Biology and Medicine*. 2016;12(2):517. doi:10.1016/j.nano.2015.12.201
65. Vintiloiu A, Lafleur M, Bastiat G, Leroux JC. In situ-forming oleogel implant for rivastigmine delivery. *Pharmaceutical Research*. 2008;25(4):845-852. doi:10.1007/s11095-007-9384-3
66. Gao Z hui, Crowley WR, Shukla AJ, Johnson JR, Reger JF. Controlled Release of Contraceptive Steroids from Biodegradable and Injectable Gel Formulations: In Vivo Evaluation. *Pharmaceutical Research: An Official Journal of the American Association of Pharmaceutical Scientists*. 1995;12(6):864-868. doi:10.1023/A:1016261004230
67. Iwanaga K, Sumizawa T, Miyazaki M, Kakemi M. Characterization of

- organogel as a novel oral controlled release formulation for lipophilic compounds. *International Journal of Pharmaceutics*. 2010;388(1-2):123-128. doi:10.1016/j.ijpharm.2009.12.045
68. Iwanaga K, Kawai M, Miyazaki M, Kakemi M. Application of organogels as oral controlled release formulations of hydrophilic drugs. *International Journal of Pharmaceutics*. 2012;436(1-2):869-872. doi:10.1016/j.ijpharm.2012.06.041
69. Maharjan P, Cho KH, Maharjan A, Shin MC, Moon C, Min KA. Pharmaceutical challenges and perspectives in developing ophthalmic drug formulations. *Journal of Pharmaceutical Investigation*. 2019;49(2):215-228. doi:10.1007/s40005-018-0404-6
70. Gulsen D, Chauhan A. Dispersion of microemulsion drops in HEMA hydrogel: A potential ophthalmic drug delivery vehicle. *International Journal of Pharmaceutics*. 2005;292(1-2):95-117. doi:10.1016/j.ijpharm.2004.11.033
71. Anand B, Pisal SS, Paradkar AR, Mahadik KR. Applications of Organogels in Pharmaceutics. *Journal of Scientific and Industrial Research*. 2001;60(4):311-318.
72. Bhasha SA, Khalid SA, Duraivel S, Bhowmik D, Kumar SKP. Recent Trends in Usage of Polymers in the Formulation of Dermatological Gels. *Indian Journal of Research in Pharmacy and Biotechnology*. 2013;1(2):2320-3471.
73. Jose J, Gopalan K. Organogels: A versatile drug delivery tool in pharmaceuticals. *Research Journal of Pharmacy and Technology*. 2018;11(3):1242-1246. doi:10.5958/0974-360X.2018.00231.7

Chapter 3: Innovation and development of an organogel based gel-in-water nanodispersion for hydrophobic drug delivery

3.1 Introduction

In the field of pharmaceutical research, the formulation of hydrophobic drugs is most challenging because of their poor water solubility¹. Different strategies like lipid-based delivery systems, nanoparticles, crystal engineering (nanocrystal technology, co-crystal technology), liquid-solid technology, self-emulsifying solid dispersions, and P-efflux inhibition strategies, nanoparticles, etc. have been used as novel drug delivery systems for hydrophobic drugs². Among the most investigated novel drug delivery systems, nanoparticle drug delivery system such as liposomes, polymeric micelles, polymeric nanoparticles and nanoemulsions (NE) has attracted much attention owing to their several advantages³. Because of their smaller particle size and higher surface-to-volume ratio, nanoparticles can improve the bioactivity of poorly water-soluble drugs⁴.

However, all of these drug delivery systems are not beyond limitations. For instance, liposomes are lipid-based spherical vesicles of about 200 nm and cause an immediate release of drugs for their large surface area and susceptible to oxidation⁵. Polymeric nanoparticles (20 – 1000 nm) have superiority over liposomes in terms of physical stability and controlled release. But these nanoparticles require surface treatment to escape rapid clearance from circulating blood by the mononuclear phagocyte system (MPS). Premature elimination of polymeric nanoparticles often leads to inadequate accumulation of particles in the target site for effective drug

release^{6, 7}. On the other hand, low structural stability in the bloodstream confined the use of polymeric micelles as an in vivo drug carrier. Polymeric micelles are prone to dissociation into the unimers upon administration, as they become diluted to a concentration below critical micelle concentration^{8,9}. Recently hydrogels are extensively studied for hydrophobic drug delivery owing to their high biocompatibility and slow drug release¹⁰. But hydrogel-based hydrophobic drug delivery represents inherent incompatibility because of limited drug loading in the gel matrix and unsuccessful drug release owing to poor aqueous solubility¹¹.

The use of organogels in nanoemulsion to enhance stability and to sustain drug release has been reported in recent days¹². Organogels have become a choice of research interest in drug delivery as organogelator molecules can entrap a large volume of organic solvent through their self-assembled fibrous structure¹³. Organogels are biocompatible and biodegradable, which can overcome the risk of toxic residual aggregation and assure sustained drug release owing to their remarkable three-dimensional nano/microstructure¹⁴. 12-Hydroxystearic acid (12-HSA) is one of the widely used low molecular weight organogelators (LMOG) and forms a three-dimensional gel structure through intermolecular forces, namely hydrogen bonding and π -interactions¹⁵. In situ gel formation of 12-HSA organogels in different organic solvents has been investigated in recent days for injectable drug delivery systems. 12-HSA is also known to increase the cellular uptake of nanoparticles owing to their gel structure¹⁶. All these characteristics make 12-HSA a suitable candidate for hydrophobic drug delivery.

3.2 Objectives

Considering all the benefits of lipiodol and organogels, the aim was to develop an emulsified system with nanogel droplets as a drug delivery system for hydrophobic drugs and termed as gel-in water (G/W) nanoemulsion. Biodegradable 12-HSA based organogels can encapsulate drugs within it and localized site-specific action was expected due to the tumor-seeking nature of lipiodol. Besides this, the sol-gel transition property of organogel molecules within the body system could ensure the sustained release of the drug along with better stability of G/W NE. Several experiments were performed to evaluate physicochemical properties of G/W nanoemulsion, to determine the optimum concentration of surfactant and gelling agent along with emulsion stability assessment. This drug delivery system could be a promising carrier for hydrophobic drugs with enhanced solubility and improved bioavailability.

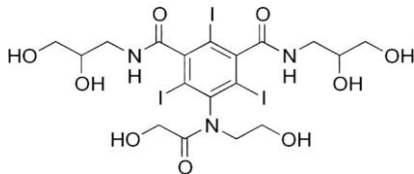
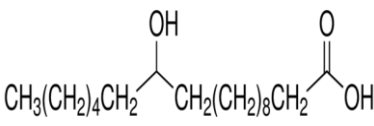
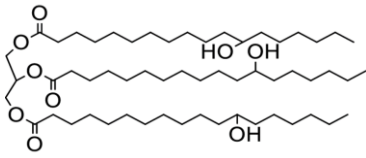
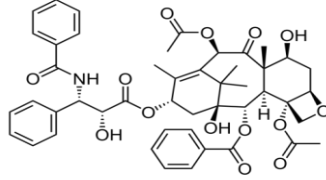
3.3 Materials and methods

3.3.1 Materials and their justification

12-Hydroxydstearic acid (12-HSA, Tokyo Chemical Industry Co., Ltd., Tokyo, Japan) of >80% purity was used as a gelling agent for the nanoemulsion. Iodinated oil lipiodol (Guerbet Japan Co., Ltd., Tokyo, Japan) serves as an organic solvent for organogelator and form the inner gel phase. The continuous phase was purified water (Arium 611VF, SARTORIUS Mechatronics Japan K.K., Tokyo, Japan) and contains the emulsifier polyoxyethylene hydrogenated castor oil (NIKKOL HCO-60, Nippon

Surfactant Industries Co., Ltd., Tokyo, Japan). HCO-60 is a non-ionic and hydrophilic surfactant with a hydrophilic-lipophilic balance (HLB) value of 14.0 and stabilizes the nanoemulsion by reducing the interfacial tension between the oil and water phase. As a hydrophobic model drug, paclitaxel of >98% purity (Tokyo Chemical Industry Co., Ltd., Tokyo, Japan) was used. All the materials used in NE preparation and related experiments were of analytical grade. Table 3-1 represents all the ingredients used in gel in water nanoemulsion formulation with their justification-

Table 3-1: List of ingredients for gel-in-water nanoemulsion

Ingredients name	Chemical Structure	Justification
Lipiodol		Organic solvent
12-Hydroxystearic acid (12-HSA)		Gelling agent
Polyoxyethylene hydrogenated castor oil-60 (HCO-60)		Emulsifying agent
Paclitaxel		Hydrophobic drug

3.3.2 Methods

3.3.2.1 *Preformulation study*

A suitable concentration of surfactant and gelling agent with optimum volumes of oil and water are required for stable NE formulation. Oil and water at volume ratios of 1:4, 1:7, 1:10, 1:20 and 1:40 were used to obtain nanosized particles. Similarly, surfactant at a concentration range of 12.5–200.0 mg/mL in water was used to develop a G/W NE formulation with desired particle size and distribution. For the gelling agent, a concentration range of 4%–12% (w/w in oil) was used. A stable G/W NE formulation was developed with an optimum concentration of each ingredient. Particle size analysis was performed by dynamic light scattering (DLS) (Malvern Zetasizer NanoZS™, Software Version 7.04; Malvern Panalytical, Tokyo, Japan).

3.3.2.2 *Formulation of gel-in-water nanoemulsion*

Various preparation conditions for NEs and paclitaxel-loaded NEs were investigated^{17,18}. Briefly, the oil phase was made by dissolving predetermined amounts of 12-HSA in lipiodol at 80 °C for 5 min in a water bath (EYELA PRO THERMO SHAKER NTS-2100, Tokyo, Japan) with continuous shaking at 100 rpm. The same experimental condition was maintained to make the aqueous phase containing HCO-60 as a surfactant in a separate tube. The oil phase was then added to the water phase, followed by emulsification through ultrasonication (BRANSON SONIFIER 250, Branson Ultrasonics Co., Danbury, USA) for 20 minutes with continuous running (1 pulse/sec) and 70% power amplitude. The temperature was maintained at 80 °C during

emulsification using a water bath (AS ONE THERMAX TM-1A, Osaka, Japan). The NE was then cooled down gradually to room temperature to form nanogel droplets. To prepare paclitaxel-loaded NEs, paclitaxel was first dissolved in lipiodol at a concentration of 2 mg/mL and centrifuged (Centrifuge Microtec 1524 R; Eppendorf, ASTEC Co., Ltd., Fukuoka, Japan) at 10000 rpm ($6160 \times g$) for 3 min to precipitate undissolved paclitaxel. The supernatant is then added to the predetermined amount of 12-HSA to form the oil phase. The rest of the method was the same as the NE preparation.

3.3.2.3 Qualitative analysis of gel-in-water nanoemulsion

(a) Measurement of particle size and zeta potential

The average particle size, its distribution (characterized by PDI), and zeta potential of the NE were measured by dynamic light scattering (DLS) using a laser scattering particle analyzer (Malvern Zetasizer NanoZS™). The measurement was performed at 20 °C and a scattering angle of 173°. G/W NE was diluted 600 times and 10 times with purified water before measurement of particle size and zeta potential, respectively.

(b) Morphology of G/W nanoemulsion

The morphology of nanoparticles was observed by using both fluorescent microscope and transmission electron microscopy (TEM). Samples for TEM images were prepared by dilution of G/W NE (100 times) and 5 μ l was placed on a carbon-coated copper grid, dried at 25 °C for 10 min, vacuumed for 48 hours, and finally observed under TEM at 120 kV (TEM, JEOL, JEM-2100). Similarly, for fluorescent imaging, G/W NE containing a fluorescent dye

Coumarin-6 (Tokyo Chemical Industry Co., Ltd., Tokyo, Japan) was diluted in the same manner (100 times) and 5 μ l of the sample was placed in a glass slide and observed under the microscope (Inverted Microscope, IX71 Olympus Corporation, Tokyo, Japan).

(c) Determination of pH

The pH value of the NEs was measured using a calibrated pH meter (Sartorius Mechatronics Japan K.K., Tokyo, Japan) at 25 ± 1 °C. As paclitaxel injection was reconstituted with 0.9% saline or 5% dextrose solution before administration to ensure isotonicity within the body system¹⁹, changes in the pH of G/W NE after dilution was also checked. Hence, samples were appropriately diluted (600 folds) with the continuous phase, i.e., water. We also checked changes in the pH of NE with the same dilution factor in the case of phosphate-buffered saline (PBS) of pH 7.4, 0.9% saline, and 5% dextrose solution. Three measurements were performed for each condition.

(d) Rheological property evaluation

The rheological property of G/W NE was measured using a rheometer (Modular Compact Rheometer: MCR 302; Anton Paar Japan KK, Tokyo, Japan) according to the method described by M. Luo et. al²⁰. The prepared NE (4 mL) was centrifuged at 15,000 rpm for 30 min to separate the continuous phase. The supernatant was removed and the solid residue was placed between the parallel plates of 25 mm diameter with a set gap of 100 μ m. The thermal sensitivity of the nanoemulsion was determined by observing the values of storage modulus (G') and loss modulus (G'') at 37°C and 70°C by keeping the strain and frequency constant at 1% and 1 Hz, respectively.

(e) Determination of encapsulation efficiency (EE)

To evaluate the encapsulation efficiency (EE) of G/W NE, 1 mL of NE was centrifuged at 15,000 rpm for 30 min at 20°C (Centrifuge Microtec 1524 R; Eppendorf, ASTEC Co., Ltd., Fukuoka, Japan). Free paclitaxel content was determined by measuring the non-incorporated drug present in a clear supernatant obtained through the separation of the aqueous phase. To establish the linearity of the proposed method, a calibration curve was constructed at six concentration levels within the range of 1–20 µg/ mL. These paclitaxel standard solutions were prepared using ethanol/PBS (3:7) as a solvent. Least square regression analysis was performed for the paclitaxel standard solutions absorbance data ($y = 0.034x + 0.006$, $R^2 = 0.996$). Beer's law was obeyed in all spectrophotometric analyses. Paclitaxel concentration in this solvent system was determined by using a UV/VIS spectrophotometer (UV-2500 PC; SHIMADZU, Japan) with detection at 230 nm. The EE percentage (EE%) of paclitaxel into NEs was calculated using equation (1)^{21,22} –

$$EE\% = \frac{(Total\ drug\ added - Non\ incorporated\ drug)}{Total\ drug\ added} \times 100 \quad (1)$$

3.3.2.4 Stability study

The physical stability of the G/W NE was determined through the analysis of particle size, PDI, zeta potential, and pH. The NEs were stored at the following three different temperatures: 4°C, 25°C, and 37°C for 6 months, and samples were subsequently tested at different time intervals. A similar stability study was performed for oil-in-water (O/W) NEs for comparison.

3.3.2.5 Statistical analysis

All test results are presented as mean \pm standard deviation. A significant difference between the two groups was analyzed using the two-tailed Student's *t*-test. A *p*-value of < 0.05 was considered statistically significant.

3.4 Results and discussion

3.4.1 Preformulation study

The particle size and PDI of G/W NE at different oil-to-water volume ratios, surfactant concentrations, and gelling agent concentrations are shown in Figure 3-1. At the oil-to-water ratio of 1:7, the particle size was in the nanoscale range (200–300 nm in diameter), with narrow size distribution (PDI < 0.2) (Figure 3-1(A)). It appeared that the diameter of NE decreased as the aqueous phase volume increased. In contrast, a slight increase in PDI value was observed with a 20% to 40% increase in water volume. These findings may be explained by changes in the viscosity of the emulsion formed during processing. Generally, the use of an emulsifier reduces particle size via a reduction of interfacial tension, followed by an increase in emulsion viscosity. Such an increase in viscosity causes high viscous resistance against the shear force during the formation of nanodroplets²³. In this study, ultrasonication was applied as external energy to form nanoemulsion. When the volume of the aqueous phase increases, but the amount of emulsifier and the applied force is kept constant, the same amount of energy has to distribute in a large volume during

emulsification. This leads to less droplet breakdown and consequently increases PDI value.

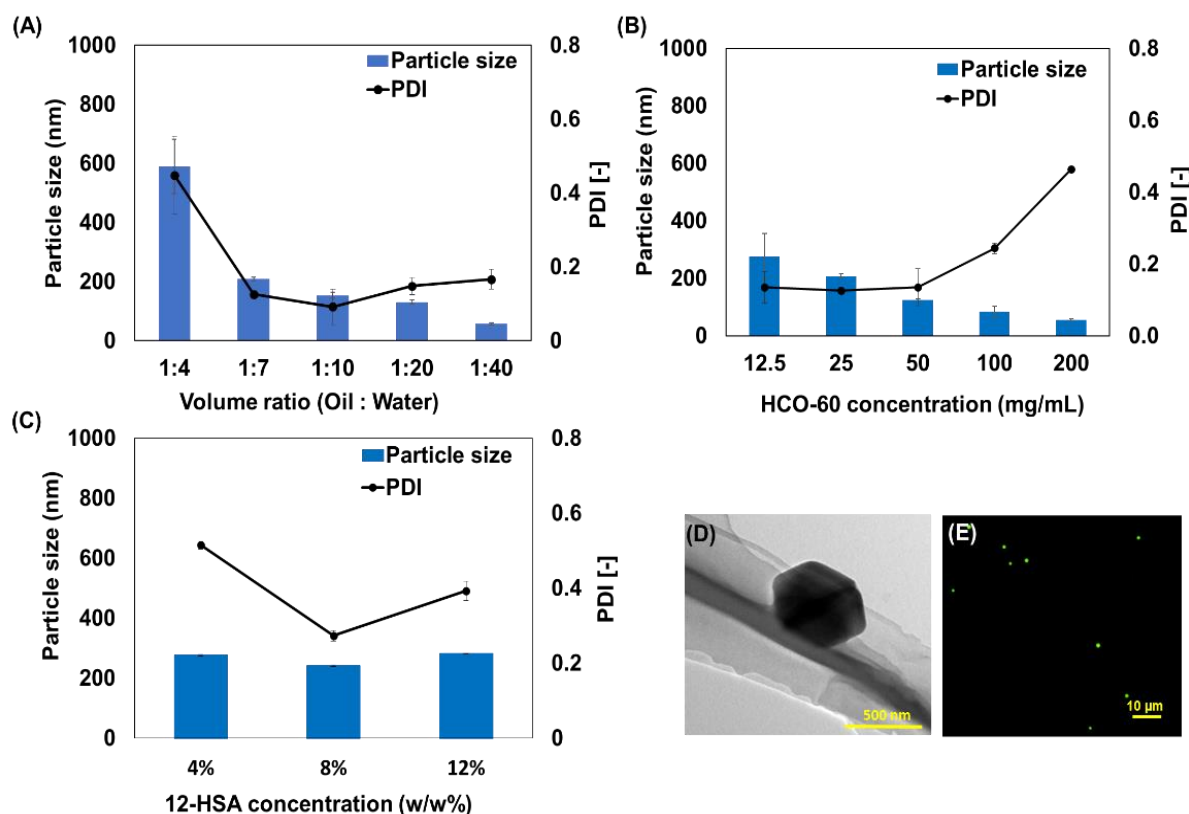


Figure 3-1: Changes in the particle size and PDI of G/W nanoemulsion with the increasing volume of water and concentration of surfactant and organogelator, (A) oil-to-water volume ratio; (B) HCO-60 concentration; (C) 12-HSA concentration; (D) TEM micrograph of G/W nanoparticle; (E) fluorescent image of G/W nanoemulsion.

In case of surfactant concentration, the optimum particle size (200–300 nm) with narrow distribution ($PDI = < 0.2$) was obtained with 25 mg/mL of HCO-60 (Figure 3-1(B)). It was found that particle size decreased as surfactant concentration increased, which might result from a large oil-water interface²⁴. Typically, surfactants adsorb on droplet surfaces, decrease the interfacial

tension between continuous and dispersed phases and thereby minimize the particle size. Hence, a greater amount of surfactant is needed to obtain a smaller particle size and to avoid instability of nanoemulsion by aggregation and coalescence²⁵.

However, a higher amount of surfactant increases the PDI value of nanoemulsion as it depends on surfactant dynamic property and is affected by the kinetics of surface adsorption²⁶. Our results also showed an increase in droplet size distribution (PDI > 0.3) at a higher concentration (200 mg/mL) of HCO-60 and limit the stability of G/W NE.

The effect of gelling agent concentration on particle size and its distribution is shown in Figures 3-1(C). The LMOG (12-HSA) forms the organogel owing to the intermolecular interactions i.e., H-bond and van der Waals bond, between organogelator molecules and the solvent. These intermolecular forces increase with the increase in 12-HSA concentration and form a strong gel that requires higher force for the gel breakdown^{27,28}. This may be a possible reason for an increase in the PDI of G/W NE when the concentration of 12-HSA increased to 12% (w/w).

The morphology and size of organogel nanoparticles in G/W NE were observed by fluorescent microscope and TEM (Figure 3-1(D) & (E)). The images showed nanosize of particles (~200 nm) and that was similar to DLS measurement.

3.4.2 Qualitative analysis of gel-in-water nanoemulsion

3.4.2.1 Particle size, zeta potential, encapsulation efficiency and pH

The results of particle size and its distribution, zeta potential, EE%, and pH of G/W NE are presented in Table 3-2. The results showed that our G/W NE has a nanosized particle of about 210 nm with narrow size distribution (PDI = 0.1). The zeta potential of prepared G/W NE was ≈ -25 mV and has a high drug loading efficiency of about 97%. The cross-linked gel structure of organogel may result in a high drug loading capacity of G/W nanoparticles. The pH of prepared NE was acidic (pH = 4) initially while pH became less acidic (5.5 - 7.4) upon dilution with different solvents. Similarly, no significant change was found in any of these parameters in the presence of the hydrophobic drug-Paclitaxel.

Figure 3-2(A) shows the narrow size distribution of nanogel droplets with a diameter of <250 nm. Researchers suggest that particle size plays an important role in drug distribution and excretion along with its biocompatibility. It is also responsible for the enhanced permeability and retention (EPR) effect upon administration within the physiological system²⁹. Nanocarriers with small particle sizes show increased drug accumulation in tumor cells because of the EPR effect³⁰. Given that the size of nanoparticles in our study was maintained at <250 nm, therefore drug accumulation in tumor cells was expected to be relatively high. Moreover, these nanodroplets cannot penetrate through the tight junction of endothelial cells in healthy tissues owing to their large size. Therefore, therapeutic action can be achieved with minimum side effects through this drug delivery system.

Table 3-2: Physicochemical properties of G/W nanoemulsion.

G/W NE	Particle size (nm)	Polydispersity index (PDI)	Zeta potential (ζ) (mV)	Encapsulation efficiency (EE%)	pH			
					Water	PBS	0.9% saline	5% Dextrose
Drug free NE	206 \pm 2.0	0.1 \pm 0.01	-25.2 \pm 1.0	-	5.9 \pm 0.02	7.4 \pm 0.01	6.02 \pm 0.02	6.4 \pm 0.01
Drug-loaded NE	210 \pm 2.0	0.1 \pm 0.02	-23.9 \pm 1.0	96.8 \pm 1.0	5.5 \pm 0.01	7.2 \pm 0.02	6.07 \pm 0.02	6.5 \pm 0.03

Safe and effective delivery of nanoparticles to target tissue largely depends on their physicochemical properties including particle size distribution. Particle size distribution is expressed by polydispersity index (PDI) which describes the degree of non-uniformity of the size distribution of particles. Nanoparticles should be monodispersed with a PDI value of 0.3 or below for being stable and efficient³¹. In this study, G/W NE has a lower PDI value (<0.3) that indicates monodisperse size distribution.

Zeta potential is the surface charge of particles and a higher charge (> ± 30 mV) indicates better NE stability. However, the use of nonionic surfactants generates charged droplets owing to the impurities of H_3O^+ and OH^- ions. These surfactants also cause a negative charge of zeta potential in the case of acidic NE (pH 3–6) and vice versa³². Results showed that the zeta potential of G/W NE was about -25.0 mV (Figure 3-2(B)). Researchers have also suggested that when a high-molecular-mass emulsifier is used, zeta potential < ± 20 mV may also provide enough stability because of steric hindrance, which is in line with our results³³.

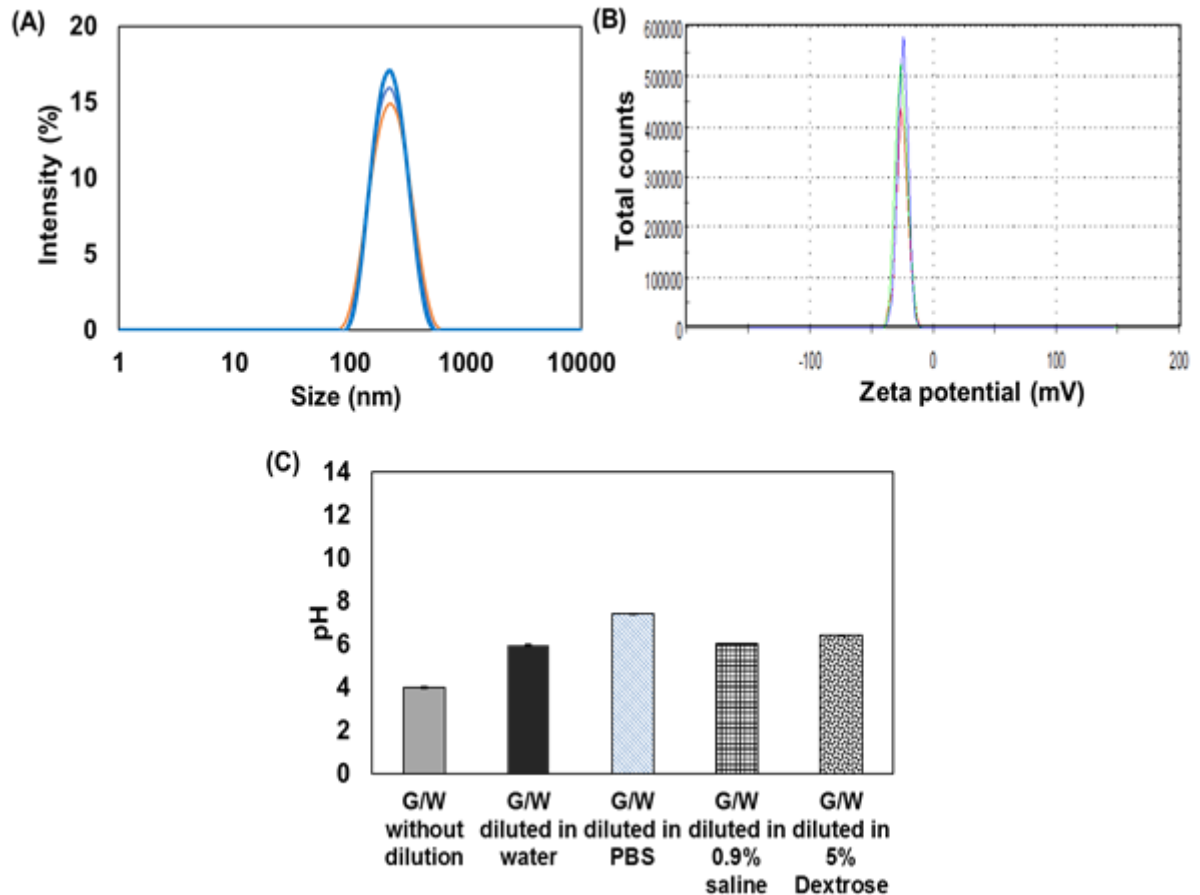


Figure 3-2: Characterization of G/W nanoemulsion by (A) particle size distribution, (B) zeta potential distribution and (C) pH of G/W nanoemulsion before and after dilution with water, PBS, 0.9% saline, 5% dextrose.

G/W nanoemulsion was found acidic with a pH of 4.0 which may result from the use of 12-HSA that contains 15-35% of fatty acid³⁴. Lipiodol with a high content of unsaturated fatty acid may also have an impact on the pH of G/W NE. On the other hand, the pH of G/W NE increased and ranging from 5.5 – 7.4 when diluted with different solvents namely PBS, water, 0.9% saline, and 5% dextrose (Figure 3-2(C)). The pH of G/W NE upon dilution is close to

blood pH and therefore assures the possible biocompatibility of this drug delivery system.

3.4.2.2 Rheological property evaluation

The results for rheological analysis are shown in Figures 3-3. As seen from the figure, storage modulus (G') and loss modulus (G'') of G/W nanoemulsion increased drastically upon decreasing the temperature from 70 °C to 37 °C, indicating the formation of gel³⁵. The changes in the viscoelastic behavior (G' , G'') of G/W nanoparticles were negligible at 50 °C compared to 37 °C (data not shown). In contrast, O/W rheological analysis showed no change in the values of G' and G'' upon lowering the temperature (data not shown), indicating that O/W has no thermal sensitivity.

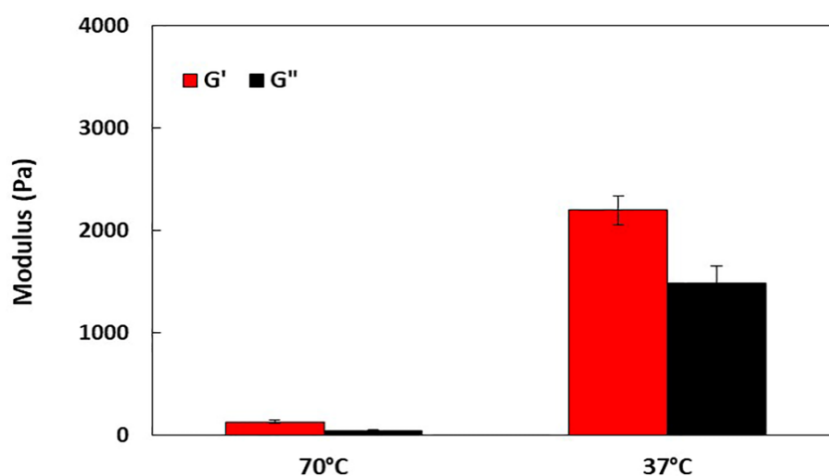


Figure 3-3: Thermal sensitivity of G/W nanoparticles.

3.4.3 Stability study

A 6-month long stability study of G/W NE was performed at different storage conditions and various parameters were observed during this period. The results are shown in Figures 3-4. The results of the stability study indicate that G/W NE remained stable over six months regardless of storage condition. The particle size of G/W NE was 202–260 nm during storage for up to 6 months and was not significantly affected by the storage temperature (Figure 3-4(A)). The same trend was observed for the size distribution. G/W NE was monodispersed during the storage period, with PDI values ranging from 0.099–0.200 (Figure 3-4(B)). The presence of a 12-HSA may be responsible for the long-term stability of G/W NE as the use of 12-HSA has been reported to improve nanoparticle stability³⁶.

On the contrary, the particle size of O/W NE was higher (> 300 nm) compared to the G/W NE and the diameter tends to increase with time. Similarly, O/W NE showed wide particle size distribution with $PDI > 0.3$ and varies with time and storage conditions. Both the particle size and polydispersity index of O/W NE showed variability at different temperatures and relatively increased with time. Besides the absence of 12-HSA, particle aggregation by Ostwald ripening may cause such instability of O/W NE. Ostwald ripening is proportionally dependent on PDI while inversely related to storage temperature. In polydispersed NE, nanodroplets tend to form larger droplets through the diffusion of smaller droplets into larger droplets as a result of concentration gradient³⁷. Our preparation also showed good stability in terms of pH and zeta potential, thereby showing no significant changes in both of these parameters over time (Figure 3-4(C) and 3-4(D)).

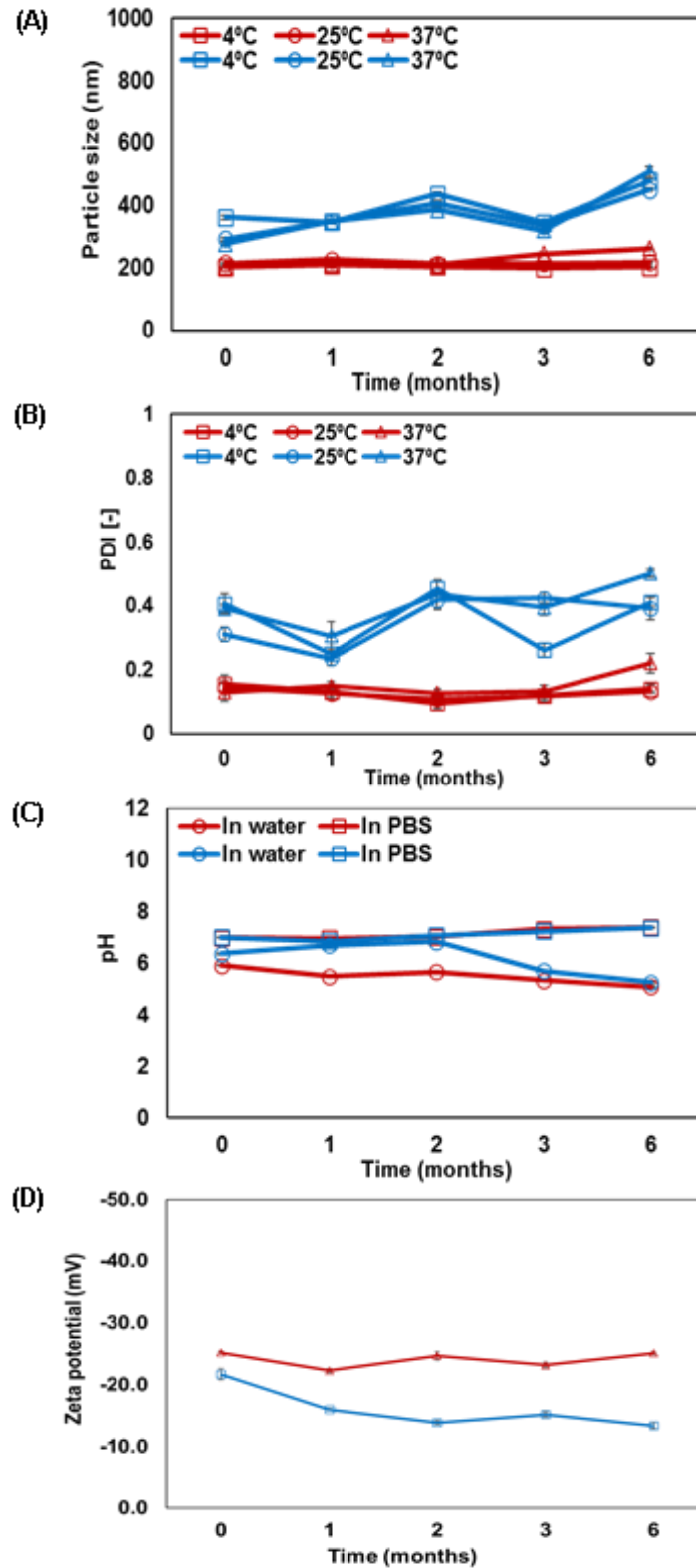


Figure 3-4: Comparative stability study of G/W NE and O/W NE, (A) particle size; (B) polydispersity index; (C) pH; (D) zeta potential, blue lines = O/W and red lines = G/W.

3.5 Conclusion

Organogel based nanoemulsion was developed with a mean diameter of ~200 nm and narrow size distribution. The higher negative surface charge of the nanogel droplets will help to resolve the stability issues that are a major challenge with nanoemulsions. The prepared G/W nanoemulsion showed stability over six months with no significant change in particle diameter, size distribution, zeta potential, and pH. Additionally, all the physicochemical properties of G/W nanoemulsion remained almost the same after the encapsulation of hydrophobic drugs. Moreover, the pH of G/W nanoemulsion is close to blood pH after dilution with saline and 5% dextrose solution suggesting the biocompatibility of this carrier within the body system. A higher encapsulation efficiency emerges the possibility of G/W nanoemulsion as an effective carrier for hydrophobic drugs.

3.6 Reference

1. Cui PF, Zhuang WR, Hu X, et al. A new strategy for hydrophobic drug delivery using a hydrophilic polymer equipped with stacking units. *Chemical Communications*. 2018;54(59):8218-8221. doi:10.1039/c8cc04363a
2. Ghadi R, Dand N. BCS class IV drugs: Highly notorious candidates for formulation development. *Journal of Controlled Release*. 2017;248:71-95. doi:10.1016/j.jconrel.2017.01.014
3. Qin C, Lv Y, Xu C, Li J, Yin L, He W. Lipid-bilayer-coated nanogels allow for sustained release and enhanced internalization. *International Journal of Pharmaceutics*. 2018;551(1-2):8-13. doi:10.1016/j.ijpharm.2018.09.008
4. Maher PG, Roos YH, Fenelon MA. Physicochemical properties of spray dried nanoemulsions with varying final water and sugar contents. *Journal of Food Engineering*. 2014;126:113-119. doi:10.1016/j.jfoodeng.2013.11.001
5. Vasir JK, Labhasetwar V. Biodegradable nanoparticles for cytosolic delivery of therapeutics. *Advanced drug delivery reviews*. 2007;59(8):718-728. doi:10.1016/j.addr.2007.06.003
6. Fam SY, Chee CF, Yong CY, Ho KL, Mariatulqabtiah AR, Tan WS. Stealth Coating of Nanoparticles in Drug-Delivery Systems. *Nanomaterials*. 2020;10(4):787. doi:10.3390/nano10040787
7. Alexis F, Pridgen E, Molnar LK, Farokhzad OC. Factors Affecting the Clearance and Biodistribution of Polymeric Nanoparticles. *Molecular*

Pharmaceutics. 2008;5(4):505-515. doi:10.1021/mp800051m

8. Cha E-J, Kim JE, Ahn C-H. Stabilized polymeric micelles by electrostatic interactions for drug delivery system. *European Journal of Pharmaceutical Sciences*. 2009;38(4):341-346. doi:10.1016/j.ejps.2009.08.006
9. Lu Y, Park K. Polymeric micelles and alternative nanonized delivery vehicles for poorly soluble drugs. *International Journal of Pharmaceutics*. 2013;453(1):198-214. doi:10.1016/j.ijpharm.2012.08.042
10. Gu D, O'Connor AJ, G.H. Qiao G, Ladewig K. Hydrogels with smart systems for delivery of hydrophobic drugs. *Expert Opinion on Drug Delivery*. 2017;14(7):879-895. doi:10.1080/17425247.2017.1245290
11. Hoare TR, Kohane DS. Hydrogels in drug delivery: Progress and challenges. *Polymer*. 2008;49(8):1993-2007. doi:10.1016/j.polymer.2008.01.027
12. Martin B, Brouillet F, Franceschi S, Perez E. Evaluation of Organogel Nanoparticles as Drug Delivery System for Lipophilic Compounds. *AAPS PharmSciTech*. 2017;18(4):1261-1269. doi:10.1208/s12249-016-0587-y
13. Murdan S. Organogels in drug delivery. *Expert Opinion on Drug Delivery*. 2005;2(3):489-505. doi:10.1517/17425247.2.3.489
14. Esposito CL, Kirilov P, Roullin VG. Organogels, promising drug delivery systems: an update of state-of-the-art and recent applications. *Journal of controlled release: official journal of the Controlled Release Society*. 2018;271:1-20. doi:10.1016/j.jconrel.2017.12.019

15. Chen W, Yang Y, Lee CH, Shen AQ. Confinement Effects on the Self-Assembly of 1,3:2,4-Di- p -methylbenzylidene Sorbitol Based Organogel. *Langmuir*. 2008;24(18):10432-10436. doi:10.1021/la801734x
16. Lv Y, Xu C, Zhao X, et al. Nanoplatfrom Assembled from a CD44-Targeted Prodrug and Smart Liposomes for Dual Targeting of Tumor Microenvironment and Cancer Cells. *ACS Nano*. 2018;12(2):1519-1536. doi:10.1021/acsnano.7b08051
17. Gupta A, Eral HB, Hatton TA, Doyle PS. Nanoemulsions: formation, properties and applications. *Soft Matter*. 2016;12(11):2826-2841. doi:10.1039/C5SM02958A
18. Le Kim TH, Jun H, Kim JH, Park K, Kim JS, Nam YS. Lipiodol nanoemulsions stabilized with polyglycerol-polycaprolactone block copolymers for theranostic applications. *Biomaterials Research*. 2017;21(1):21. doi:10.1186/s40824-017-0108-4
19. Panchagnula R. Pharmaceutical aspects of paclitaxel. *International Journal of Pharmaceutics*. 1998;172(1-2):1-15. doi:10.1016/S0378-5173(98)00188-4
20. Luo M, Wang M, Niu W, et al. Injectable self-healing anti-inflammatory europium oxide-based dressing with high angiogenesis for improving wound healing and skin regeneration. *Chemical Engineering Journal*. 2021;412:128471. doi:10.1016/j.cej.2021.128471
21. Rodrigues F, Diniz L, Sousa R, et al. Preparation and characterization of nanoemulsion containing a natural naphthoquinone. *Química Nova*. 2018.

doi:10.21577/0100-4042.20170247

22. Bolourchian N, Bahjat M. Design and *In Vitro* Evaluation of Eudragit-Based Extended Release Diltiazem Microspheres for Once- and Twice-Daily Administration: The Effect of Coating on Drug Release Behavior. *Turkish Journal of Pharmaceutical Sciences*. 2019;16(3):340-347. doi:10.4274/tjps.galenos.2018.24861
23. Sharma N, Madan P, Lin S. Effect of process and formulation variables on the preparation of parenteral paclitaxel-loaded biodegradable polymeric nanoparticles: A co-surfactant study. *Asian Journal of Pharmaceutical Sciences*. 2016;11(3):404-416. doi:10.1016/j.ajps.2015.09.004
24. Chuacharoen T, Prasongsuk S, Sabliov CM. Effect of Surfactant Concentrations on Physicochemical Properties and Functionality of Curcumin Nanoemulsions Under Conditions Relevant to Commercial Utilization. *Molecules*. 2019;24(15):2744. doi:10.3390/molecules24152744
25. Chong W-T, Tan C-P, Cheah Y-K, et al. Optimization of process parameters in preparation of tocotrienol-rich red palm oil-based nanoemulsion stabilized by Tween80-Span 80 using response surface methodology. Kuksenok O, ed. *PLOS ONE*. 2018;13(8):e0202771. doi:10.1371/journal.pone.0202771
26. Silva HD, Cerqueira MA, Vicente AA. Influence of surfactant and processing conditions in the stability of oil-in-water nanoemulsions. *Journal of Food Engineering*. 2015;167:89-98. doi:10.1016/j.jfoodeng.2015.07.037
27. Abdallah DJ, Weiss RG. Organogels and Low Molecular Mass Organic

- Gelators. *Advanced Materials*. 2000;12(17):1237-1247. doi:10.1002/1521-4095(200009)12:17<1237::AID-ADMA1237>3.0.CO;2-B
28. Marangoni AG. Organogels: An Alternative Edible Oil-Structuring Method. *Journal of the American Oil Chemists' Society*. 2012;89(5):749-780. doi:10.1007/s11746-012-2049-3
29. Fang J, Nakamura H, Maeda H. The EPR effect: Unique features of tumor blood vessels for drug delivery, factors involved, and limitations and augmentation of the effect. *Advanced Drug Delivery Reviews*. 2011;63(3):136-151. doi:10.1016/j.addr.2010.04.009
30. Kim JE, Park YJ. Paclitaxel-loaded hyaluronan solid nanoemulsions for enhanced treatment efficacy in ovarian cancer. *International Journal of Nanomedicine*. 2017;12:645-658. doi:10.2147/IJN.S124158
31. Danaei M, Dehghankhold M, Ataei S, et al. Impact of Particle Size and Polydispersity Index on the Clinical Applications of Lipidic Nanocarrier Systems. *Pharmaceutics*. 2018;10(2):57. doi:10.3390/pharmaceutics10020057
32. Mitri K, Shegokar R, Gohla S, Anselmi C, Müller RH. Lipid nanocarriers for dermal delivery of lutein: Preparation, characterization, stability and performance. *International Journal of Pharmaceutics*. 2011;414(1-2):267-275. doi:10.1016/j.ijpharm.2011.05.008
33. Rai VK, Mishra N, Yadav KS, Yadav NP. Nanoemulsion as pharmaceutical carrier for dermal and transdermal drug delivery: Formulation development, stability issues, basic considerations and applications. *Journal of Controlled*

Release. 2018;270:203-225. doi:10.1016/j.jconrel.2017.11.049

34. Mallia VA, Weiss RG. Self-assembled fibrillar networks and molecular gels employing 12-hydroxystearic acid and its isomers and derivatives. *Journal of Physical Organic Chemistry*. 2014;27(4):310-315. doi:10.1002/poc.3193
35. Singh YP, Bandyopadhyay A, Mandal BB. 3D Bioprinting Using Cross-Linker-Free Silk–Gelatin Bioink for Cartilage Tissue Engineering. *ACS Applied Materials & Interfaces*. 2019;11(37):33684-33696. doi:10.1021/acsami.9b11644
36. Siqueira-Moura MP, Franceschi-Messant S, Blanzat M, et al. Gelled oil particles: A new approach to encapsulate a hydrophobic metallophthalocyanine. *Journal of Colloid and Interface Science*. 2013;401:155-160. doi:10.1016/j.jcis.2013.03.029
37. Dalmaschio CJ, Ribeiro C, Leite ER. Impact of the colloidal state on the oriented attachment growth mechanism. *Nanoscale*. 2010;2(11):2336. doi:10.1039/c0nr00338g

Chapter 4: In vitro and in vivo evaluation of gel-in-water nanodispersion as a novel drug delivery system

4.1 Introduction

The emerging trend in the drug delivery system is mostly focusing on the effective delivery of hydrophobic drugs in recent times. Formulation of hydrophobic drugs without compromising safety and efficacy is challenging because of their oil-loving nature¹. Approximately 40% of approved drugs and 90% of drugs under development have shown poor water solubility². Despite numerous advancements in drug discovery and development, hydrophobic drug formulations have shown poor bioavailability and subtherapeutic effect until today³. According to Biopharmaceutics Classification System (BCS), class IV drugs are characterized with low solubility and low permeability and possess plenty of hurdles during formulation⁴. The need for effective delivery of poorly water-soluble drugs has led to adopting newer strategies and technologies in drug development in the last few decades⁵.

Cancer is one of the worst diseases we are facing today and the number of cancer patients is increasing day by day⁶. Drugs used in cancer therapy have been a key issue for several decades as most of the neoplastic drugs are hydrophobic in nature⁷. In most cases, anticancer drugs fail to differentiate between rapidly-growing healthy cells and abnormally growing tumorous cells and lead to several adverse effects. Hence, targeted therapy with a higher bioavailability and fewer adverse effects is demanding for designing chemotherapeutic agents until today⁸.

Chapter 4: In vitro in vivo evaluation of GW nanodispersion

Nanoemulsion is an important tool and has been studied widely in the nanotechnological field intended for the clinical and therapeutic application of hydrophobic drugs⁹⁻¹². Among different nano-carriers, nanoemulsions are considered efficient drug delivery systems for the targeted delivery of lipophilic cytotoxic chemotherapeutic agents. Nanometric size, large surface area, ease of preparation, and kinetic stability along with higher drug encapsulation, sustained release of drug take the attention of researchers for using nanoemulsion as cancer drug carrier^{13,14}.

Nanoemulsion has become popular as a suitable strategy for cancer drug delivery and has been studied for the treatment of several types of cancers like ovarian cancer, breast cancer, prostate cancer, melanoma etc¹⁵⁻¹⁷. Melanoma is one of the fatal types of skin cancer and causes 80% of skin cancer-related deaths. Currently available treatment for melanoma exhibits less response and poor therapeutic efficacy of anticancer drugs owing to their poor solubility and bioavailability^{18,19}. Therefore nanotechnology-based drug delivery systems like nanoemulsions have become popular as a vehicle for anticancer drugs.

4.2 Objectives

This chapter aims to determine the functionality of gel-in-water nanoemulsion both in vitro and in vivo as a drug delivery system for hydrophobic anticancer drugs. Organogels form the core phase of G/W nanoemulsion and capable to encapsulate the hydrophobic drug molecules within it as shown in the previous chapter. As a model anticancer drug, paclitaxel was used which is also widely used for the treatment of melanoma. Since melanoma treatment with paclitaxel is challenging for several

Chapter 4: In vitro in vivo evaluation of GW nanodispersion

reasons including poor water solubility, decreased bioavailability, the inherent resistance of melanoma cells to the neoplastic agents, G/W nanoemulsion would be a possible solution to overcome these drawbacks. In vitro biocompatibility study of G/W nanoemulsion to healthy cells along with in vivo cytotoxicity against melanoma cell lines has been discussed in this chapter to define the feasibility of G/W nanoemulsion as a carrier for anticancer drugs.

4.3 Materials and methods

4.3.1 Biocompatibility of G/W nanoemulsion

To assess the biocompatibility of the prepared G/W NE in normal cells, freshly isolated rat hepatocytes were cultured in the presence of G/W NE for 7 days, as the liver is a major metabolic organ.

(a) Isolation of hepatocytes

Primary hepatocytes were isolated from 6–8-weeks old male Sprague-Dawley rats (Japan SLC, Inc., Hamamatsu, Japan). Hepatocytes were prepared using a two-step collagenase perfusion method²⁰. The culture medium was the Dulbecco's modified Eagle medium (DMEM, Funakoshi, Tokyo, Japan) supplemented with 0.05 mg/L Epidermal Growth Factor (Funakoshi Co., Ltd., Tokyo, Japan), 10 mg/L insulin obtained from bovine pancreas (Sigma, Tokyo, Japan), 7.5 mg/L hydrocortisone (Sigma, Tokyo, Japan) and 60 mg/L L-proline (Sigma, Tokyo, Japan). This culture medium is hereafter referred to as D-HDM²¹. This protocol was reviewed and approved by the Ethics Committee on Animal Experiments of Kyushu University (A29-413-1; 29 Jun 2018).

(b) Culture of hepatocytes

Freshly isolated hepatocytes were inoculated in a 96-well cell culture plate under standard conditions (37°C, 5% CO₂, 95% air) at a seeding density of 2.5×10^4 cells/cm². The culture medium was replaced with fresh medium after 4 h and 1, 3 and 5 days. G/W NE diluted (1000 times) with D-HDM was added to the cells after 24 h of seeding and changed at the same intervals as D-HDM.

(c) Hepatocyte function

The live-cell activity of hepatocytes was evaluated using highly water-soluble tetrazolium salt, WST-8 (Cell Counting Kit-8; Dojindo, Kumamoto, Japan), and albumin secretion was tested using an enzyme-linked immunosorbent assay (ELISA) kit (Protein detector ELISA Kit HRP/ABTS System; Kirkegaard & Perry Laboratories, Gaithersburg, MD, USA). To measure live-cell activity, cells were incubated with CCK-8 supplemented D-HDM for 2 hours followed by absorbance measurement at 450 nm by spectroscopy. In WST-8 assay, yellow-colored formazan dye is produced via the reduction of WST-8 by the activities of cell dehydrogenases. This formazan dye is soluble in a cell culture medium and the amount (measured at an absorbance of 450 nm by spectroscopy) is directly proportional to the number of living cells present. Albumin was measured as per previously described methods²². Rat albumin standard and anti-rat albumin antibody were purchased from ICN Pharmaceuticals (Aurora, OH, USA). In addition, Ethoxyresorufin-O-deethylase (EROD) activity - an indicator of CYP1A1 (Cytochrome P450 family 1 subfamily A member 1) activity was also tested to evaluate the effect of G/W on the liver-specific function of hepatocytes. EROD activity was

Chapter 4: In vitro in vivo evaluation of GW nanodispersion

estimated by measuring the intensity of resorufin fluorescence in the medium. Briefly, enzyme induction was conducted for 24 h by adding 0.5% (v/v) 3-methylchloranthrene (Sigma, Tokyo, Japan) to the culture medium. After that, the medium was replaced with 10 μ M Ethoxyresorufin (Wako, Japan) supplemented D-HDM and incubated for 1 h and enzyme activity was assessed by measuring the O-dealkylation reaction of ethoxyresorufin using an ARVO MX Spectro fluorometer (PerkinElmer, USA)²².

4.3.2 In vitro cytotoxicity against cancer cells

Melanoma cells (cell line B16F10) were purchased from RIKEN Bioresource Research Center, Tsukuba, Japan. B16F10 cells were cultured in a 96-well cell plate at a seeding density of 5×10^3 cells/cm² using media DMEM (Hyclone Laboratories, Utah) supplemented with 10% fetal bovine serum (FBS) and penicillin/ streptomycin. Cells were incubated under standard conditions (37°C, 5% CO₂, 95% air) and treated with paclitaxel-loaded G/W NEs (0.2 mg/ml) after 24 h of seeding. The live-cell activity of melanoma cells was determined by using WST-8 assay in the same manner as described earlier (hepatocyte function).

4.3.3 In vitro cellular uptake by cancer cells

To assess the cellular uptake of G/W NE, 0.03% of Coumarin-6 (C-6) was incorporated into the organogel particles of the emulsion. B16F10 cells were cultured in a 35-mm glass dish at a density of 5×10^3 cells/cm². Cells were

Chapter 4: In vitro in vivo evaluation of GW nanodispersion

incubated in DMEM containing 10% FBS and antibiotics for 48 h at 37°C with 5% CO₂. Next, the cells were incubated with the prepared G/W NE containing C-6 (0.03%) for 1 h at 37°C, washed several times with PBS, fixed with 10% neutral formalin buffer (Fujifilm Wako Pure Chemicals, Ltd., Japan), and stained with Rhodamine B and Hoechst 33258 for 20 min (Thermo Fisher Scientific, Waltham, MA, USA). The cells were then washed several times with PBS to remove free dyes. Afterward, the cells were observed under confocal laser scanning microscopy (CLSM) (FV1000; Olympus, Tokyo, Japan).

4.3.4 In vivo antitumor efficacy

The in vivo antitumor efficacy of the paclitaxel-loaded G/W (G/W-PTX) was assessed by injecting B16F10 melanoma cancer cells into 6-week-old ICR male mice. The antitumor efficacy of G/W-PTX was also compared with commercially available paclitaxel injection (Taxol[®], 30 mg/ 5 ml, Bristol-Myers Squibb, Japan). The cells were cultured under a 5% CO₂ atmosphere at 37°C in DMEM containing 10% (v/v) FBS and penicillin/streptomycin. B16F10 cells were treated with a trypsin solution, isolated from the 100-mm culture dish, and suspended in DMEM at a concentration of 2×10^6 cells/ mL.

To transplant the cancer cells into the mice, 0.1 mL of the respective cell suspension was subcutaneously injected into the flank of each mouse using a 1-mL, 26-gauge syringe. At 24 h after injection, accumulation of tumor cells was observed beneath the mouse skin. The mice were divided into three groups (n=3 per group) of similar average tumor size. The groups were treated as follows: Group 1 (G1)- untreated (control) group; Group 2 (G2)- treated with Taxol

Chapter 4: In vitro in vivo evaluation of GW nanodispersion

(positive control) and Group 3 (G3)- treated with G/W-PTX. The same volume of Taxol and G/W-PTX (0.18 mg/100 μ L) was injected into each mouse of group G2 and G3, respectively. The formulations were administered directly at the tumor site through subcutaneous injection. The administration dosage was once after every 48h for 11 days and the mice were sacrificed on day 12.

To evaluate the anticancer activity of each treatment, changes in tumor size were determined three times per week. Tumors were measured with a vernier caliper and their size was calculated from the length and width according to equation (2)^{23, 24}

$$\text{Tumor volume (mm}^3\text{)} = \frac{\text{Tumor length (mm)} \times [\text{Tumor width (mm)}]^2}{2} \quad (2)$$

where width is the shortest diameter and length is the longest diameter.

Bodyweight changes in mice were measured using a precision electronic balance at 2-day intervals for 11 days. After sacrifice, the tumors were collected and weighed using a precision electronic balance. All animals were treated and used according to the protocol approved by the Ethics Committee on Animal Experiments of Kyushu University (A29-413-1; 29 Jun 2018).

4.3.5 Statistical analysis

All test results are presented as mean \pm standard deviation. A significant difference between the two groups was analyzed using the two-tailed Student's *t*-test. A *p*-value of < 0.05 was considered statistically significant.

4.4 Results and discussion

4.4.1 Biocompatibility of G/W nanoemulsion

The biocompatibility study of G/W NE to primary rat hepatocytes is shown in figure 4-1. Firstly, hepatocytes morphology was similar in the absence and presence of G/W NE up to 7 days as shown in figure 4-1(A) & (B), respectively. Results also showed that G/W NE was biocompatible with hepatocytes as the live-cell activity was similar for both conditions - cells incubated with D-HDM (G/W (-)) and cells incubated with G/W NE containing D-HDM (G/W (+)). Mitochondrial activity of hepatocytes was maintained for 1 week without any significant decrease (Figure 4-1(C)). The same trend was observed for liver-specific functions i.e. metabolic activity and albumin synthesis rate. A slight increase in metabolic activity (CYP1A1) was found for G/W NE (Figure 4-1(D)). The presence of organogelator 12-HSA in G/W NE may be a possible reason for such an increase in CYP1A1 activity. The crosslinked structure of organogel and its unsaturated fatty acid content may contribute to cell function maintenance^{25,26}.

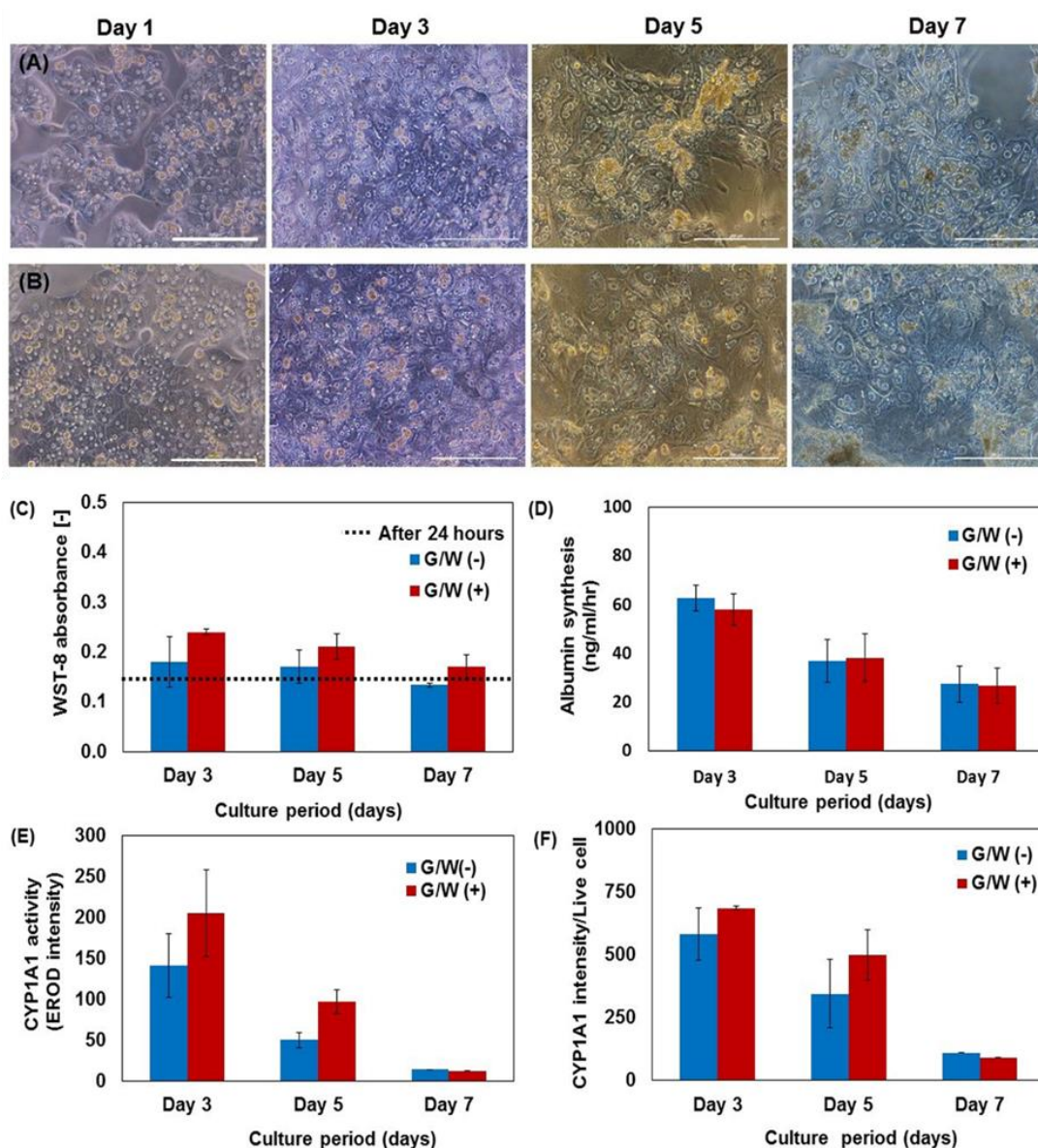


Figure 4-1: Changes in hepatocytes morphology and expression of liver functions, (A) hepatocyte morphology without G/W; (B) hepatocyte morphology with G/W; (C) live-cell activity of hepatocytes; (D) albumin secretion rate by hepatocytes; (E) metabolic activity of hepatocytes; (F) metabolic activity per live cell. Bars represent standard deviation, n=3, scale bars = 200 μ m. G/W (+) = Cells incubated with G/W nanoemulsion, G/W (-) = Cells incubated with D-HDM.

Chapter 4: In vitro in vivo evaluation of GW nanodispersion

On the other hand, albumin synthesis by primary hepatocytes was almost parallel for G/W (-) and G/W (+) during 7 days culture period (Figure 1(E)). No significant change was observed in the albumin synthesis rate for G/W NE. Additionally, CYP1A1 activity per live cell was also alike for both in the absence and presence of G/W NE (Figure 1(F)). All these findings revealed the biocompatibility of G/W NE, as there were no significant changes in the morphology and functionality of primary rat hepatocytes.

4.4.2 In vitro anticancer efficacy

Paclitaxel-loaded G/W NE (G/W-PTX) caused a significant decrease in the growth of melanoma cells (B16F10) (Figure 4-2(A)). This result suggests the successful entrapment of paclitaxel within organogels and effective drug delivery after application. A significant difference in melanoma cell activity was observed after 24 h of G/W-PTX administration in comparison with cell culture medium (DMEM). Cytotoxicity of G/W-PTX was almost the same as the paclitaxel solution in dimethyl sulfoxide (DMSO). Changes in cell morphology also ensure cytotoxicity of G/W-PTX against melanoma cells (Figure 4-2(B) & (C)). However, further in vivo studies and animal experiments are needed to confirm the efficacy of G/W NE as a hydrophobic drug delivery system.

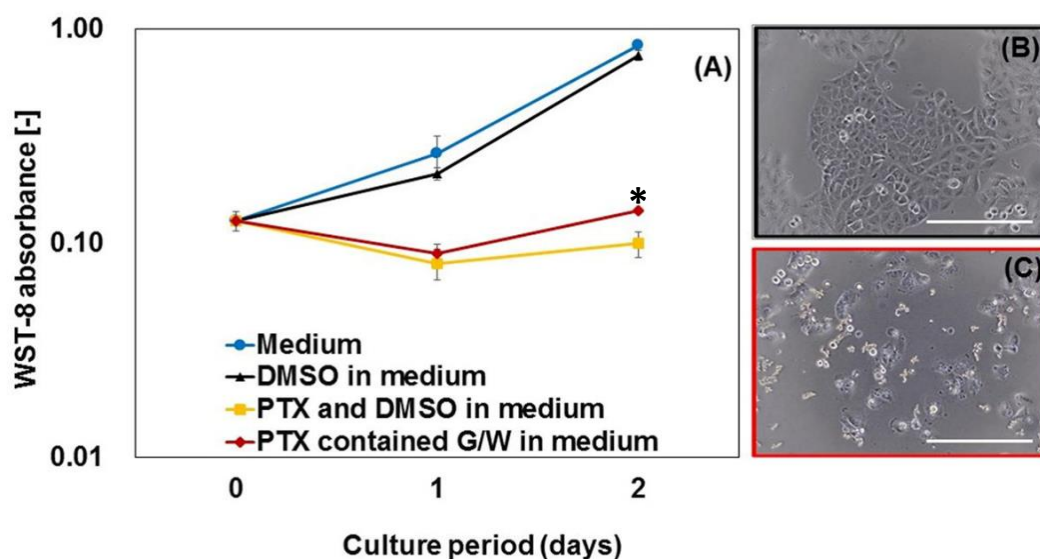


Figure 4-2: In vitro cytotoxicity of paclitaxel-loaded G/W on melanoma cells, (A) live cell activity showing significant cell death; bars represent standard deviation, $n=3$; (B) melanoma cell morphology in the culture medium; (C) melanoma cell morphology after treatment with paclitaxel-loaded G/W NE. Scale bars = 200 μm . * $p < 0.05$.

4.4.3 In vitro cellular uptake by cancer cells

In vitro cellular uptake was observed using confocal laser microscopy (CLSM) after incubation of melanoma cells with coumarin-6-loaded G/W NE. Cellular uptake was confirmed as the cells exhibited green fluorescence and indicated the possible sites of coumarin-6 accumulation (Figure 4-3). Cellular internalization of hydrophobic C-6 may occur either by passive exchange or by active endocytosis²⁷. The gel structure of nanoparticles can enhance cellular uptake via enhancing the

Chapter 4: In vitro in vivo evaluation of GW nanodispersion

internalization of nanoparticles²⁸. Moreover, this high cellular uptake assumes the potential for G/W NE to improve the therapeutic efficacy of hydrophobic drugs.

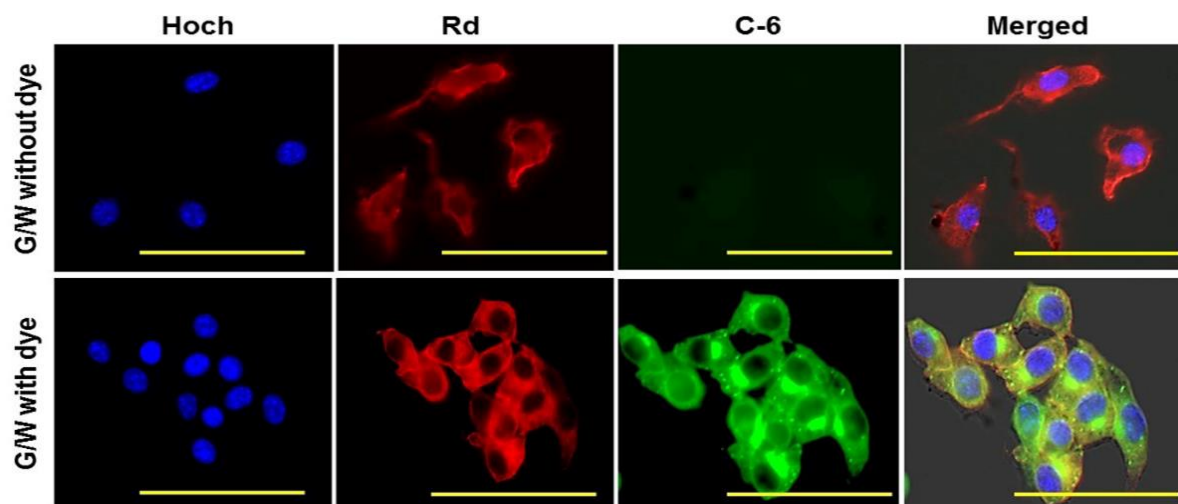


Figure 4-3: In vitro cellular uptake of G/W nanoemulsion observed under CLSM. Hoch = Hoechst, Rd = Rhodamine, C-6 = Coumarin-6, CLSM = Confocal laser scanning microscopy. Scale bars = 20 μm .

4.4.4 In vivo antitumor efficacy

ICR mice were injected with a bolus dose of G/W-PTX for 11 days and the antitumor activity of G/W-PTX was evaluated by measuring tumor volume and tumor weight. Tumor growth considerably decreased following G/W-PTX injection, thereby showing results that were similar to those observed after Taxol administration (Figure 4-4(A) and (B)). Conversely, tumor volume increased rapidly in untreated mice during the experimental period. Treatment with Taxol often causes hypersensitivity reactions and peripheral neuropathy due to the presence of Cremophor EL and thereby requires pretreatment with corticosteroids and antihistamines^{29,30}. Since similar antitumor

Chapter 4: In vitro in vivo evaluation of GW nanodispersion

efficacy was attained with paclitaxel-loaded G/W nanoemulsion, it could be a choice of carrier for paclitaxel to avoid Cremophor EL-associated side effects. Although tumor volume decreased over time after paclitaxel administration, no significant change in mice body weight was observed in all cases (Figure 4-4(C)). Therefore, we assume that paclitaxel could exert the anti-tumor activity in vivo upon administration as G/W NE.

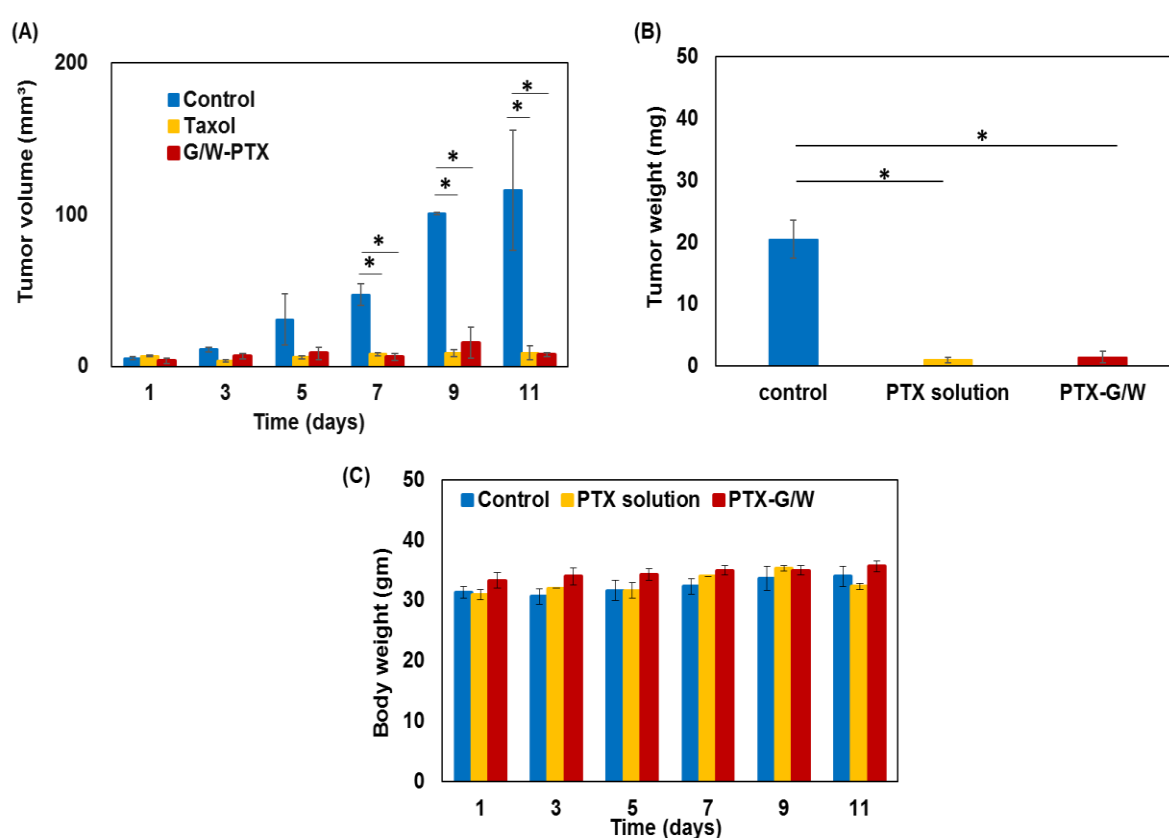


Figure 4-4: In vivo cytotoxicity study, (A) changes in tumor volume over time; (B) changes in tumor weight over time; (C) changes in mice body weight. Bars represent standard deviation, $n=3$, $*p < 0.05$.

4.5 Conclusion

In this chapter, an evaluation of the developed G/W nanoemulsion using in vitro and in vivo experiments was executed. This G/W nanoemulsion would be a novel drug delivery system for a poorly water-soluble drug. This drug delivery system was novel in terms of its organogel structure with thermos-reversible property and stability over a long period. Prepared nanoemulsions can effectively encapsulate and deliver hydrophobic drugs at the site of application. Physicochemical properties of G/W nanoemulsion were not affected by storage temperature. In vitro study showed the biocompatible nature of the G/W NE, as it did not affect the mitochondrial and metabolic activities of primary rat hepatocytes. Both in vitro and in vivo studies revealed the cytotoxicity of PTX-loaded G/W NE against skin cancer. Therefore, the G/W nanoemulsion can be a promising carrier for hydrophobic drugs which may improve the effectiveness of drug delivery in the body. This nanoemulsion can be used in melanoma treatment with fewer side effects and site-specificity.

4.6 Reference

1. Kalepu S, Nekkanti V. Insoluble drug delivery strategies: review of recent advances and business prospects. *Acta Pharmaceutica Sinica B*. 2015;5(5):442-453. doi:10.1016/j.apsb.2015.07.003
2. Loftsson T, Brewster ME. Pharmaceutical applications of cyclodextrins: basic science and product development. *Journal of Pharmacy and Pharmacology*. 2010;62(11):1607-1621. doi:10.1111/j.2042-7158.2010.01030.x
3. Tambosi G, Coelho PF, Luciano S, et al. Challenges to improve the biopharmaceutical properties of poorly water-soluble drugs and the application of the solid dispersion technology. *Matéria (Rio de Janeiro)*. 2018;23(4). doi:10.1590/s1517-707620180004.0558
4. Abhinav M, Neha J, Anne G, Bharti V. Role of Novel Drug Delivery Systems in Bioavailability Enhancement: At A Glance. *International Journal of Drug Delivery Technology*. 2016;6(1). doi:10.25258/ijddt.v6i1.8884
5. Bhagwat R, Vaidhya I. Novel Drug Delivery Systems: An Overview. *International Journal of Pharmaceutical Sciences and Research*. 2013;4(3):970-982. doi.org/10.13040/IJPSR.0975-8232.4(3).970-82
6. Sahu P, Das D, Mishra VK, Kashaw V, Kashaw SK. Nanoemulsion: A Novel Eon in Cancer Chemotherapy. *Mini reviews in medicinal chemistry*. 2017;17(18):1778-1792. doi:10.2174/1389557516666160219122755
7. Sánchez-López E, Guerra M, Dias-Ferreira J, et al. Current Applications of

Chapter 4: In vitro in vivo evaluation of GW nanodispersion

- Nanoemulsions in Cancer Therapeutics. *Nanomaterials*. 2019;9(6):821. doi:10.3390/nano9060821
8. Praveen Kumar G. Nanoemulsion Based Targeting in Cancer Therapeutics. *Medicinal Chemistry*. 2015;5(6). doi:10.4172/2161-0444.1000275
 9. Kumar M, Bishnoi RS, Shukla AK, Jain CP. Techniques for Formulation of Nanoemulsion Drug Delivery System: A Review. *Preventive Nutrition and Food Science*. 2019;24(3):225-234. doi:10.3746/pnf.2019.24.3.225
 10. Qian C, McClements DJ. Formation of nanoemulsions stabilized by model food-grade emulsifiers using high-pressure homogenization: Factors affecting particle size. *Food Hydrocolloids*. 2011;25(5):1000-1008. doi:10.1016/j.foodhyd.2010.09.017
 11. Mu H, Holm R, Müllertz A. Lipid-based formulations for oral administration of poorly water-soluble drugs. *International Journal of Pharmaceutics*. 2013;453(1):215-224. doi:10.1016/j.ijpharm.2013.03.054
 12. Karthik P, Ezhilarasi PN, Anandharamakrishnan C. Challenges associated in stability of food grade nanoemulsions. *Critical Reviews in Food Science and Nutrition*. 2017;57(7):1435-1450. doi:10.1080/10408398.2015.1006767
 13. Patel RB, Patel MR, Thakore SD, Patel BG. Nanoemulsion as a Valuable Nanostructure Platform for Pharmaceutical Drug Delivery. In: *Nano- and Microscale Drug Delivery Systems: Design and Fabrication*. ; 2017:321-341. doi:10.1016/B978-0-323-52727-9.00017-0

Chapter 4: In vitro in vivo evaluation of GW nanodispersion

14. Anton N, Vandamme TF. Nano-emulsions and micro-emulsions: Clarifications of the critical differences. *Pharmaceutical Research*. 2011;28(5):978-985. doi:10.1007/s11095-010-0309-1
15. Ahmad G, El Satta R, Botchkina G, Ojima I, Egan J, Amiji M. Nanoemulsion formulation of a novel taxoid DHA-SBT-1214 inhibits prostate cancer stem cell-induced tumor growth. *Cancer letters*. 2017;406:71-80. doi:10.1016/j.canlet.2017.08.004
16. Ganta S, Singh A, Patel NR, et al. Development of EGFR-Targeted Nanoemulsion for Imaging and Novel Platinum Therapy of Ovarian Cancer. *Pharmaceutical Research*. 2014;31(9):2490-2502. doi:10.1007/s11095-014-1345-z
17. Periasamy VS, Athinarayanan J, Alshatwi AA. Anticancer activity of an ultrasonic nanoemulsion formulation of Nigella sativa L. essential oil on human breast cancer cells. *Ultrasonics Sonochemistry*. 2016;31:449-455. doi:10.1016/j.ultsonch.2016.01.035
18. Monge-Fuentes V, Muehlmann LA, Longo JPF, et al. Photodynamic therapy mediated by acai oil (*Euterpe oleracea* Martius) in nanoemulsion: A potential treatment for melanoma. *Journal of photochemistry and photobiology B, Biology*. 2017;166:301-310. doi:10.1016/j.jphotobiol.2016.12.002
19. Maranhao R, Kretzer I, Maria D, Guido MC, Contente T. Simvastatin increases the antineoplastic actions of paclitaxel carried in lipid nanoemulsions in melanoma-bearing mice. *International Journal of Nanomedicine*. March

Chapter 4: In vitro in vivo evaluation of GW nanodispersion

2016:885. doi:10.2147/IJN.S88546

20. Seglen PO. Chapter 4 Preparation of Isolated Rat Liver Cells. In: *Methods in Cell Biology.* ; 1976:29-83. doi:10.1016/S0091-679X(08)61797-5
21. Yoshida K, Ono F, Chouno T, et al. Cryoprotective enhancing effect of very low concentration of trehalose on the functions of primary rat hepatocytes. *Regenerative Therapy.* 2020;15:173-179. doi:10.1016/j.reth.2020.08.003
22. Bual R, Kimura H, Ikegami Y, Shirakigawa N, Ijima H. Fabrication of liver-derived extracellular matrix nanofibers and functional evaluation in in vitro culture using primary hepatocytes. *Materialia.* 2018;4:518-528. doi:10.1016/j.mtla.2018.11.014
23. Liu D, Liu F, Liu Z, Wang L, Zhang N. Tumor Specific Delivery and Therapy by Double-Targeted Nanostructured Lipid Carriers with Anti-VEGFR-2 Antibody. *Molecular Pharmaceutics.* 2011;8(6):2291-2301. doi:10.1021/mp200402e
24. Yang X, Li Y, Li M, Zhang L, Feng L, Zhang N. Hyaluronic acid-coated nanostructured lipid carriers for targeting paclitaxel to cancer. *Cancer Letters.* 2013;334(2):338-345. doi:10.1016/j.canlet.2012.07.002
25. Zohuriaan-Mehr MJ, Kabiri K, Kheirabadi M. Extraordinary swelling behavior of poly(AMPS) organogel in solvent/DMSO binary mixed media. *Journal of Applied Polymer Science.* 2010;117(2):1127-1136. doi:10.1002/app.31912
26. Wiesenfeld PW, Babu US, O'Donnell MW. Effect of long-chain fatty acids in

Chapter 4: In vitro in vivo evaluation of GW nanodispersion

the culture medium on fatty acid composition of WEHI-3 and J774A.1 cells.

Comparative Biochemistry and Physiology Part B: Biochemistry and Molecular Biology. 2001;128(1):123-134. doi:10.1016/S1096-4959(00)00305-5

27. Rivolta I, Panariti A, Lettiero B, et al. Cellular uptake of coumarin-6 as a model drug loaded in solid lipid nanoparticles. *Journal of physiology and pharmacology: an official journal of the Polish Physiological Society*. 2011;62(1):45-53. <http://www.ncbi.nlm.nih.gov/pubmed/21451209>.
28. Yu M, Xu L, Tian F, et al. Rapid transport of deformation-tuned nanoparticles across biological hydrogels and cellular barriers. *Nature Communications*. 2018;9(1):2607. doi:10.1038/s41467-018-05061-3
29. Gelderblom H, Verweij J, Nooter K, Sparreboom A. Cremophor EL: The drawbacks and advantages of vehicle selection for drug formulation. *European Journal of Cancer*. 2001;37(13):1590-1598. doi:10.1016/S0959-8049(01)00171-X
30. Hino H, Yang M, Dalvi P, et al. In vitro effects of paclitaxel and cremophor EL on human riboflavin transporter SLC52A2. *Biological and Pharmaceutical Bulletin*. 2020;43(1):175-178. doi:10.1248/bpb.b19-00377

Chapter 5: Gel-in-water nanodispersion for potential application in intravenous delivery of anticancer drugs

5.1 Introduction

Nanoemulsions are pharmaceutical formulations that are used as a vehicle for drug molecules particularly with poor water solubility¹. Nanoemulsions are heterogeneous colloidal dispersions comprising particles of nanometer size range and result in high solubility, stability, and bioavailability of hydrophobic drugs². The hydrophobic core phase of oil-in-water type nanoemulsion encapsulates the hydrophobic drug and aids to raise plasma half-life by avoiding drug degradation within the body system³.

Drugs used in cancer therapy are challenging to deliver successfully to the target site mainly due to low solubility, unspecific toxicity, multidrug resistance etc³. Research on nanoemulsion for chemotherapeutic agents has been focused on recent days since they possess a large surface area, superficial charge, higher drug loading capacity⁴. Nanoemulsions can easily accumulate in tumor sites because of their smaller particle diameter and could provide site-specific action⁵.

The burden of cancer incidences and mortality is increasing daily, with a subsequent increase in the need for a potential drug delivery system⁶. Some of the widely used anticancer drugs, such as doxorubicin, paclitaxel, and docetaxel, have been studied as nanoemulsions⁷⁻¹⁰, and to date, only a limited number of studies have been performed on organogel-based nanoemulsions for anticancer drug delivery. Most anticancer drugs are hydrophobic and toxic and exhibit a range of side effects upon administration¹¹. The development of an effective carrier for anticancer drugs, notably

hydrophobic ones with a higher bioavailability and minimal adverse effects, is an emerging demand.

5.2 Objectives

In Chapter 4, gel-in-water (G/W) nanoemulsion was developed as a novel drug delivery system, in which 12-HSA successfully encapsulated the hydrophobic drug molecules. The G/W nanoemulsion was found to be stable over time, with higher encapsulation efficiency. Paclitaxel-loaded G/W nanoemulsions showed antitumor efficacy against melanoma cells *in vitro* and *in vivo* after subcutaneous injection¹². This chapter tends to evaluate the potential of G/W nanoemulsions for the intravenous delivery of anticancer drugs that will verify site-specific action by nanogel droplets. Besides, as nanoemulsions cause the burst release of drugs owing to their increased surface area, estimation of the sustained drug release over time from organogel-based G/W nanoemulsions was analyzed here in this chapter. Additionally, the biocompatibility of G/W nanoemulsions against primary rat hepatocytes and mouse fibroblast cells to determine whether any of the G/W components have toxic effects on cells was performed. The drug release performance of paclitaxel (anticancer model drug)-loaded G/W nanoemulsion was kinetically evaluated, followed by an *in vitro* cytotoxicity study against a human lung cancer cell line (A549). Consequently, ectopic xenograft models of lung cancer were developed using A549 cells and severe combined immunodeficient (SCID) mice for the *in vivo* evaluation of paclitaxel-loaded G/W nanoemulsions. The therapeutic efficacy of paclitaxel-loaded G/W nanoemulsions after intravenous injection was assessed to reveal the possibility of G/W as an emerging carrier for anticancer drugs.

5.3 Materials and methods

5.3.1 Preparation of Paclitaxel-loaded G/W nanoemulsion

Paclitaxel (>98% purity, Tokyo Chemical Industry Co., Ltd., Tokyo, Japan) was used as a model anticancer drug with poor water solubility (0.1 µg/mL in water)¹³. The G/W nanodispersion of paclitaxel was prepared in the same manner as stated previously in Chapter 3¹². In brief, paclitaxel (2 mg/mL) was added to the oil phase, which comprised 8% w/v 12-HSA (LMOG) in iodinated (37% w/w) poppyseed oil known as Lipiodol (Guerbet Japan Co., Ltd., Tokyo, Japan). The oil phase was immediately added to the aqueous phase and emulsified by ultrasonication (BRANSON SONIFIER 250, Branson Ultrasonics Co., Danbury, CT, USA) for 20 min with continuous running (1 pulse/sec) and 70% power amplitude. Polyoxyethylene hydrogenated castor oil (NIKKOL HCO-60, Nippon Surfactant Industries Co., Ltd., Tokyo, Japan) was used at a concentration of 25 mg/mL to stabilize the emulsion. The temperature was maintained at 80 °C during emulsification using a water bath (AS ONE THERMAX TM-1A, Osaka, Japan), and paclitaxel-loaded nanogel droplets were formed upon gradual cooling to room temperature. The prepared G/W-PTX was acidic (pH ~ 4.0) and had a mean diameter of 210 nm with a narrow size distribution (polydispersity index, PDI = 0.1) and higher encapsulation efficiency (~97%).

5.3.2 In-vitro biocompatibility study

The biocompatibility of G/W nanoemulsions was assessed using freshly isolated rat hepatocytes cultured with G/W nanoemulsions for 7 days. In addition, the in vitro biocompatibility of the G/W nanoemulsion was evaluated for the mouse fibroblast cell line (L929).

(a) Isolation of hepatocytes: Primary hepatocytes were isolated from 6–8-weeks old male Sprague-Dawley rats (Japan SLC, Inc., Hamamatsu, Japan) using a two-step collagenase perfusion method¹⁴. The culture medium consisted of Dulbecco's modified Eagle medium (DMEM, Funakoshi, Tokyo, Japan) supplemented with 0.05 mg/L epidermal growth factor (Funakoshi Co., Ltd., Tokyo, Japan), 10 mg/L insulin obtained from bovine pancreas (Sigma, Tokyo, Japan), 7.5 mg/L hydrocortisone (Sigma, Tokyo, Japan), and 60 mg/L L-proline (Sigma, Tokyo, Japan). This culture medium is hereafter referred to as D-HDM¹⁵. This protocol was reviewed and approved by the Ethics Committee on Animal Experiments of Kyushu University (A29-413-1; 29 June 2018; A10-381: Feb 25, 2020).

(b) Culture of hepatocytes and mouse fibroblast cells: Freshly isolated hepatocytes were cultured in D-HDM in a 96-well plate at 37 °C in a humidified atmosphere with 5% CO₂. Similarly, mouse fibroblast (L929) cells were cultured in DMEM (Hyclone Laboratories, Utah) supplemented with 10% fetal bovine serum (FBS) under standard conditions (37 °C, 5% CO₂, 95% air). The seeding densities of primary hepatocytes and L929 cells were 2.5×10^4 cells/cm² and 5.0×10^3 cells/cm², respectively. The cell culture medium was used as a control and replaced with a fresh medium at one-day intervals for 7

Chapter 5: Intravenous injection of GW nanodispersion

days of the cell culture period. G/W nanoemulsion diluted (1000 times) with the respective culture medium (D-HDM/DMEM) was added to the cells (hepatocytes/ L929) after 24 h of seeding and replaced with a freshly diluted one at the same intervals as the control.

(c) WST-8 analysis: The live-cell activity of the hepatocytes was evaluated using a highly water-soluble tetrazolium salt, WST-8 (Cell Counting Kit-8; Dojindo, Kumamoto, Japan). Cell dehydrogenases reduce WST-8 to formazan dye and change the cell culture medium color to yellow. The amount of formazan dye was measured by spectroscopy at 450 nm and was directly proportional to the number of living cells present. Therefore, cells were incubated with CCK-8 supplemented with the respective culture medium of hepatocytes and fibroblasts for 2 h followed by absorbance measurement at 450 nm using a Multiskan FC Microplate Reader (Thermo Fisher Scientific, Tokyo, Japan). The final absorbance used to estimate the live-cell activity was obtained by subtracting the background absorbance from the sample absorbance. The relative cell viability of the L929 cells in the presence of G/W nanoemulsion was calculated from absorbance using the following equation (Equation 1)¹⁶:

$$\% \text{ Cell viability} = \frac{\text{Absorbance}(\frac{G}{W})}{\text{Absorbance (Control)}} \times 100 \quad (1)$$

A sample was considered cytotoxic when the cell viability was <70% in comparison to the control, which was considered to have 100% viability¹⁶.

(d) Cell proliferation assay of L929 cell line: L929 cells were seeded in a 6-well plate at a density of 3×10^3 cells/cm² and maintained at 37 °C in a humidified 5% CO₂ atmosphere. After 24 h of seeding, the cells were treated with the G/W nanoemulsion (1000 times dilution) and replaced with fresh emulsion in the same interval as the WST-8 assay. The cells were trypsinized and counted using trypan blue staining at 48 h intervals over 9 days to evaluate the cell proliferation rate.

5.3.3 In vitro drug release from G/W nanodispersion

The in vitro release profile of paclitaxel from a gel-in-water (G/W) nanoemulsion was tested by centrifugation as described by Abouelmagd et. al with slight modifications¹⁷. One milliliter of paclitaxel-loaded G/W nanoemulsion (G/W-PTX) was centrifuged ($13860 \times g$) for 30 min to obtain the nanoparticles. Afterward, the nanoparticles were suspended in 1 mL of release medium (PBS with 0.1% Tween 80) and incubated at 37 ± 0.5 °C with continuous shaking (100 rpm). At predetermined time points, the nanoparticle suspension was centrifuged at 10000 rpm or $6160 \times g$ for 10 min to separate the nanoparticle pellets and supernatants; 0.8 mL of supernatant was collected and replaced with the same volume of the fresh release medium. The nanoparticles were resuspended in a fresh medium and incubated with continuous agitation. The sampled aliquot was analyzed immediately, and the paclitaxel concentration was calculated by measuring the UV absorbance at 230 nm (UV-2500 PC; Shimadzu, Kyoto, Japan). Paclitaxel standard solutions at six concentration levels within the range of 1–20 µg/mL were prepared using ethanol/PBS (3:7) as a solvent. Least square regression analysis was performed for the paclitaxel standard solution

Chapter 5: Intravenous injection of GW nanodispersion

absorbance data ($y = 0.0352x - 0.0141$, $R^2 = 0.99$). The percentage of paclitaxel released as a function of time was determined using the standard plot of paclitaxel as follows (Equation 2)¹⁸:

$$\text{Drug released (\%)} = \frac{\text{Paclitaxel released at time, } t}{\text{Total amount of Paclitaxel}} \times 100 \quad (2)$$

The drug release mechanism was further examined using two different mathematical models: the Korsmeyer-Peppas model and the Higuchi model. The Korsmeyer-Peppas model is preferred for pharmaceutical polymeric dosage forms. The model describes the release mechanism that follows both diffusion and erosion of polymer chains^{19,20}. According to the Korsmeyer-Peppas model,

$$\frac{M_t}{M} = K t n \quad (3)$$

where M_t is the amount of paclitaxel released at time t , M is the total amount of paclitaxel used for the release study, K is the release rate constant incorporating structural and geometric characteristics of the drug dosage form, and n is the release exponent. K , n , and regression coefficient values were determined by plotting the first 60% of cumulative drug release i.e. M_t/M against time, t in logarithmic scale in an Excel spreadsheet followed by experimental data fitting to estimated data.

The Higuchi model describes the square root of the time-dependent drug release from hydrophilic matrices based on Fick's diffusion law.

$$\frac{M_t}{M} = K_H \sqrt{t}, \quad (4)$$

where K_H is the Higuchi dissolution constant. This model mainly depicts diffusion-controlled drug release. The percentage of paclitaxel released (cumulative) was

plotted against the square root of time, and regression coefficient values were determined^{19,20}.

5.3.4 In vitro cellular uptake of nanoparticles

A hydrophobic fluorescent dye, Coumarin-6 (Tokyo Chemical Industry Co., Ltd., Tokyo, Japan) was incorporated into the inner gel phase of the G/W nanoemulsion. The human lung cancer cell line A549 was used to determine the cellular uptake of nanoparticles in vitro. A549 cells were cultured in a 35-mm glass dish using D-HDM and 10% FBS DMEM as media at a seeding density of 5.0×10^3 cells/cm². The cells were incubated at 37 °C with 5% CO₂ for 48 h, followed by incubation with Coumarin-6 (0.03%) containing G/W nanoemulsion for another 1 h. The cells were subsequently washed several times with PBS, fixed with 10% neutral formalin buffer (Fujifilm Wako Pure Chemicals, Ltd., Osaka, Japan), and stained with Rhodamine B and Hoechst 33258 for 20 min (Thermo Fisher Scientific, Waltham, MA, USA). Any free dye was removed from the cells by washing with PBS several times before microscopic observation. Subsequently, the cells were observed under confocal laser scanning microscopy (CLSM; FV1000; Olympus, Tokyo, Japan) to determine the cellular uptake of the nanoparticles.

5.3.5 In vitro anticancer effect of G/W nanoemulsion

The in vitro anticancer efficacy of Paclitaxel-loaded G/W nanoemulsion (G/W-PTX) was evaluated against two different types of cancer cell lines. Human lung cancer cells (A549) were purchased from the RIKEN Bioresource

Research Center, Tsukuba, Japan. Both of these cancer cells were cultured in a 96-well plate at a seeding density of 5×10^3 cells/cm² in DMEM supplemented with 10% fetal bovine serum (FBS) and penicillin/streptomycin as culture media. The cells were incubated under standard conditions (37°C, 5% CO₂, 95% air) and treated with G/W-PTX (0.2 mg/ml paclitaxel) after 24 h of seeding. The live-cell activity of A549 cells was determined using the WST-8 assay in the same manner as described earlier.

5.3.6 In vivo antitumor efficacy of paclitaxel-loaded G/W nanoemulsion

5.3.6.1 Development of animal model with lung cancer

(a) Animals: Animal models or xenografts for in vivo anticancer efficacy studies were developed using severe combined immunodeficient (SCID) mice (C. B-17/IcrHsd-Prkdc, Japan SLC Inc. Hamamatsu, Japan) inoculated with the human lung cancer cell line (A549). Six-week-old male SCID mice weighing 17–22 g were maintained under pathogen-free conditions with a standard diet and water. All animals were treated and used according to the protocol approved by the Ethics Committee on Animal Experiments of Kyushu University (A29-413-1; 29 June 2018; A10-381: Feb 25, 2020).

(b) Cell line culture: Human lung cancer cell lines (A549) were maintained in DMEM supplemented with 10% FBS and penicillin/streptomycin. The cells were cultured in an incubator with a humidified atmosphere of 5% CO₂ in air at 37 °C.

(c) Preparation of cell suspension for subcutaneous injection: Cancer cells were harvested from subconfluent culture dishes by mechanical pipetting. The cells were washed with PBS, resuspended in serum-free DMEM, and the floating cells were collected after centrifugation at 1000 rpm for 3 min. Trypan blue staining was used to assess cell viability, and cell suspensions with >90% confluency were used for injection. The cells were resuspended at a density of 1×10^6 cells/100 μ L in serum-free DMEM and diluted with an equal volume of Matrigel (Corning Matrigel Matrix Basement Membrane, REF 354234). Matrigel acts as an anchor to prevent the spreading and diffusion of cells from the site of injection, as it rapidly forms a gel at room temperature or above. Cell suspensions and injection kits were kept on ice until injection to avoid the solidification of the Matrigel.

The animals were anesthetized with isoflurane, and 1×10^6 cells were injected subcutaneously into the left flank of the mice using a 1-mL, 26-gauge syringe. Seven days after the cell inoculation, the cancer cell lines formed tumors under the mouse skin.

5.3.6.2 Intravenous injection of paclitaxel-loaded G/W nanoemulsion

The mice were divided into three groups (control, Taxol, and G/W-PTX) with comparable tumor sizes. The antitumor efficacy of G/W-PTX was also compared with commercially available paclitaxel injection (Taxol[®], 30 mg/ 5 ml, Bristol-Myers Squibb, Japan). The same concentration (0.18 mg/ 100 μ L PBS) of Taxol and G/W-PTX were administered via the tail vein to the Taxol group and G/W-PTX group, respectively. Whereas PBS was administered intravenously to the mice of a control group. The administration dosage was once after every 48 h for 11 days, and the mice

Chapter 5: Intravenous injection of GW nanodispersion

were sacrificed on day 12. To avoid tail vein damage during administration, the formulations were administered first from the tip of the tail, and then gradually moved upward until the point where the tail vein entered the mouse body.

To evaluate the anticancer activity of each treatment, changes in the tumor size were determined three times per week. The tumor dimensions were measured using a Vernier caliper, and calculated from the length and width according to equation (5)^{21,22}:

$$\text{Tumor volume (mm}^3\text{)} = \frac{\text{Tumor length (mm)} \times [\text{Tumor width (mm)}]^2}{2} \quad (5)$$

where the width and length are the shortest and longest diameters, respectively.

5.3.7 Statistical analysis

All data are reported as the mean \pm standard deviation. A significant difference between the two groups was analyzed using a two-tailed Student's *t*-test. A two-tailed *p*-value of less than 0.05 ($*p < 0.05$) was considered statistically significant.

5.4 Results and discussion

5.4.1 In vitro biocompatibility study

The biocompatibility of the G/W nanoemulsions with primary rat hepatocytes and mouse fibroblasts (L929) is shown in Figure 5-1. First, there was no noticeable change

Chapter 5: Intravenous injection of GW nanodispersion

in the cell morphology during the seven days of cell culture. Hepatocytes cultured with G/W supplemented D-HDM (G/W) have a cellular structure similar to that of cells cultured with D-HDM (Figure 5-1(A) & (B)). Fibroblasts maintained in G/W-supplemented media also showed consequent cell growth like fibroblasts cultured with media (10% FBS DMEM) only (Figure 5-1(C) & (D)).

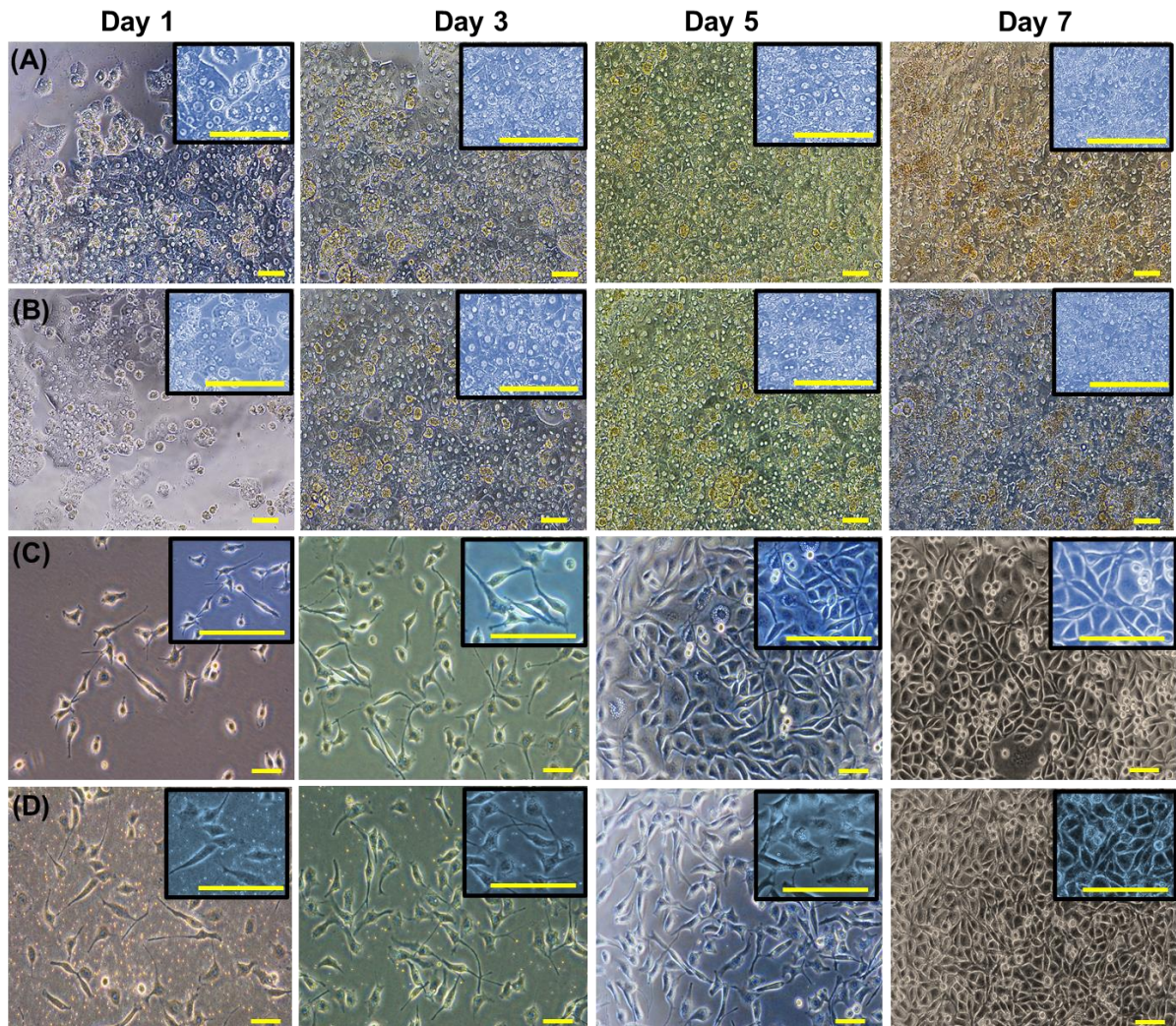


Figure 5-1: Changes in cell morphology at day 1, 3, 5, and 7 days of culture under a phase-contrast microscope, (A) hepatocytes morphology incubated with D-HDM; (B) hepatocytes morphology incubated with G/W; (C) fibroblasts (L929) morphology incubated with DMEM; (D) fibroblasts morphology incubated with G/W. Scale bars = 200 μm .

Chapter 5: Intravenous injection of GW nanodispersion

The biocompatibility of the G/W with primary hepatocytes was ensured by live-cell activity. Because primary hepatocytes are quiescent and do not undergo cell division, they do not proliferate *in vitro*²³. Consequently, maintaining the cell number is considered an index. Our results showed that primary hepatocytes maintained mitochondrial activity (proportional to WST-8 absorbance) during the culture period, even in the presence of G/W nanodispersion, and assured G/W nanodispersion biocompatibility to primary hepatocytes (Figure 5-2(A)). No significant change in the live cell activity (WST-8 absorbance) was observed for G/W nanoemulsions in primary rat hepatocytes.

However, the biocompatibility of the G/W nanoemulsion to L929 cells was evaluated using a cell proliferation assay, as L929 cells could proliferate *in vitro*. The G/W nanoemulsion was found to be biocompatible and supported L929 cell proliferation over 9 days (Figure 5-2(B)). The cell proliferation rate for the G/W nanoemulsion was almost the same as that of the control group, indicating the biocompatibility of the G/W nanoemulsion to mouse fibroblasts. Similarly, G/W nanoemulsion had no cytotoxic effect on mouse fibroblasts as the cell viability was $\geq 90\%$ during the experimental period (Figure 5-2(C)). Based on Cannella et al. 2020, L929 cells with a percentage cell viability of $< 70\%$ were considered cytotoxic, and noncytotoxic when the cell viability was $> 70\%$ ²⁴. Therefore, our results confirm no possible cytotoxicity of G/W nanoemulsions with a cell viability of $\geq 90\%$. Hence, all the above results suggest the biocompatibility of G/W nanoemulsions for both primary hepatocytes and mouse fibroblasts.

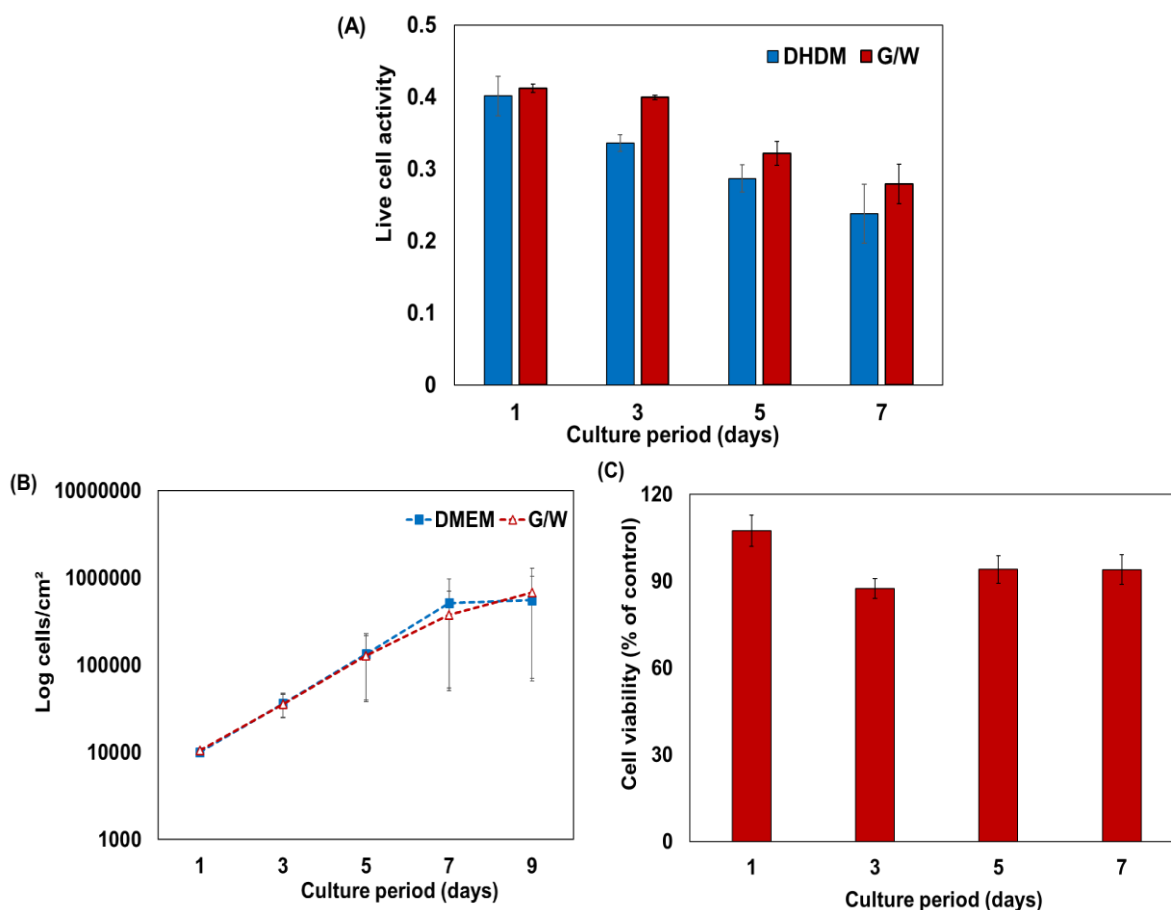


Figure 5-2: In vitro biocompatibility study of G/W nanodispersion, (A) live-cell activity of hepatocytes; (B) cell proliferation assay of L929 cell line; (C) relative cell viability of L929 cell line incubated with G/W. Bars represent standard deviation, n= 3.

5.4.2 In vitro drug release from nanodispersion

The release of paclitaxel from the organogel droplets of G/W nanoemulsions is shown in Figures 5-3(A). The results showed an initial burst release of paclitaxel from the nanoparticles, followed by a constant rate of drug release. Initially, approximately 20% of the encapsulated paclitaxel was released after 1h. The cumulative amount of paclitaxel released was approximately 66% after 48 h. The use of 12-HSA may sustain

the release of paclitaxel from nanoparticles. Generally, drug release from organogels may occur through diffusion, erosion, or drug dissolution²⁵. The initial burst release of paclitaxel (~20%) may be due to the adsorption of drug molecules on the nanoparticle surface by weak bonds, while a sustained drug release was obtained for the next 48h, which was controlled by erosion or diffusion²⁶.

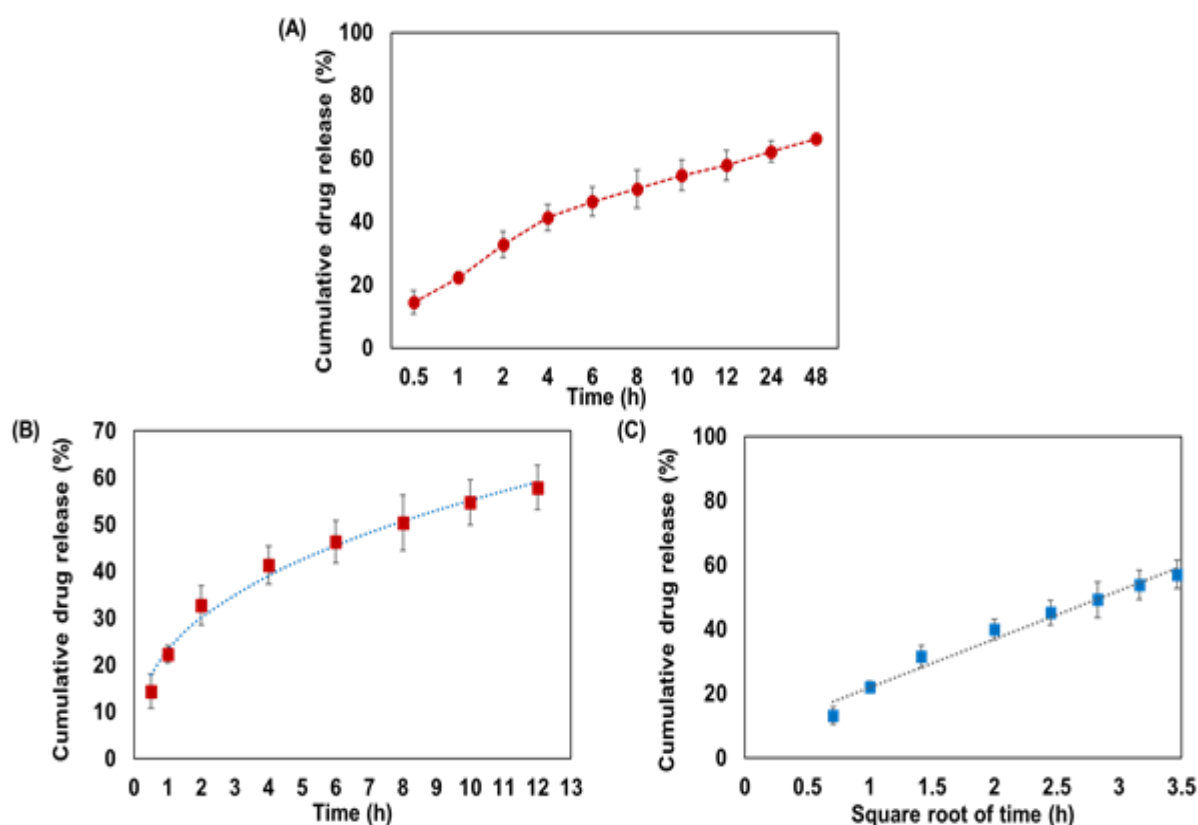


Figure 5-3: In vitro drug release of paclitaxel from G/W nanodispersion and kinetic evaluation of release profile, (A) cumulative release of paclitaxel from nanoparticles; (B) paclitaxel release data fitted to Korsmeyer-Peppas model; (C) paclitaxel release data fitted to Higuchi model. Bars represent standard deviation, n= 3.

The mechanism of paclitaxel release from the nanogel particles was kinetically analyzed using the Korsmeyer-Peppas model (Figure 5-3(B)). Paclitaxel release from

the G/W nanoemulsion showed a better linear fit to the Korsmeyer-Peppas model with a regression coefficient value of 0.99. The release rate constant (K) was estimated as 18.5 ± 3.0 , and the release exponent, n , was 0.43 on average. When the n value is < 0.5 , it indicates a Fickian diffusion mechanism²⁷. Therefore, drug release from nanoparticles occurs primarily via diffusion. Similarly, the fitting of cumulative drug release data to the Higuchi model had a regression coefficient value of 0.97, suggesting that the release kinetics was diffusion-controlled¹⁸ (Figure 5-3(C)).

5.4.3 In vitro cellular uptake by lung cancer cells

The uptake of coumarin-6 loaded G/W nanoemulsion was observed using confocal laser scanning microscopy (CLSM). Cellular uptake by lung cancer cells (A549) was confirmed as the cells exhibited green fluorescence (Figure 5-4). The image indicates the internalization of coumarin-6 within the cytoplasm of A549 cells.

The cellular uptake of fluorescence molecules encapsulated in organogel particles may be driven either by passive exchange or by active endocytosis²⁸. The cross-linked gel structure may enhance cellular uptake by enhancing the internalization of nanoparticles. Organogels prevent the deformation of nanoparticle structures, resulting in reduced membrane fluidity of nanoparticles^{29,30}. Hence, it is presumed that a decrease in membrane fluidity of nanogel droplets promotes cellular uptake of coumarin-6 loaded nanoparticles. Moreover, this high cellular uptake indicates the potential for G/W nanoemulsion as an effective carrier for anticancer drugs.

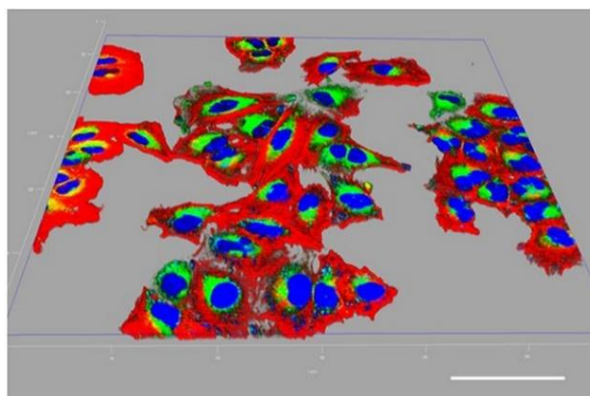


Figure 5-4: 3D reconstruction of confocal analysis of the A549 cells exposed to coumarin-6 loaded G/W nanoemulsion. The staining of the cells is as follows: Blue - Hoechst-stained nuclei, Red – Rhodamine-stained cytoplasm, Green – Coumarin-6 loaded G/W nanoemulsion. Scale bar = 20 μm .

5.4.4 In vitro anticancer effect against lung cancer cells

The anticancer efficacy of paclitaxel-loaded G/W nanoemulsion (G/W-PTX) was determined against lung cancer cells (A549) in vitro. A significant decrease in the live cell activity of A549 cells was observed after 24h of G/W-PTX administration (Figure 5-5(A)). This result suggests the effective delivery of paclitaxel from nanogel droplets, resulting in the inhibition of cancer cell growth. The mechanism hypothesized for such cytotoxicity is pH-responsive drug release from G/W nanoparticles at the cellular level. The intracellular compartments, that is, endosomes and lysosomes, became acidic ($\text{pH} < 6.0$) owing to ATP-ase-mediated proton influx after the endocytosis of foreign particles. This acidic environment promotes cellular internalization of nanoparticles, followed by drug release into the cytoplasm³¹.

Additionally, the higher fatty acid (15%–35% stearic acid) content of 12-HSA, and the tumor-seeking nature of lipiodol may also aid in the cellular uptake of G/W nanoparticles by cancer cells³². The cytotoxicity of G/W-PTX was almost the same as that of paclitaxel solution in dimethyl sulfoxide (DMSO). Changes in the cell morphology also ensured the cytotoxicity of G/W-PTX against A549 cells (Figure 5-5(B) and (C)). However, further *in vivo* studies are required to confirm the efficacy of G/W nanoemulsions as carriers for anticancer drugs.

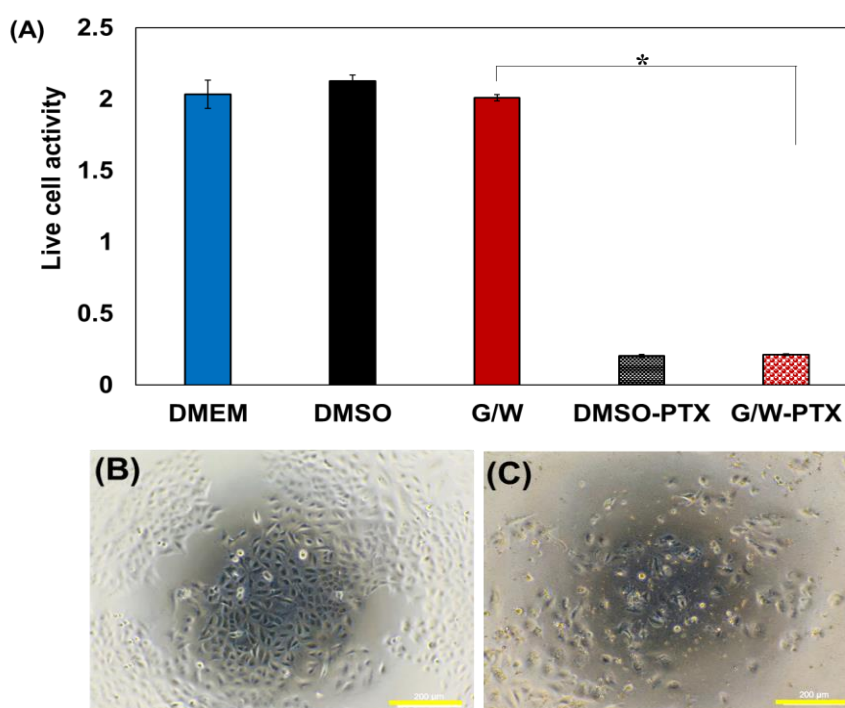


Figure 5-5: In vitro cytotoxicity of paclitaxel-loaded G/W nanoemulsion to lung cancer cells (A549), (A) live cell activity of A549 cells; (B) A549 cell morphology with DMEM; (C) A549 cell morphology with G/W-PTX. Bars represent standard deviation, $n = 3$, $*p < 0.05$. Scale bars = 200 μm.

5.4.5 In vivo antitumor efficacy of paclitaxel-loaded G/W nanoemulsion

Tumors developed in the SCID mice after 7 days subcutaneous injection of A549 cells followed by treatment with a bolus dose of G/W-PTX injection for 11 days. The antitumor activity of the G/W-PTX nanoemulsion was evaluated by measuring the tumor volume and weight. Tumor growth was significantly decreased ($*p < 0.05$) following intravenous injection of G/W-PTX via the tail vein (Figure 5-6(A)). Conversely, an increase in tumor volume was observed in mice of the control group (mice received an intravenous injection of PBS only) during the experimental period.

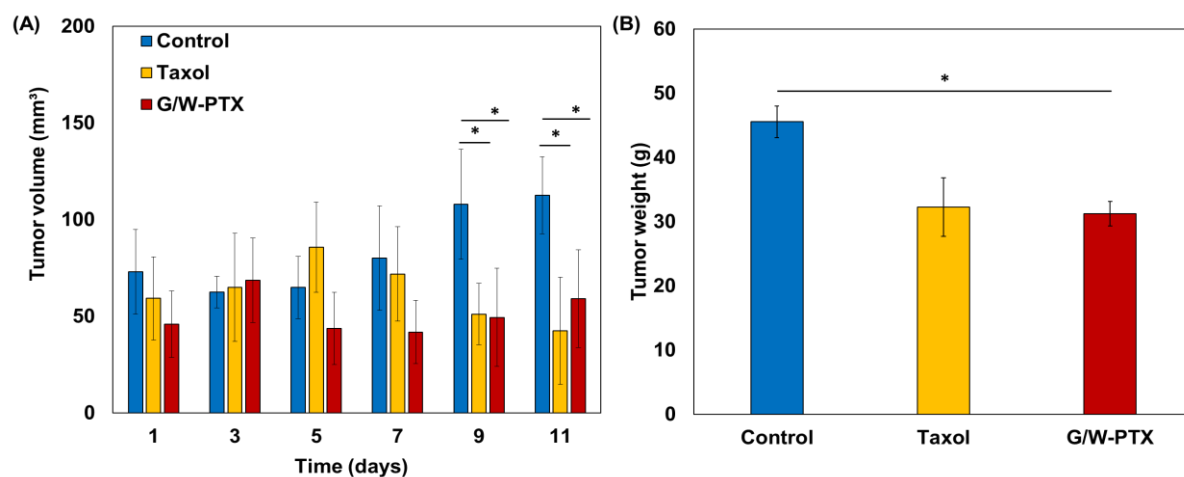


Figure 5-6: Anti-tumor efficacy of paclitaxel-loaded G/W nanodispersion after intravenous injection on the tail vein, (A) changes in tumor volume over time, (B) tumor weight in control and treatment groups. Bars represent standard deviation, $n = 5$, $*p < 0.05$.

Simultaneously, G/W-PTX-treated mice also showed a decrease in tumor weight compared to the control group (Figure 5-6(B)). Antitumor efficacy of G/W-PTX was similar to that of mice treated with Taxol[®]. The acidic nature of the tumor

Chapter 5: Intravenous injection of GW nanodispersion

microenvironment (pH 6.5 – 7.2) owing to their enhanced lactic acid production, insufficient blood supply, and poor lymphatic drainage enables the release of anticancer drugs in the tumor extracellular environment. Studies have also shown that paclitaxel release from nanoparticles was improved at a slightly acidic pH^{31,33}.

Therefore, G/W-PTX nanoparticles may take advantage of the acidic pH of the tumor microenvironment and prevent the rapid growth of A549 tumors in SCID mice. Although the tumor volume decreased over time after paclitaxel administration, no significant change in the mice's body weight (20 ± 2 mg) was observed in any of the two groups during the experiment (data not shown). Hence, our results suggest that the therapeutic efficacy of G/W-PTX could be achieved by intravenous administration of G/W nanoemulsion.

5.5 Conclusion

The current study showed the successful delivery of paclitaxel from organogel-based nanodispersion (G/W) through intravenous injection. No change in the mitochondrial activity of primary hepatocytes and fibroblasts in the presence of G/W nanoemulsion ensured biocompatibility. Drug encapsulation within organogels enabled sustained release of paclitaxel over time, which may provide several advantages including dose reduction, decreased risk of local inflammation, and a lower cost of therapy. The cytotoxicity of paclitaxel against A549 cells, both in vitro and in vivo, revealed the potential of G/W nanoemulsions to improve the therapeutic efficacy of anticancer drugs. Moreover, organogels improve the cellular uptake of nanoparticles, which will elevate the cytotoxicity of chemotherapeutic agents. In

Chapter 5: Intravenous injection of GW nanodispersion

summary, organogel-based G/W nanodispersion could be a promising carrier for the intravenous delivery of anticancer drugs with sustained drug release and enhanced therapeutic outcomes.

5.6 Reference

1. Ganta S, Talekar M, Singh A, Coleman TP, Amiji MM. Nanoemulsions in translational research - Opportunities and challenges in targeted cancer therapy. *AAPS PharmSciTech*. 2014;15(3):694-708. doi:10.1208/s12249-014-0088-9
2. Sánchez-López E, Guerra M, Dias-Ferreira J, et al. Current Applications of Nanoemulsions in Cancer Therapeutics. *Nanomaterials*. 2019;9(6):821. doi:10.3390/nano9060821
3. Maeda H, Wu J, Sawa T, Matsumura Y, Hori K. Tumor vascular permeability and the EPR effect in macromolecular therapeutics: A review. *Journal of Controlled Release*. 2000;65(1-2):271-284. doi:10.1016/S0168-3659(99)00248-5
4. Jaiswal M, Dudhe R, Sharma PK. Nanoemulsion: an advanced mode of drug delivery system. *3 Biotech*. 2015;5(2):123-127. doi:10.1007/s13205-014-0214-0
5. Tiwari S, Tan Y-M, Amiji M. Preparation and In Vitro Characterization of Multifunctional Nanoemulsions for Simultaneous MR Imaging and Targeted Drug Delivery. *Journal of Biomedical Nanotechnology*. 2006;2(3):217-224. doi:10.1166/jbn.2006.038
6. Sung H, Ferlay J, Siegel RL, et al. Global Cancer Statistics 2020: GLOBOCAN Estimates of Incidence and Mortality Worldwide for 36 Cancers in 185 Countries. *CA: a cancer journal for clinicians*. 2021;71(3):209-249. doi:10.3322/caac.21660

Chapter 5: Intravenous injection of GW nanodispersion

7. Jiang SP, He SN, Li YL, et al. Preparation and characteristics of lipid nanoemulsion formulations loaded with doxorubicin. *International Journal of Nanomedicine*. 2013;8:3141-3150. doi:10.2147/IJN.S47708
8. Shakhwar S, Darwish R, Kamal MM, Nazzal S, Pallerla S, Abu Fayyad A. Development and evaluation of paclitaxel nanoemulsion for cancer therapy. *Pharmaceutical Development and Technology*. 2020;25(4):510-516. doi:10.1080/10837450.2019.1706564
9. Kim JE, Park YJ. Paclitaxel-loaded hyaluronan solid nanoemulsions for enhanced treatment efficacy in ovarian cancer. *International Journal of Nanomedicine*. 2017;12:645-658. doi:10.2147/IJN.S124158
10. Li X, Du L, Wang C, Liu Y, Mei X, Jin Y. Highly efficient and lowly toxic docetaxel nanoemulsions for intravenous injection to animals. *Pharmazie*. 2011;66(7):479-483. doi:10.1691/ph.2011.1015
11. Narvekar M, Xue HY, Eoh JY, Wong HL. Nanocarrier for poorly water-soluble anticancer drugs - Barriers of translation and solutions. *AAPS PharmSciTech*. 2014;15(4):822-833. doi:10.1208/s12249-014-0107-x
12. Fardous J, Omoso Y, Joshi A, et al. Development and characterization of gel-in-water nanoemulsion as a novel drug delivery system. *Materials Science and Engineering: C*. 2021;124(February):112076. doi:10.1016/j.msec.2021.112076
13. Konno T, Watanabe J, Ishihara K. Enhanced solubility of paclitaxel using water-soluble and biocompatible 2-methacryloyloxyethyl phosphorylcholine polymers. *Journal of Biomedical Materials Research*. 2003;65A(2):209-214.

Chapter 5: Intravenous injection of GW nanodispersion

doi:10.1002/jbm.a.10481

14. Seglen PO. Chapter 4 Preparation of Isolated Rat Liver Cells. In: *Methods in Cell Biology.* ; 1976:29-83. doi:10.1016/S0091-679X(08)61797-5
15. Yoshida K, Ono F, Chouno T, et al. Cryoprotective enhancing effect of very low concentration of trehalose on the functions of primary rat hepatocytes. *Regenerative Therapy.* 2020;15:173-179. doi:10.1016/j.reth.2020.08.003
16. Srivastava GK, Alonso-Alonso ML, Fernandez-Bueno I, et al. Comparison between direct contact and extract exposure methods for PFO cytotoxicity evaluation. *Scientific Reports.* 2018;8(1):1425. doi:10.1038/s41598-018-19428-5
17. Abouelmagd SA, Sun B, Chang AC, Ku YJ, Yeo Y. Release Kinetics Study of Poorly Water-Soluble Drugs from Nanoparticles: Are We Doing It Right? *Molecular Pharmaceutics.* 2015;12(3):997-1003. doi:10.1021/mp500817h
18. Kini S, Bahadur D, Panda D. Mechanism of anti-cancer activity of benomyl loaded nanoparticles in multidrug resistant cancer cells. *Journal of Biomedical Nanotechnology.* 2015;11(5). doi:10.1166/jbn.2015.1998
19. Costa P, Sousa Lobo JM. Modeling and comparison of dissolution profiles. *European Journal of Pharmaceutical Sciences.* 2001;13(2):123-133. doi:10.1016/S0928-0987(01)00095-1
20. Pereira Camelo SR, Franceschi S, Perez E, Girod Fullana S, Ré MI. Factors influencing the erosion rate and the drug release kinetics from organogels

Chapter 5: Intravenous injection of GW nanodispersion

designed as matrices for oral controlled release of a hydrophobic drug. *Drug Development and Industrial Pharmacy*. 2016;42(6):985-997. doi:10.3109/03639045.2015.1103746

21. Yang X, Li Y, Li M, Zhang L, Feng L, Zhang N. Hyaluronic acid-coated nanostructured lipid carriers for targeting paclitaxel to cancer. *Cancer Letters*. 2013;334(2):338-345. doi:10.1016/j.canlet.2012.07.002
22. Liu D, Liu F, Liu Z, Wang L, Zhang N. Tumor Specific Delivery and Therapy by Double-Targeted Nanostructured Lipid Carriers with Anti-VEGFR-2 Antibody. *Molecular Pharmaceutics*. 2011;8(6):2291-2301. doi:10.1021/mp200402e
23. Cho CH, Berthiaume F, Tilles AW, Yarmush ML. A new technique for primary hepatocyte expansion in vitro. *Biotechnology and Bioengineering*. 2008;101(2):345-356. doi:10.1002/bit.21911
24. Cannella V, Altomare R, Leonardi V, et al. In Vitro Biocompatibility Evaluation of Nine Dermal Fillers on L929 Cell Line. *BioMed Research International*. 2020;2020. doi:10.1155/2020/8676343
25. Lupi FR, Gabriele D, Baldino N, Mijovic P, Parisi OI, Puoci F. Olive oil/policosanols organogels for nutraceutical and drug delivery purposes. *Food & Function*. 2013;4(10):1512. doi:10.1039/c3fo60259a
26. Li XP, Zhan Q, Qi HZ, et al. Paclitaxel formulation with stable sustained-release behavior and its biological safety evaluation. *Science China Technological Sciences*. 2019;62(7). doi:10.1007/s11431-018-9334-6

Chapter 5: Intravenous injection of GW nanodispersion

27. Gao Y, Zuo J, Bou-Chacra N, et al. In vitro release kinetics of antituberculosis drugs from nanoparticles assessed using a modified dissolution apparatus. *BioMed Research International*. 2013;2013. doi:10.1155/2013/136590
28. Rivolta I, Panariti A, Lettiero B, et al. Cellular uptake of coumarin-6 as a model drug loaded in solid lipid nanoparticles. *Journal of physiology and pharmacology: an official journal of the Polish Physiological Society*. 2011;62(1):45-53. <http://www.ncbi.nlm.nih.gov/pubmed/21451209>.
29. Qin C, Lv Y, Xu C, Li J, Yin L, He W. Lipid-bilayer-coated nanogels allow for sustained release and enhanced internalization. *International Journal of Pharmaceutics*. 2018;551(1-2):8-13. doi:10.1016/j.ijpharm.2018.09.008
30. Yu M, Xu L, Tian F, et al. Rapid transport of deformation-tuned nanoparticles across biological hydrogels and cellular barriers. *Nature Communications*. 2018;9(1):2607. doi:10.1038/s41467-018-05061-3
31. Shetab Boushehri M, Dietrich D, Lamprecht A. Nanotechnology as a Platform for the Development of Injectable Parenteral Formulations: A Comprehensive Review of the Know-Hows and State of the Art. *Pharmaceutics*. 2020;12(6):510. doi:10.3390/pharmaceutics12060510
32. Pesapane F, Nezami N, Patella F, Geschwind JF. New concepts in embolotherapy of HCC. *Medical Oncology*. 2017;34(4):58. doi:10.1007/s12032-017-0917-2
33. Gao W, Chan JM, Farokhzad OC. PH-responsive nanoparticles for drug delivery. *Molecular Pharmaceutics*. 2010;7(6). doi:10.1021/mp100253e

Chapter 6: Delivery of hydrophobic drug to the posterior region of eye as gel-in-water nanodispersion

6.1 Introduction

According to World Health Organization (WHO), about 2.2 billion people in the world are suffering from near or distance vision impairment. Vision impairment hampers the quality of life along with poses an enormous burden on global finance estimated to be US\$ 224 billion annually¹. The number of patients with ocular diseases is increasing day by day as it has a linear relation with patient age². Generally, the eye can be divided into two major segments- the anterior segment and the posterior segment. The posterior segment comprises two-thirds of the eye and consists of the choroid, the sclera, the retina and the vitreous humor³. Adult peoples mainly suffer from posterior segment eye diseases (PSEDs) which affect the tissues in the posterior eye segment including glaucoma, age-related macular degeneration (AMD), diabetic retinopathy^{4,5}. Between two different forms of AMD, wet AMD is most common in Japan that emerges abruptly and affects the central part of the retina⁶. In case of wet AMD, abnormal growth of new blood vessels outside of the retina causes edema and bleeding in the retina and may lead to various degrees of blindness or even permanent loss of sight⁵.

Drug delivery to the posterior segment of the eyes is challenging owing to the unique structural features of the eye and the physiological ocular barriers⁷. The nasolacrimal drainage, lacrimation rate, tear film, blinking, efflux pumps, and metabolism in ocular tissues are common physiological ocular barriers that impede drug delivery to both anterior and posterior regions of the eye⁸. The popular treatment

option for AMD, diabetic retinopathy is intravitreal injection where the drug is directly placed in the vitreous humor. However, this treatment method is inconvenient to the patient for being an invasive route⁹. Other routes to target the posterior eye section include topical, systemic, and periocular drug delivery¹⁰. Laser treatment has recently become popular for wet AMD and diabetic retinopathy although laser treatment causes significant post-treatment complications like retinal detachment, rupture of retina, macular edema and fibrose etc¹¹.

Nanocarriers for ocular drug delivery have gained attention in recent days to overcome the limitations associated with currently available treatments of PSEDs¹². Nanocarriers are distinct particulate systems of nanosize range (10-1000 nm) and include liposomes, nanoemulsions, polymeric nanoparticles, etc¹³. Among these nanocarriers, nanoemulsion has been explored as a suitable alternative to the conventional options due to their enhanced bioavailability, improved stability, higher retention time and so on¹⁴. Oil-in-water (O/W) type nanoemulsions are suitable for ocular administration due to lesser ocular irritation and better tolerance¹⁵. Nanoemulsions for ocular drug delivery are mostly aqueous dispersions that can be easily formulated as an eye drop or injection. Studies also showed that emulsions improve corneal permeability, retards drug release followed by enhanced bioavailability¹⁶. Furthermore, the presence of surfactant in nanoemulsion serves as a penetration enhancer leading to increased permeability to deep layers of ocular structure^{14,17}.

6.2 Objectives

In this chapter, an effort was made to develop an effective nanocarrier as a non-invasive measure for PSEDs treatment. Nanoparticles are successfully employed as an alternative strategy for drug delivery to the posterior segment of ocular tissues. However, nanoparticles result in immediate drug release owing to their smaller size and also cause rapid clearance from the site of administration because of removal by conjunctival, periocular circulatory system^{18,19}. Research showed that nanoparticles of 200-2000 nm could retain in ocular site for a prolonged period and effectively deliver drugs to the back of eye¹⁹. Hence, the goal was development of a nanogel dispersion of < 250 nm in diameter where the organogel will encapsulate the hydrophobic drug substance within it. This G/W nanodispersion will be a suitable drug delivery candidate with sustained drug release and enhanced ocular retention time. The development of G/W nanoemulsion as topical eye drops will be a promising option for ocular drug delivery in the posterior eye segment with minimal side effects. Moreover, G/W eye drops would be a choice of treatment in PSEDs as eye drops are a patient preferred ocular form due to their ease of administration which is noninvasive and pain-free in addition to low cost.

6.3 Materials and methods

6.3.1 Preparation of G/W nanoemulsion

The nanoemulsion was prepared in the same manner as described by Fardous et. al. with slight modification²⁰. Beeswax was used as an organogelator that dissolves in

castor oil (Fujifilm Wako Pure Chemical Corporation, Osaka, Japan) above its melting point (62 – 65) °C²¹ and forms the inner gel phase of the emulsion. On the other hand, phosphate buffer saline of pH 7.4 was used as an aqueous phase and contains polyoxyethylene hydrogenated castor oil -60 (HCO-60) (NIKKOL HCO-60, Nippon Surfactant Industries Co., Ltd., Tokyo, Japan) as the emulsifying agent. In brief, beeswax (5% wt. of oil) was dissolved in castor oil at 80 °C in a water bath with continuous shaking (100 rpm) for 5 min and forms the oil phase. Non-ionic surfactant HCO-60 was dissolved in PBS at a concentration of 50 mg/ mL in the same experimental condition as the oil phase. Afterward, the oil phase was added to the aqueous phase immediately and homogenized by ultrasonication. Emulsification was performed for 20 min at 80 °C using an ultrasonic probe (BRANSON SONIFIER 250, Branson Ultrasonics Co., Danbury, USA) running at 70% power amplitude and 1 pulse/sec. Here, the ultrasonic waves provide cavitation forces that subsequently form nano-size droplets²². The emulsion was cool down slowly to room temperature and organogel droplets were formed that remain dispersed in the aqueous phase.

6.3.2 Development of G/W nanoemulsion as an eyedrop

Nanosized particles (diameter < 250 nm) with narrow size distribution which is characterized by polydispersity index (PDI) are desired for better stability and biocompatibility of the nanoemulsion. The particle diameter and size distribution of G/W nanoemulsion changed with changes in oil and aqueous phase volume ratio, surfactant concentration, gelling agent concentration. Therefore, a screening study was performed by changing the volume or concentration of nanoemulsion components to obtain the optimum concentration of each ingredient. Aqueous phase i.e. PBS volume

was increased from 1 to 10 mL corresponding to the oil phase volume to obtain the optimum volume ratio of dispersed medium to continuous medium. Similarly, HCO-60 at a concentration ranging from 25-200 mg/ mL of PBS was used to determine the suitable concentration of surfactant for a stable nanoemulsion. For the gelling agent, beeswax concentration varied from 1-12% (w/w of oil). Particle size and its distribution were determined for each condition by dynamic light scattering (DLS) (MALVERN Zetasizer NanoZS™, Software version 7.04, Malvern Panalytical, Tokyo, Japan) at 20 °C and scattering angle 173°. All the samples were diluted 600 times with the continuous phase before particle size analysis. The optimum concentration of surfactant and organogelator including oil to water volume ratio for stable nanoemulsion with a mean particle diameter of < 250 nm and narrow size distribution (PDI < 0.3) was determined from particle size analysis.

6.3.3 Characterization of G/W eyedrop

(a) Particle size analysis and zeta potential: A dynamic scattering particle analyzer (MALVERN Zetasizer NanoZS™, Software version 7.04, Malvern Panalytical, Tokyo, Japan) was employed to monitor the particle diameter and its distribution of nanoemulsion. The sample was diluted in the same manner as mentioned before (600 times with PBS) and three measurements were taken each time. Light scattering was monitored at a 173° angle and 20 °C. Zeta potential of prepared nanoemulsion was also measured using the same instrument. The sample was diluted 100 times with the water before zeta potential measurement.

(b) Measurement of nanoemulsion pH: pH of the prepared nanoemulsion was measured by a calibrated pH meter (SARTORIUS Mechatronics, Japan K.K., Tokyo,

Japan) at 25 °C. The 4.0 and 7.0 pH buffer solutions were used for calibration of the pH meter. The samples were repeated in a triplicate manner and mean values were calculated.

(c) Rheological study of G/W nanoemulsion: Viscoelastic behavior of G/W nanoemulsion was determined by oscillatory rheometer (Modular Compact Rheometer: MCR 302, Anton Paar Japan K.K., Tokyo, Japan) and compared with oil-in-water (O/W) nanoemulsion. The dynamic viscoelasticity G^* was measured that representing the modulus of elasticity based on Hooke's law and the viscosity based on Newton's law. The nanoemulsion was centrifuged at 15000 rpm or $13860 \times g$ for 20 min to separate the nanoparticles followed by placement of particles between the parallel plates of the rheometer. The plate gap was set at 100 μm and measurement was performed at 0.1 -100% strain at a constant frequency of 1 Hz. Simultaneously, thermal sensitivity of beeswax organogel was also observed by taking measurements at 25 °C and 37 °C at constant strain (0.1%) and frequency (1 Hz).

6.3.4 Effect of sterilization on particle size and its distribution

Sterilization is a must for eye drops as they undergo intimate contact with the eye tissue. Different sterilization techniques are applied for ophthalmic preparations including moist heat sterilization using autoclave, sterile filtration, irradiation with ultraviolet (UV) light, gamma irradiation, high hydrostatic pressure sterilization, etc²³. In this study, we have applied two sterilization methods namely moist heat sterilization by autoclave and UV light irradiation to determine the effect of sterilization on particle size analysis. G/W nanoemulsion was autoclaved (High-Pressure Steam Sterilizer LBS 325, TOMY Seiko Co., Ltd., Tokyo, Japan) at 121 °C

under a pressure of 1 atm for 15 min followed by particle size analysis. At the same time, G/W nanoemulsion was also exposed to UV radiation for 20 min for sterilization. Changes in particle size and PDI after autoclaving and UV irradiation were determined from particle size analysis by DLS in the same manner as described earlier.

6.3.5 In vitro biocompatibility study of G/W nanoemulsion

Biocompatibility of G/W nanoemulsion was tested in vitro using both proliferative cells and non-proliferative cells. Human umbilical vein endothelial cells (HUVECs) and primary rat hepatocytes were used as proliferative cells and non-proliferative cells, respectively. Both of these cells are highly susceptible to foreign particles and hence we choose these two types of cells for biocompatibility study.

(a) Primary rat hepatocyte isolation: Primary rat hepatocytes were isolated from 6-8 weeks old male Sprague-Dawley (SD) rats (Japan SLC Inc., Hamamatsu, Japan) of 160-230 g weight. A two-step collagenase perfusion method was applied for hepatocytes isolation and cell viability was ~ 90% according to the trypan blue dye exclusion assay. Primary rat hepatocytes were cultured in a serum-free medium supplemented with Dulbecco's Modified Eagle Medium (DMEM; Funakoshi Co., Ltd., Tokyo, Japan), 0.05 mg/L Epidermal Growth Factor (Funakoshi Co., Ltd., Tokyo, Japan) 10 mg/L insulin obtained from bovine pancreas (Sigma, Tokyo, Japan), 7.5 mg/L hydrocortisone (Sigma), and 60 mg/L L-proline (Sigma). This culture medium was referred to as DHDM. This protocol was reviewed and approved by the

Ethics Committee on Animal Experiments of Kyushu University, Japan (A29-413-1; 29 Jun 2018; A10-381: Feb 25, 2020).

(b) Hepatocytes and HUVEC cell culture for mitochondrial activity: Freshly isolated primary rat hepatocytes suspended in DHDM were seeded (2.5×10^4 cells/cm²) in a collagen-I-C coated 96-well plate. Cells were incubated at 37 °C in a humidified atmosphere with 5% CO₂ and the medium was replaced at 4h after cell inoculation. Similarly, HUVECs (RIKEN Bioresource Research Center, Tsukuba, Japan) were cultured in a 96-well plate under standard condition (37 °C, 5% CO₂, 95% air) using Endothelial Growth Medium-2 (EGM-2, LONZA, Walkersville, MD, USA) at a seeding density of 2.0×10^4 cells/cm². Both of the cells were incubated with organogel based G/W nanoemulsion of three different concentrations ranging from 0.1 -10% after 24 h of post-inoculation. Mitochondrial activity of hepatocytes and HUVECs in the presence of G/W nanoemulsion was evaluated after 24 h of inoculation using Cell Counting Kit-8 (CCK-8, Dojindo, Kumamoto, Japan). The bioavailability of G/W nanoemulsion to these cells was compared with their corresponding control (cells incubated with culture medium DHDM/ EGM-2 only). The relative cell viability of the HUVECs at different concentrations of G/W nanoemulsion was calculated from WST-8 absorbance using the following equation (Equation 1)²⁴:

$$\% \text{ Cell viability} = \frac{\text{Absorbance} \left(\frac{\text{G}}{\text{W}} \right)}{\text{Absorbance (Control)}} \times 100 \quad (1)$$

A sample was considered cytotoxic when the cell viability was <70% in comparison to the control, which was considered to have 100% viability.

6.3.6 Ocular surface irritation test in vivo

Ocular irritation by G/W nanoemulsion was evaluated using 6 weeks old, male, ICR mice (Slc: ICR, Japan SLC Inc., Shizuoka, Japan). Animals were housed in standard cages and were provided with a standard pellet diet and water ad libitum for 24 h. The experimental procedures conform to the Ethics Committee on Animal Experiments of Kyushu University, Japan (A29-413-1; 29 Jun 2018; A10-381: Feb 25, 2020), on the use of animals.

Mice were divided into three groups (3 mice per group) - a) no treatment group or negative control, b) mice treated with castor oil or positive control, and c) mice treated with G/W nanoemulsion or G/W. In vivo ocular irritation study was performed according to the Draize technique²⁵. For the negative control group, 15 μ L of saline was administered on each eye of mice at 24 h intervals for 6 days. Similarly, mice of positive control and G/W groups received the same volume (15 μ L on each eye) of castor oil and G/W nanoemulsion, respectively for 6 successive days. After 24 h of instillation, eyes were examined under general anesthesia during the experimental period.

Ocular irritation scores for every mouse were calculated by adding together the irritation scores for the iris, cornea, and conjunctiva and dividing the total score of all mice in a group by the number of mice. Furthermore, eyes were stained with 2 μ L fluorescein (0.5% fluorescein in saline) and examined under a fluorescence microscope (IX71, Olympus Corporation, Tokyo, Japan) for possible corneal lesions. Ocular irritation was classified according to four grades: practically non-irritating, score 0–3; slightly irritating, score 4–8; moderately irritating, score 9–12; and severely

irritating (or corrosive), score 13–16²⁶. Mice were also observed for any swelling or watering of the eyes.

6.3.7 In vivo permeability study

Eye permeability of G/W nanoemulsion was performed using a hydrophobic fluorescent dye Coumarin-6 (Tokyo Chemical Industry Co., Ltd., Tokyo, Japan) as a model drug that was incorporated in the inner gel phase of G/W nanoemulsion. 6-weeks old male ICR mice (Slc: ICR, Japan SLC Inc., Shizuoka, Japan) mice were used in this study and divided into three groups (n=3). Group A represents negative control (no treatment), group B mice were treated with coumarin-6 loaded castor oil (positive control), and group C was treated with coumarin-6 (0.03%) loaded G/W nanoemulsion (G/W with C-6).

5 μ L of respective emulsion for each condition (group B and C) was carefully administered on each eye and kept the eye leads closed for 10 sec to avoid drainage out of emulsion. The emulsion was instilled once daily for 5 consecutive days. On day 6, mice were sacrificed, eyeballs collected after disinfecting the eyeball surrounding with 70% ethanol and preserved in 10% neutral formalin buffer (Fujifilm Wako Pure Chemicals, Ltd., Japan). Eyeballs were then embedded in the OCT compound (Sakura Finetek USA, Inc., Torrance, USA) and frozen at -80 °C, followed by a cut to a thickness of 20 μ m using a microtome (LEICA CM 1860 UV, Leica Microsystems K.K, Tokyo, Japan). Eyeball slices were then placed on a glass slide and observed under a fluorescence microscope (IX71, Olympus Corporation, Tokyo, Japan). The numerical evaluation of fluorescence intensity in the retinal layer of the eye was performed using ImageJ software. The relative fluorescence intensity of coumarin-6

from castor oil solution and G/W nanoemulsion was calculated considering the fluorescence intensity of control as 1.

6.3.8 Statistical analysis

Statistical analysis of results was performed using the two-tailed Student's *t*-test. A *p*-value of < 0.05 was considered statistically significant. All the results are presented as mean \pm standard deviation.

6.4 Results and discussion

6.4.1 Determination of optimum concentration of oil to aqueous phase volume ratio, surfactant, and gelling agent concentration

The particle size and PDI of G/W nanoemulsion at different oil to aqueous phase volume ratios are shown in figure 6-1(A). A subsequent decrease in particle size along with their distribution was observed with the increase in PBS volume. Particles have a diameter of > 300 nm and wide size distribution (PDI > 0.4) when the relative volume of castor oil lies between 33 – 50% of PBS. Further decrease in oil volume leads to the formation of monodispersed (PDI < 0.3) nanoparticles with < 300 nm in diameter. This may result from changes in the viscosity of emulsion during emulsification. A higher extent of castor oil increases the viscosity and causes higher resistance against the shear force applied in the form of ultrasonication²⁷. To ensure higher bioavailability and permeability of eye drop in the posterior eye segment, nanoparticles of < 300 nm with narrow size distribution (PDI < 0.2) are desired²⁸.

Therefore, the optimum volume ratio of castor oil to PBS was chosen 1:7 for G/W nanoemulsion where the mean particle diameter was ~ 200 nm and PDI was 0.15.

Therefore, the optimum volume ratio of castor oil to PBS was chosen 1:7 for G/W nanoemulsion where the mean particle diameter was ~ 200 nm and PDI was 0.15.

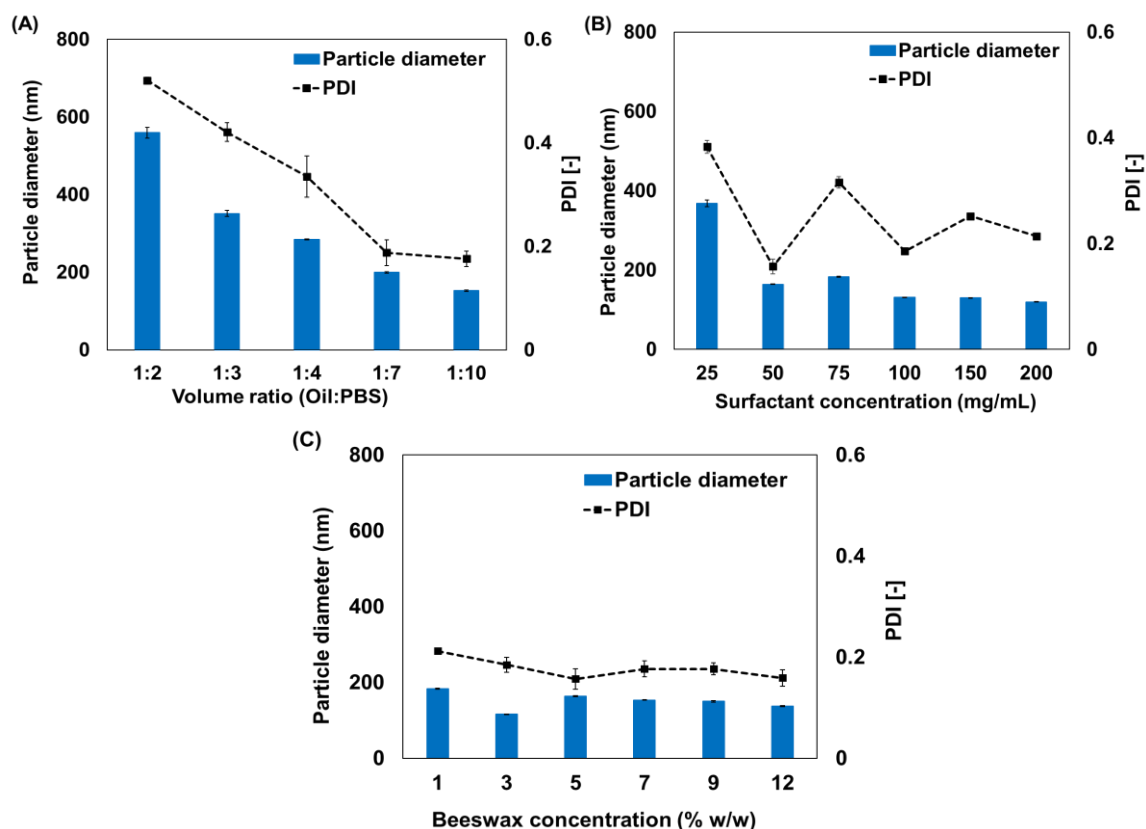


Figure 6-1: Formulation optimization for a stable G/W nanoemulsion, (A) selection of oil:PBS volume ratio; (B) selection of surfactant concentration; (C) selection of organogelator concentration. Bars represent standard deviation, $n=3$.

Screening results for surfactant concentration showed that particle diameter decrease from 360 nm to 150 nm with an increase in surfactant concentration (Figure 6-1(B)). Surfactants adsorb on the particle surface and reduce the interfacial tension between the dispersed phase and continuous phase. An increased amount of surfactant

leads to a large oil-water interface, reduced surface tension, and thereby minimizes the particle size^{29,30}. In contrast, a higher concentration of surfactant increases the polydispersity index of nanoemulsion. Particle size distribution or PDI largely depends on surfactant's dynamic property and is affected by their adsorption kinetics. As a result, a greater amount of surfactant leads to higher PDI and affects the stability of nanoemulsion³¹. Our results also showed a fall in PDI value from 0.4 to 0.15 with the increase in HCO-60 concentration from 25 mg/mL to 50 mg/mL. While an increase in PDI value > 0.2 was observed with a further increase in the concentration of HCO-60 ranging from 75 – 200 mg/mL. The optimum surfactant concentration was determined 50 mg/mL as nanoparticles with narrow size distribution were found at this concentration.

The effect of beeswax concentration on particle size distribution was shown in figure 6-1(C). Results showed an increase in gelling agent concentration has no significant effect on particle size and its distribution. The mean particle diameter was < 200 nm and the PDI value was ≤ 0.2 for beeswax concentration ranging from 1 – 12%. Martins et. al. showed that beeswax can form stable organogel and sustain its gel behavior only at a concentration of 4% w/w of oil or higher³². Therefore, beeswax was used at a concentration of 5% w/w of castor oil in G/W nanoemulsion. Concisely, the optimized formulation for a stable G/W nanoemulsion consists of 50 mg/mL surfactant, 5% w/w beeswax with an oil aqueous volume ratio of 1:7.

6.4.2 Characterization of G/W eyedrop

Various physicochemical characteristics of prepared G/W nanoemulsion were determined and presented in figure 2.

(a) Particle size analysis: Particle size analysis by DLS showed that G/W nanoemulsion has nanosized particles of about 200 nm in diameter. The polydispersity index value 0.15 – 0.20 indicates homogenous, uniformly sized, spherical vesicles (Figure 6-2(A)). Generally, nanoparticles with < 250 nm in diameter are easily taken up by the retina via endocytosis³³. So, our G/W nanoemulsion could be an effective carrier for drug delivery in the posterior eye segment.

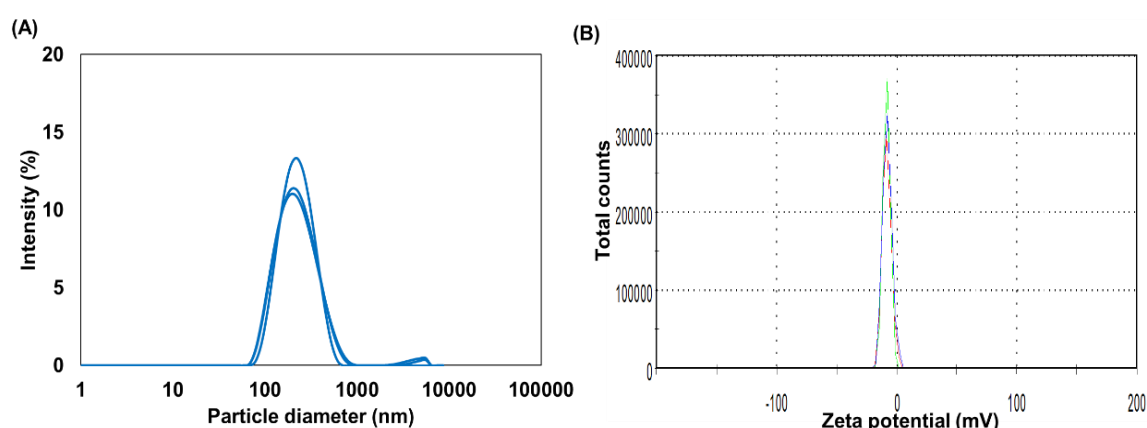


Figure 6-2: Characterization of G/W nanoemulsion, (A) particle size distribution analysis by DLS; (B) zeta potential of G/W nanoparticles, n=3.

(b) Zeta potential: Surface charge i.e. zeta-potential of nanodroplets influences precorneal residence of emulsion at the ocular surface along with formulation stability during storage³⁴. The observed zeta potential value of G/W nanoemulsion was - 8.1 mV on average (Figure 6-2(B)). According to the classical electrical double layer theory, a zeta potential value of about ± 20 mV provides short-term stability, above ± 30 mV demonstrates good stability, and above ± 60 mV excellent stability. But this is valid for low molecular weight surfactants and pure electric stabilization³⁵. High molecular weight surfactants stabilize a nanoemulsion by steric hindrance and hence

zeta potential value of only ± 20 mV or much lower can provide sufficient stability³⁶. Studies also suggest that formation of the shear plane to a far distance from the particle surface often leads to reduction in measured zeta potential and emulsions showed better stability even at a lower zeta potential³⁷. HCO-60 is a high molecular weight (939.5 g/mol) surfactant used in G/W nanoemulsion and the zeta potential value of - 8.1 mV suggests sufficient stability of the nanoemulsion.

(c) pH: The mean values of the above-mentioned physicochemical properties along with the pH of G/W nanoemulsion are given in Table 6-1. The pH of the prepared nanoemulsion was about 7.3 and was within the acceptable range of pH for ophthalmic preparations (6.07 – 8.45). Eye drops having pH within this range are easily buffered by lacrimal fluid and hence avoid ocular irritation, reflex tears, or rapid eye blinking^{34,35}. Therefore, G/W nanoemulsion could be administered as an eye drop without causing possible irritations on the eye.

Table 6-1: Featured characteristics of G/W nanoemulsion

Particle diameter	PDI	Zeta potential	pH
182 \pm 1.7 nm	0.17 \pm 0.02	- 8.1 \pm 0.4 mV	7.3 \pm 0.1

(d) Rheological analysis: Dynamic viscoelasticity (G^*) of beeswax nanogel particles was measured and compared with that of O/W nanoparticles (Figure 6-3(A)). In general, organogels are viscoelastic systems, and G^* is the most relevant parameter for assessing viscoelasticity. It is a quantitative measurement of material stiffness^{38,39}. Results showed that G/W nanoemulsion has a higher value of G^* compared to O/W nanoemulsion suggesting a highly cross-linked microstructure of nanogel particles

leading to higher stiffness of gel. Thus, this gel microstructure will enhance the corneal retention time of eye drop and will help to maintain the stability of G/W nanoemulsion.

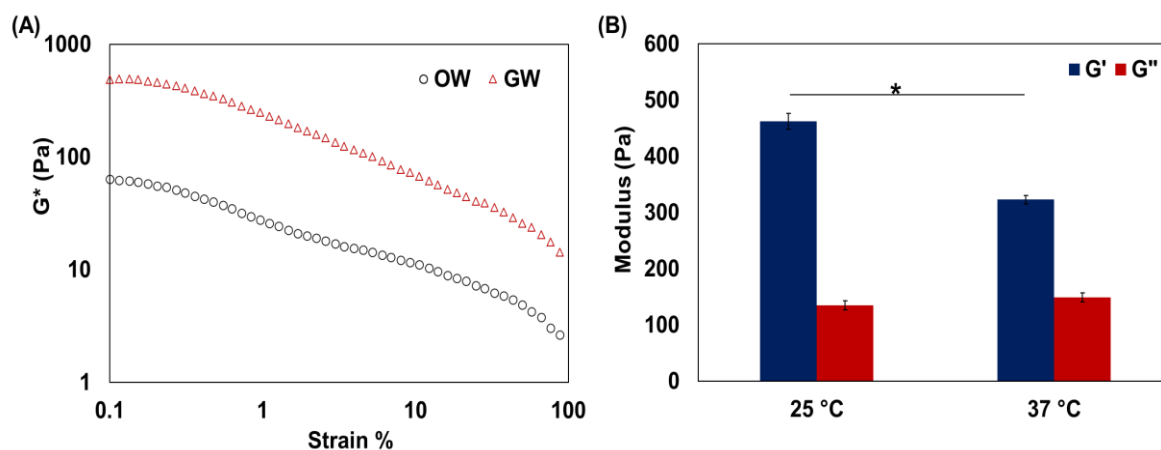


Figure 6-3: Rheological analysis of G/W nanoparticles, (A) comparative dynamic viscoelasticity of G/W and O/W nanoemulsion; (B) thermal sensitivity of G/W nanoparticles. Bars represent standard deviation, $n=3$, $*p < 0.05$.

Additionally, the thermal sensitivity of beeswax organogel was confirmed from rheological analysis at different temperatures. Gel formation was confirmed as the storage modulus (G') of G/W nanoparticles decreased significantly with an increase in temperature from 25 °C to 37 °C (Figure 6-3(B)). Effect of temperature on elastic behavior (G') and viscous behavior (G'') of G/W nanoparticle indicates gel formation⁴⁰. On the other hand, O/W nanoparticles did not show any thermal sensitivity as no significant change (data not shown) in G' and G'' was found with temperature changes.

6.4.3 Effect of sterilization on the particle size distribution

In order to avoid contamination and disease transmission, ophthalmic preparations should be sterilized to remove microorganisms like bacteria, fungi, spores. It is important to ensure that sterilization does not cause any degradation to the physicochemical properties of the nanoemulsion. Autoclaves based on moist heat sterilization and UV irradiation were applied to sterilize G/W nanoemulsion and changes in particle size distribution were observed.

For moist heat sterilization, particle diameter remained unchanged while the PDI value increased from 0.2 to 0.4 (Table 6-2). Autoclaving has a destructive influence on nanoemulsions containing materials of a melting point lower than 120 °C. The increase in temperature (120 °C) and the cooling during autoclaving may lead to rearrangements of nanoparticles structure and hence increase the particle size distribution⁴¹.

In contrast, sterilization of G/W nanoemulsion using UV light did not cause any change in particle size distribution. The particle diameter was found 200 nm PDI value of 0.2 after UV irradiation. Therefore, UV irradiation would be an effective sterilization technique for preventing bacterial growth in G/W nanoemulsion without causing any change in the physicochemical properties of nanogel particles.

Table 6-2: Particle size analysis of G/W nanoemulsion before and after sterilization.

Sterilization method	Moist heat sterilization (Autoclaving)		UV irradiation	
	Diameter (nm)	PDI	Diameter (nm)	PDI
Before sterilization	226.0 ± 4.0	0.2 ± 0.01	174.0 ± 3.0	0.2 ± 0.01
After sterilization	205.0 ± 5.0	0.4 ± 0.02	200.0 ± 2.0	0.2 ± 0.01

6.4.4 In vitro biocompatibility study

Biocompatibility of G/W nanoemulsion to primary rat hepatocytes and HUVECs was determined from WST-8 assay. Live cell activity of these cells at different concentrations ranging from 0.1 – 10% is shown in figure 6-4.

There was no significant change in live cell activity of primary rat hepatocytes in comparison to control after 24 h of emulsion administration (Figure 6-4(A)). Similarly, an increase in the concentration of G/W nanoemulsion from 0.1% to 1% has no cytotoxic effect on cell viability. For the dormant nature of hepatocytes, they do not undergo cell division in vitro and lose their cuboidal morphology and liver-specific functions within few days of culture. As a result, maintaining the cell number is considered an index for hepatocytes^{42,43}. Our results are in line with them as the WST-8 absorbance (proportional to live cell activity) in the presence of G/W nanoemulsion was almost similar to that of control.

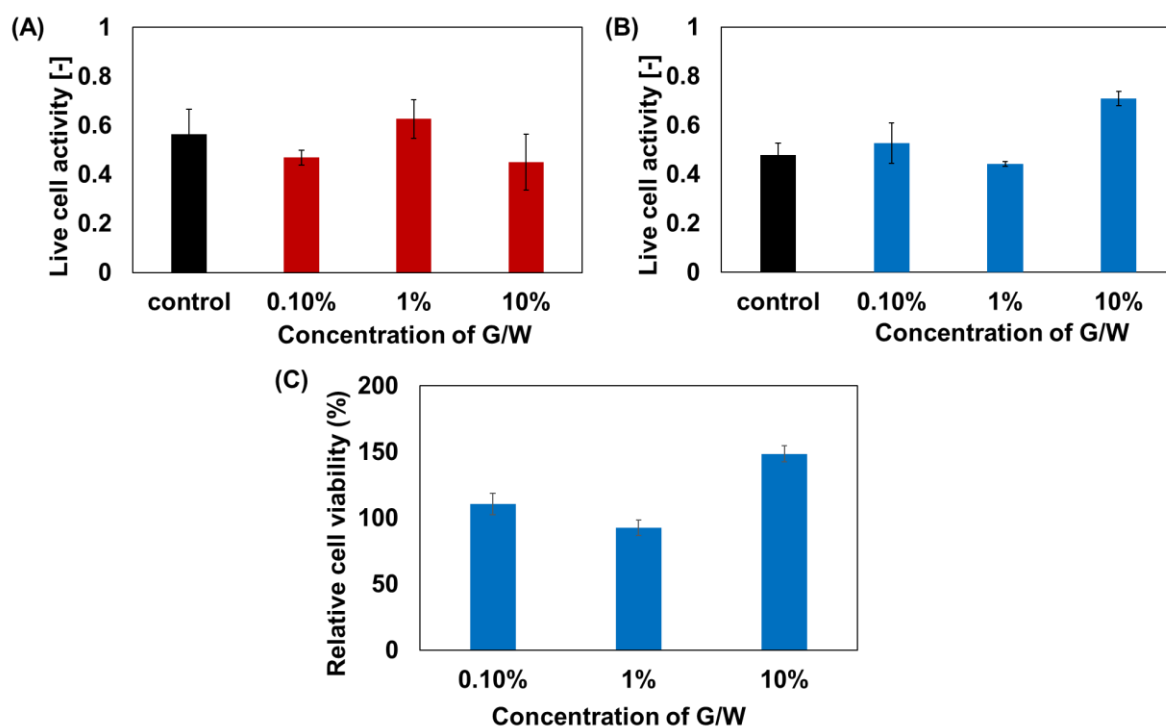


Figure 6-4: In vitro biocompatibility of G/W nanoemulsion at different concentrations, (A) live cell activity of primary hepatocytes; (B) live cell activity of HUVECs; (C) cell viability of HUVECs in the presence of G/W nanoemulsion. Bars represent standard deviation, $n = 3$.

In case of proliferative cells, G/W nanoemulsion was also found biocompatible with HUVECs with no significant decrease in live cell activity (Figure 6-4(B)). The relative cell viability after 24 h was $\geq 90\%$ for all the concentration ranges i.e. 0.1%, 1%, and 10% (v/v) of G/W nanoemulsion (Figure 6-4(C)).

Additionally, cell morphology of both primary rat hepatocytes and HUVECs remains unchanged with the increase in concentration and assures biocompatibility of G/W nanoemulsion (Figure 6-5(A) & (B)). Therefore, G/W nanoemulsion was found biocompatible to both proliferative and non-proliferative cells in vitro and suggesting its feasibility for use as ophthalmic preparations.

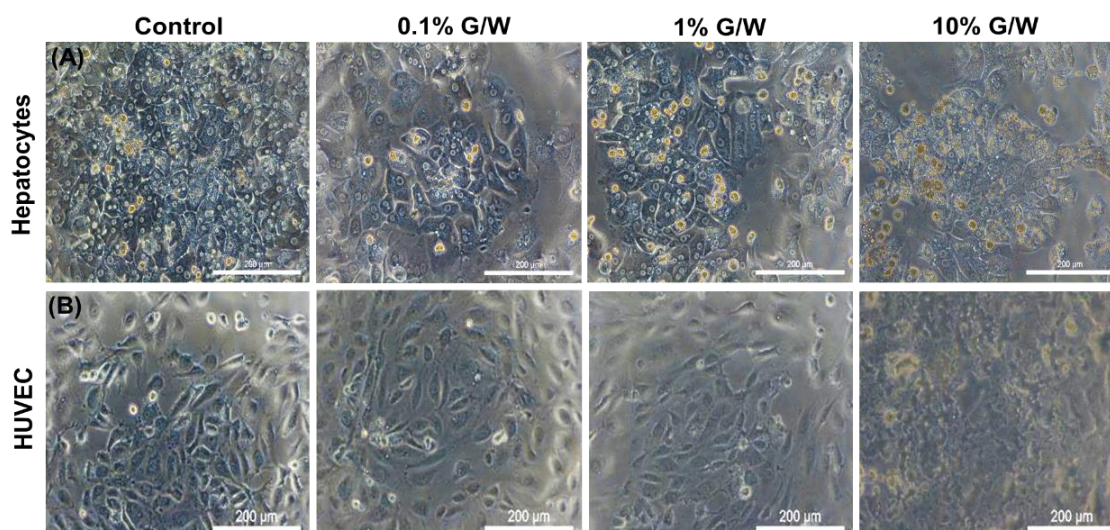


Figure 6-5: Effect of G/W nanoemulsion on cell morphology at different concentrations, (A) hepatocytes morphology; (B) HUVECs morphology. Scale bars = 200 μm .

6.4.5 Ocular surface irritation test in vivo

The eye irritation probability of G/W nanoemulsion was tested in vivo based on corneal lesion scores after G/W nanoemulsion administration and was considered non-irritating when the score is 0-3. The total number of lesions of all mice in a group was divided by the total number of mice tested to calculate the eye irritation score. The observed eye irritation score for all three groups (control, positive control, and G/W) was between 0.71 – 0.98 which implying an excellent ocular tolerance of G/W nanoemulsion (Figure 6-6). Moreover, no ocular damage was found on the cornea or conjunctiva. Likewise, any swelling or watering of eyes was absent for both control and G/W groups. Hence, the results of this study reveal the safety of G/W nanoemulsion for ophthalmic application.

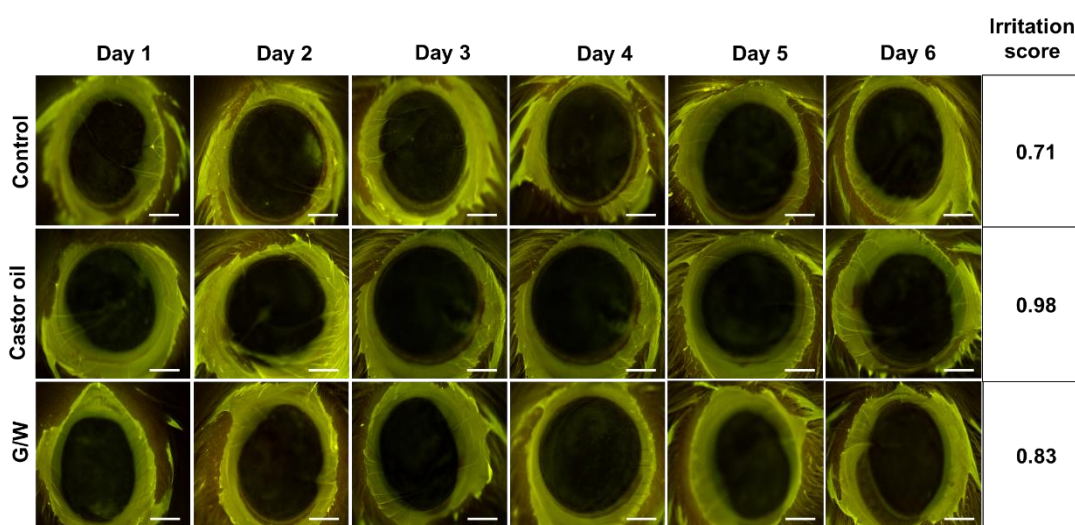


Figure 6-6: Ocular surface irritation test for G/W nanoemulsion. Scale bars = 50 μ m.

6.4.6 In vivo permeability study

Coumarin-6 incorporated in organogel droplets was used to observe in vivo permeability of G/W nanoemulsion through the cornea. Results showed a significant increase in corneal permeability for G/W nanoemulsion compared to control (Figure 6-7(A)). The fluorescence intensity of coumarin-6 was significantly higher for G/W nanoemulsion than the solution of coumarin-6 in castor oil. Owing to the nanosize and high surface area along with the presence of surfactants, G/W nanoparticles may overcome the ocular barriers followed by increased permeability to the posterior segment of the eye.

Consistently, the negative surface charge (zeta potential = - 8.1 mV) of nanogel droplets may also help to penetrate the nanoparticles to the retina and leads to enhanced fluorescence intensity⁴⁴. The microscopic observation also ensures the higher permeability of coumarin-6 loaded G/W nanoemulsion (Figure 6-7(B), (C) & (D)).

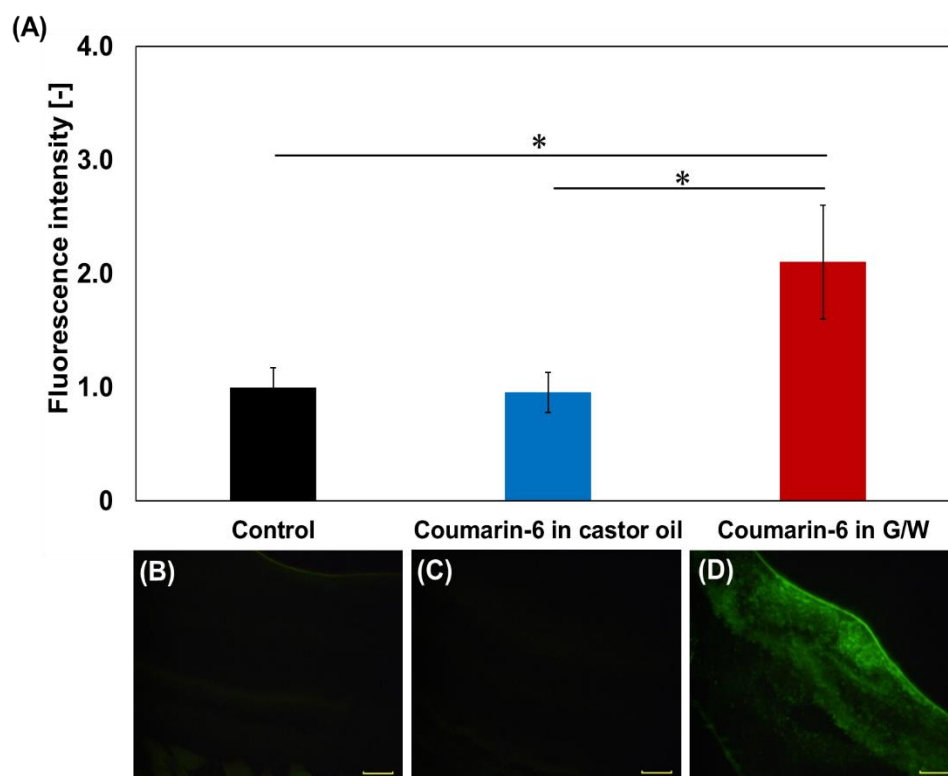


Figure 6-7: In vivo corneal permeability of G/W nanoemulsion, (A) relative fluorescence intensity of coumarin-6 in the retinal layer; (B) permeability for control group; (C) permeability of coumarin-6 in castor oil; (D) permeability of coumarin-6 loaded G/W nanoemulsion. Bars represent standard deviation, $n=3$, $*p < 0.05$. Scale bars = 50 μm .

6.5 Conclusion

The nanoemulsion system containing organogel nanodroplets for topical delivery of ophthalmic drugs in PSEDs treatment has been successfully developed in this study. Beeswax forms the organogel nanoparticles able to encapsulate hydrophobic drug molecules within it and remain dispersed in the aqueous phase by HCO-60. The mean particle diameter was ~ 200 nm with a narrow size distribution ($\text{PDI} \leq 0.2$) which will ensure effective uptake of nanoparticles by retinal cells. Rheological study suggests

Chapter 6: Nanogel dispersion as eye drop

gel formation via higher dynamic viscoelasticity (G^*) along with the thermal sensitivity of nanoparticles. The prepared G/W nanoemulsion showed biocompatibility to both primary rat hepatocytes and HUVECs in vitro. Furthermore, no ocular irritation was observed upon the instillation of G/W nanoemulsion as an eye drop. Besides, the higher permeability of G/W nanoemulsion through the cornea assures possible drug delivery to the retina. In a nutshell, the optimized formulation of G/W nanoemulsion could be a promising and viable drug delivery system for the non-invasive treatment of posterior segment eye diseases.

6.6 Reference

1. WHO. Blindness and vision impairment prevention. *Https://WwwWhoInt/News-Room/Fact-Sheets/Detail/Blindness-and-Visual-Impairment*. 2019;(8 October 2019):Accessed March 15, 2019. <https://www.who.int/news-room/fact-sheets/detail/blindness-and-visual-impairment>.
2. World Health Organization. World report on vision. *World health Organization*. 2019;214(14):1-160.
3. Gorantla S, Rapalli VK, Waghule T, et al. Nanocarriers for ocular drug delivery: current status and translational opportunity. *RSC Advances*. 2020;10(46):27835-27855. doi:10.1039/D0RA04971A
4. Varela-Fernández R, Díaz-Tomé V, Luaces-Rodríguez A, et al. Drug Delivery to the Posterior Segment of the Eye: Biopharmaceutic and Pharmacokinetic Considerations. *Pharmaceutics*. 2020;12(3):269. doi:10.3390/pharmaceutics12030269
5. Cheng K-J, Hsieh C-M, Nepali K, Liou J-P. Ocular Disease Therapeutics: Design and Delivery of Drugs for Diseases of the Eye. *Journal of Medicinal Chemistry*. 2020;63(19):10533-10593. doi:10.1021/acs.jmedchem.9b01033
6. Gomi F, Migita H, Sakaguchi T, et al. Vision-related quality of life in Japanese patients with wet age-related macular degeneration treated with intravitreal aflibercept in a real-world setting. *Japanese Journal of Ophthalmology*. 2019;63(6):437-447. doi:10.1007/s10384-019-00687-2

7. Kaur IP, Smitha R. Penetration Enhancers and Ocular Bioadhesives: Two New Avenues for Ophthalmic Drug Delivery. *Drug Development and Industrial Pharmacy*. 2002;28(4):353-369. doi:10.1081/DDC-120002997
8. Yadav D, Varma LT, Yadav K. Drug Delivery to Posterior Segment of the Eye: Conventional Delivery Strategies, Their Barriers, and Restrictions. In: *Drug Delivery for the Retina and Posterior Segment Disease*. Cham: Springer International Publishing; 2018:51-67. doi:10.1007/978-3-319-95807-1_3
9. Kaur IP, Kakkar S. Nanotherapy for posterior eye diseases. *Journal of Controlled Release*. 2014;193:100-112. doi:10.1016/j.jconrel.2014.05.031
10. Hughes PM, Olejnik O, Chang-Lin JE, Wilson CG. Topical and systemic drug delivery to the posterior segments. *Advanced Drug Delivery Reviews*. 2005;57(14 SPEC. ISS.):2010-2032. doi:10.1016/j.addr.2005.09.004
11. Alimanović-Halilović E. Complications in anterior eye segment after Nd-YAG laser capsulotomy. *Medicinski arhiv*. 2004;58(3):157-159.
12. Singhvi G, Patil S, Girdhar V, Dubey SK. Nanocarriers for Topical Drug Delivery: Approaches and Advancements. *Nanoscience & Nanotechnology-Asia*. 2019;9(3):329-336. doi:10.2174/2210681208666180320122534
13. Patra JK, Das G, Fraceto LF, et al. Nano based drug delivery systems: recent developments and future prospects. *Journal of Nanobiotechnology*. 2018;16(1):71. doi:10.1186/s12951-018-0392-8
14. Eljarrat-Binstock E, Pe'er J, Domb AJ. New Techniques for Drug Delivery to

- the Posterior Eye Segment. *Pharmaceutical Research*. 2010;27(4):530-543. doi:10.1007/s11095-009-0042-9
15. Gallarate M, Chirio D, Bussano R, et al. Development of O/W nanoemulsions for ophthalmic administration of timolol. *International Journal of Pharmaceutics*. 2013;440(2):126-134. doi:10.1016/j.ijpharm.2012.10.015
 16. Liang H, Brignole-Baudouin F, Rabinovich-Guilatt L, et al. Reduction of quaternary ammonium-induced ocular surface toxicity by emulsions: an in vivo study in rabbits. *Molecular vision*. 2008;14:204-216. <http://www.ncbi.nlm.nih.gov/pubmed/18347566>.
 17. Ammar HO, Salama HA, Ghorab M, Mahmoud AA. Nanoemulsion as a Potential Ophthalmic Delivery System for Dorzolamide Hydrochloride. *AAPS PharmSciTech*. 2009;10(3):808. doi:10.1208/s12249-009-9268-4
 18. Amrite AC, Kompella UB. Size-dependent disposition of nanoparticles and microparticles following subconjunctival administration. *Journal of Pharmacy and Pharmacology*. 2010;57(12):1555-1563. doi:10.1211/jpp.57.12.0005
 19. Amrite AC, Edelhauser HF, Singh SR, Kompella UB. Effect of circulation on the disposition and ocular tissue distribution of 20 nm nanoparticles after periocular administration. *Molecular Vision*. 2008;14:150-160. <http://www.ncbi.nlm.nih.gov/pubmed/18334929>.
 20. Fardous J, Omoso Y, Joshi A, et al. Development and characterization of gel-in-water nanoemulsion as a novel drug delivery system. *Materials Science and Engineering: C*. 2021;124(February):112076. doi:10.1016/j.msec.2021.112076

21. Ögütçü M, Arifoğlu N, Yılmaz E. Preparation and Characterization of Virgin Olive Oil-Beeswax Oleogel Emulsion Products. *Journal of the American Oil Chemists' Society*. 2015;92(4):459-471. doi:10.1007/s11746-015-2615-6
22. Kumar M, Bishnoi RS, Shukla AK, Jain CP. Techniques for Formulation of Nanoemulsion Drug Delivery System: A Review. *Preventive Nutrition and Food Science*. 2019;24(3):225-234. doi:10.3746/pnf.2019.24.3.225
23. Zielińska A, Soles BB, Lopes AR, et al. Nanopharmaceuticals for Eye Administration: Sterilization, Depyrogenation and Clinical Applications. *Biology*. 2020;9(10):336. doi:10.3390/biology9100336
24. Srivastava GK, Alonso-Alonso ML, Fernandez-Bueno I, et al. Comparison between direct contact and extract exposure methods for PFO cytotoxicity evaluation. *Scientific Reports*. 2018;8(1):1425. doi:10.1038/s41598-018-19428-5
25. Gonzalez-Mira E, Egea MA, Garcia ML, Souto EB. Design and ocular tolerance of flurbiprofen loaded ultrasound-engineered NLC. *Colloids and Surfaces B: Biointerfaces*. 2010;81(2):412-421. doi:10.1016/j.colsurfb.2010.07.029
26. Gan L, Gan Y, Zhu C, Zhang X, Zhu J. Novel microemulsion in situ electrolyte-triggered gelling system for ophthalmic delivery of lipophilic cyclosporine A: In vitro and in vivo results. *International Journal of Pharmaceutics*. 2009;365(1-2):143-149. doi:10.1016/j.ijpharm.2008.08.004
27. Sharma N, Madan P, Lin S. Effect of process and formulation variables on the preparation of parenteral paclitaxel-loaded biodegradable polymeric

- nanoparticles: A co-surfactant study. *Asian Journal of Pharmaceutical Sciences*. 2016;11(3):404-416. doi:10.1016/j.ajps.2015.09.004
28. Ali HSM, York P, Ali AMA, Blagden N. Hydrocortisone nanosuspensions for ophthalmic delivery: A comparative study between microfluidic nanoprecipitation and wet milling. *Journal of Controlled Release*. 2011;149(2):175-181. doi:10.1016/j.jconrel.2010.10.007
29. Chuacharoen T, Prasongsuk S, Sabliov CM. Effect of Surfactant Concentrations on Physicochemical Properties and Functionality of Curcumin Nanoemulsions Under Conditions Relevant to Commercial Utilization. *Molecules*. 2019;24(15):2744. doi:10.3390/molecules24152744
30. Chong W-T, Tan C-P, Cheah Y-K, et al. Optimization of process parameters in preparation of tocotrienol-rich red palm oil-based nanoemulsion stabilized by Tween80-Span 80 using response surface methodology. Kuksenok O, ed. *PLOS ONE*. 2018;13(8):e0202771. doi:10.1371/journal.pone.0202771
31. Silva HD, Cerqueira MA, Vicente AA. Influence of surfactant and processing conditions in the stability of oil-in-water nanoemulsions. *Journal of Food Engineering*. 2015;167:89-98. doi:10.1016/j.jfoodeng.2015.07.037
32. Martins AJ, Cerqueira MA, Fasolin LH, Cunha RL, Vicente AA. Beeswax organogels: Influence of gelator concentration and oil type in the gelation process. *Food Research International*. 2016;84:170-179. doi:10.1016/j.foodres.2016.03.035
33. Joseph RR, Venkatraman SS. Drug delivery to the eye: what benefits do

- nanocarriers offer? *Nanomedicine*. 2017;12(6):683-702. doi:10.2217/nnm-2016-0379
34. Dukovski BJ, Bračko A, Šare M, Pepić I, Lovrić J. In vitro evaluation of stearylamine cationic nanoemulsions for improved ocular drug delivery. *Acta pharmaceutica (Zagreb, Croatia)*. 2019;69(4). doi:10.2478/acph-2019-0054
35. Shah J, Nair AB, Jacob S, et al. Nanoemulsion Based Vehicle for Effective Ocular Delivery of Moxifloxacin Using Experimental Design and Pharmacokinetic Study in Rabbits. *Pharmaceutics*. 2019;11(5):230. doi:10.3390/pharmaceutics11050230
36. Rai VK, Mishra N, Yadav KS, Yadav NP. Nanoemulsion as pharmaceutical carrier for dermal and transdermal drug delivery: Formulation development, stability issues, basic considerations and applications. *Journal of Controlled Release*. 2018;270:203-225. doi:10.1016/j.jconrel.2017.11.049
37. Honary S, Zahir F. Effect of zeta potential on the properties of nano-drug delivery systems - A review (Part 2). *Tropical Journal of Pharmaceutical Research*. 2013;12(2):265-273. doi:10.4314/tjpr.v12i2.20
38. Esposito CL, Kirilov P, Roullin VG. Organogels, promising drug delivery systems: an update of state-of-the-art and recent applications. *Journal of controlled release: official journal of the Controlled Release Society*. 2018;271:1-20. doi:10.1016/j.jconrel.2017.12.019
39. Gilsenan PM, Ross-Murphy SB. Viscoelasticity of thermoreversible gelatin gels from mammalian and piscine collagens. *Journal of Rheology*. 2000;44(4):871-

883. doi:10.1122/1.551118

40. Singh YP, Bandyopadhyay A, Mandal BB. 3D Bioprinting Using Cross-Linker-Free Silk–Gelatin Bioink for Cartilage Tissue Engineering. *ACS Applied Materials & Interfaces*. 2019;11(37):33684-33696. doi:10.1021/acsami.9b11644
41. Subbarao N. Nanoparticle Sterility and Sterilization of Nanomaterials. In: *Handbook of Immunological Properties of Engineered Nanomaterials: Second Edition*. ; 2016:53-75. doi:10.1142/9789813140431_0003
42. Shulman M, Nahmias Y. Long-Term Culture and Coculture of Primary Rat and Human Hepatocytes. In: *Methods in Molecular Biology*. Vol 945. ; 2012:287-302. doi:10.1007/978-1-62703-125-7_17
43. Cho CH, Berthiaume F, Tilles AW, Yarmush ML. A new technique for primary hepatocyte expansion in vitro. *Biotechnology and Bioengineering*. 2008;101(2):345-356. doi:10.1002/bit.21911
44. Tsai C-H, Wang P-Y, Lin I-C, Huang H, Liu G-S, Tseng C-L. Ocular Drug Delivery: Role of Degradable Polymeric Nanocarriers for Ophthalmic Application. *International Journal of Molecular Sciences*. 2018;19(9):2830. doi:10.3390/ijms19092830

Chapter 7: Conclusion

7.1 Concluding remarks

The current study aimed to develop an effective drug delivery system for hydrophobic drugs. The emulsion concept is innovative compared to the currently available nanotechnology-based DDSs in terms of organogel that encapsulate the drug molecules and showed better stability and biocompatibility. A nanogel dispersion as novel DDS was successfully developed that emerges the immense possibility of effective delivery of poorly soluble drugs. Subsequently, G/W nanodispersion may aid to overcome the current challenges of nanoparticle DDSs in many instances.

In the development stage of nanogel dispersion, 12-HSA and lipiodol were selected to form the organogel and remain homogeneously dispersed in the aqueous phase by a non-ionic surfactant. The nanoemulsion met the basic characteristics of an ideal nanoemulsion with a high drug loading capacity. Particle diameter was maintained in the range of 200-300 nm with narrow size distribution that can avoid extravasation to other organs and rapid clearance from circulating blood and will assure increased drug bioavailability. Stability of G/W nanoemulsion over six months independent of storage temperature is one of the key findings of this research.

G/W nanoemulsion was found biocompatible to primary rat hepatocytes and fibroblasts with no significant change in cell viability. Additionally, *in vitro* studies indicate no change in liver-specific functions in the presence of G/W nanoemulsion, hence indicates biocompatibility of this DDS. *In vitro* and *in vivo* cytotoxicity against

skin cancer cells confirms the feasibility of G/W nanoemulsion as a hydrophobic drug carrier.

Next, sustained release of encapsulated drug by diffusion mechanism from the cross-linked organogel structure was indicated from kinetic evaluation of *in vitro* drug release profile. Anticancer efficacy of paclitaxel against lung cancer cells was assessed both *in vitro* and *in vivo* upon intravenous administration of G/W nanoemulsion and suggests the potential application of nanogel dispersion as an intravenous injection. Hence, it is possible to deliver anticancer drugs by G/W nanoemulsion as a safe and effective drug carrier.

Finally, this research work concentrated on ocular drug delivery by using organogel nanodispersion as an eye drop since this route is least investigated for organogel based DDSs until today. The unique features of G/W nanoemulsion including particle size, surface charge, use of non-ionic surfactants and pH will help to deliver the hydrophobic drugs to the back of the eye. *In vivo* permeability of G/W nanoemulsion to the retina emerges a new hope for the treatment of posterior segment eye diseases in a non-invasive way.

7.2 Future Prospects

Currently, the cellular uptake of nanogel particles and their drug release mechanism was assessed *in vitro*. Further study including flow cytometry, *in vivo* drug accumulation determination by CT scan, may be performed to confirm the application of organogel based nanodispersion in lipophilic drug delivery. At the same time, the biocompatibility of G/W nanoparticles towards rat hepatocytes and fibroblasts was

assessed *in vitro*. Further investigation on *in vivo* biocompatibility and biocompatibility towards human derived cell lines is necessary.

Based on the current research, it is considered that this organogel based DDS may be applied for a range of poorly soluble drugs of class II and class IV. The incorporation of lipophilic drugs of other therapeutic classes in the inner gel phase may be a new branch of this research.

Using the basic concept of this research, this research work could be further extended to the development and evaluation of a multiple emulsion for transdermal delivery of drugs. This could be an excellent study as an expansion of this current research. G/W nanoemulsion will be dispersed in the oil phase and homogenized by ultrasonication to form a gel-in-water-in-oil (G/W/O) multiple emulsion. Fabrication of G/W/O has been performed initially and monodispersed particles of less than 200 nm in diameter were obtained. This multiple emulsion could deliver both hydrophilic and hydrophobic drugs at a time and will be a promising carrier in DDS by means of combinational therapy with minimal side effects.

Acknowledgements

This work was carried out at the Laboratory of Biomaterials and Medical Engineering, Department of Chemical Engineering, Kyushu University, under the supervision of Professor Hiroyuki IJIMA. I would like to express a lot of thanks to many people for their help in the present work.

First and foremost, I would like to express my sincere gratitude to my supervisor, Professor Hiroyuki IJIMA. Without his guidance and persistent help, this thesis would not have been possible. I have learned a lot from him not only about drug delivery system itself but also logical thinking and sincere attitude towards scientific research. His comments and supports are always valuable and precious.

My great thanks are also expressed to Professors Masahiro GOTO and Professor Yoshiko MIURA for careful reading of this thesis and valuable comments. I am grateful to these professors for developing my understanding of many important parts of this thesis.

I am thankful to Assistant Professor Yusuke SAKAI for his valuable comments during discussion. His kind and friendly attitude always helped me to stay motivated.

I would like to thank Professor Fumiyasu ONO of the Global Innovation Center, Kyushu University for his generous support during this research work.

Furthermore, I would like to thank all the members of the Ijima laboratory, especially, Mr. Yuji OMOSO, Dr. Akshat JOSHI, Dr. Kozue YOSHIDA, Mr. Yuuta INOUE, Postdoctoral Researcher Dr. Nana SHIRAKIGAWA for their warmhearted help, kind support and motivation during my research period.

I gratefully acknowledge the Japanese Government (Monbukagakusho: MEXT) Scholarship for their financial support to complete my study. I would like to pay my gratitude to all Japanese taxpayers for their eternal contribution to this financial support.

I would like to thank the authority of Comilla University (CoU), Bangladesh, and my colleagues in the Department of Pharmacy of CoU for official support in study leave purposes.

My great thanks expressed to my parents, my dear sister, my beloved husband, family, and friends to support me with their love. They are the source of my motivation and power. Without their supports, I could not finish this work.

Finally, it is a pleasure to express my gratitude to everyone who supports me to complete this thesis.